1 *Review*

2 Aptamer-based Biosensors for Antibiotic Detection:
3 A Review

4 **Asol Mehlhorn [1], Parvaneh Rahimi [1] and Yvonne Joseph [1,*]**

5 [1] Institute of Electronic and Sensory Materials, Faculty of Materials Science and Materials Technology,
6   Technological University Freiberg, Akademie Str. 6, 09599 Freiberg, Germany
7 * Correspondence: Yvonne.Joseph@esm.tu-freiberg.de; Tel.: +49-3731-39-2146

8 **Abstract:** Antibiotic resistance and accordingly their pollution because of uncontrolled usage has
9 emerged as a serious problem in recent years. Hence, there is an increased demand to develope
10 robust, easy, and sensitive methods for rapid evaluation of antibiotic and their residues. Among
11 different analytical methods, the aptamer-based biosensors (aptasensors) have attracted
12 considerable attention because of good selectivity, specificity, and sensitivity. This review gives an
13 overview about recent developed aptasensors for antibiotic detection. The use of various aptamer
14 assays to determine different groups of antibiotics like β-lactams, Aminoglycosides, Anthracyclines,
15 Chloramphenicol, (Fluoro)Quinolones, Lincosamide, Tetracyclines and Sulfonamides are presented
16 in this paper.

17 **Keywords:** biosensor; aptasensor; aptamer; antibiotic; ampicillin; penicillin; gentamicin;
18 kanamycin; neomycin; tobramycin; streptomycin; daunomycin; chloramphenicol; ciprofloxacin;
19 danofloxacin; enrofloxacin; ofloxacin; lincomycin; oxytetracycline; tetracycline; sulfadimethoxine

21 1. Introduction

22   The increase of antibiotic-resistant germs is an acute challenge for the consumer health
23 protection and veterinary medicine. Inappropriate and prophylactic use of antibiotics (especially in
24 the field of animal care) is common and associated with contamination of the environment with
25 antibiotics and their metabolites. On one hand, this favors the development of antibiotic resistances
26 of bacteria [1–3], while on the other hand this harms the environment e.g. by uncontrolled
27 disturbance of the ground flora. To minimize the resistance towards antibiotics the use and the release
28 of them into the environment must be first detected and thereupon can be limited [1, 3].
29   In their original sense antibiotics are naturally built low molecular weight metabolites of bacteria
30 or fungi, which either kill or slow the growth of other microorganisms [1, 4]. In the widest sense,
31 partial synthetic derivates and chemically synthesized compounds with antimicrobial effect belongs
32 to antibiotics. They are generally used for treating infections in modern healthcare [1]. According to
33 their chemical structure and the resulting mode of action, antibiotics can be classified into different
34 groups inter alia ß-lactams, aminoglycosides, anthracyclines, (fluoro)quinolones, tetracyclines,
35 lincosamide and sulfonamides.
36   Currently residue levels of antibiotics in aqueous samples are mainly detected by high-pressure
37 liquid chromatography (HPLC) [5–8], gas chromatography-mass spectrometry (GC-MS) [9] and
38 liquid chromatography-tandem mass spectrometry (LC-MS/MS) [10–13]. Despite their wide range of
39 applications, these methods are usually time-consuming, require laborious pretreatment of samples,
40 sophisticated instrumentation, and trained technical personnel. The use of biosensors circumvent
41 these problems and could ensure a fast-on-site analysis. Biosensors are analytical devices that contain
42 two important functional components: a target recognition element (i. a. enzyme, protein, nucleic
43 acid, cell) and a signal transduction element [14]. According to their transducing element biosensors
44 can be divided into mass based, optical and electrochemical ones [14, 15]. Recently several possible
45 aptamer-based biosensors, known as aptasensors, have been developed for antibiotic detection.
46 Aptamers, are single-stranded DNA or RNA oligonucleotides, which can specifically bind to a wide

range of target molecules like nucleic acids, proteins, metal ions and other small molecules with high affinity, selectivity and sensitivity [16, 17] . Due to such advantages in comparison to antibodies, aptamers are promising alternatives for most applications. [18, 19]. Suitable aptamers can be identified using a process called Systematic Evolution of Ligands by EXponential enrichment (SELEX) [16, 17], first reported by Ellington et al. [16] and Tuerk & Gold [20]. In this approach, suitable binding sequences are first isolated from large oligonucleotide libraries and subsequently amplified. Aptamers can be produced at low costs and easily be modified with signal moieties [21]. Since the first publication of an aptamer-based biosensor in 1998 by Potyrailo et al. [22] a variety of biosensors and assay have been successfully developed for aptamer-based analysis (recognition and detection) of different targets. Similar to the classical immunosorbent assays, aptamer assays can be designed as single-site binding format, as dual-site (sandwich) binding format, in which the analyte is sandwiched by a pair of aptamers, or a sandwich binding format with an aptamer and an antibody [23].

Aptasensors can be fabricated with various transducers like mass sensitive, optical or electrochemical. The corresponding transduction principles are given in Figure 1. In *quartz crystal microbalance* (QCM, Figure 1(a)) and *surface acoustic wave sensors* (SAW, (Figure 1(b)) the change of the oscillation frequency of an acoustic wave due to a target binding is measured [15, 23]. In QCM the acoustic wave is produced as a bulk acoustic wave while in SAW sensors the wave travels along the surface of an elastic material with an amplitude that typically decreases exponentially with substrate depth [24]). In *micromechanical cantilever arrays* (MCA, Figure 1(c)) aptamer-target binding leads to a change in the resonance frequency of the microcantilever (dynamic mode) or to a steric crowding that forces the cantilever to bend (static mode). The bending is detected optically or electronically [15, 23].

The most commonly used optical biosensors are based on colorimetric or fluorometric detection [25]. Colorimetry is the determination of the concentration of a substance in a (mostly) liquid phase by comparison with a color scale which in turn corresponds to a known concentration of the substance [26]. Colloid gold nanoparticles (AuNPs) has been broadly considered as a label for molecular sensing, because of diverse electronic and optical properties. They absorb and scatter light with high efficiency, are known as strong quenchers and exhibit a wide range of colors [27]. Responsible for the colors is the phenomena of localized surface plasmon resonance (LSPR), in which the conducting electrons onto the AuNPs surface collective oscillate in resonance with incident light [28]. AuNPs possess a high surface free energy, a good biocompatibility and a large surface area, where molecules can be immobilized (e.g. aptamers), and are catalytic active [27, 29]. In the gold nanoparticle based *colorimetric assay* (CoA, Figure 1(d)) the aptamer is bound onto the surface of AuNPs and thus prevents their aggregation. Upon target binding the conformation of the aptamer changes from random coil structure to folded rigid structure, in consequence the adsorbed aptamers detach from the AuNPs and the AuNPs aggregates. This leading to a visible color change of the solution [25]. A limitation of AuNPs based colorimetric assays is the tendency of AuNPs to aggregate non-specifically in the presence of salt and other molecules present in the complex biological fluids [30]. In the *fluorometric assay* (FA, Figure 1(e)) the aptamer is labelled with a fluorophore and an appropriate quencher. The binding of the target causes a conformational change of the aptamer and brings fluorophore and quencher into close contact, whereupon the fluorescence is quenched [31]. This is known as "signal-off" mode. The reverse case, the "signal-on" mode, is possible too. Thereby the conformational change upon target binding leads to a divergence of fluorophore and quencher, resulting in a fluorescence signal. Graphene oxide (GO) have been widely used as a fluorescence sensing platform, because of its good biocompatibility, low cytotoxicity, and excellent capabilities for conjugation of target molecules. Graphene can bind single stranded DNA (ssDNA) via hydrophobic and π-π stacking interactions between the ring structures in the nucleobases and the hexagonal cells of graphene, but it hardly interacts with double stranded DNA (dsDNA) or aptamer-target complexes [32]. GO and surface modified graphene are highly efficient fluorescence quencher based on either electron or energy transfer mechanism [33, 34]. *Förster resonance energy transfer* (FRET) is the mechanism of non-radiation (dipole-dipole) energy transfer from an excited chromophore (donor) to a second chromophore (acceptor) [35]. Upconversion nanoparticles (UCNPs) are nanoscale particles, exhibiting photon upconversion, which means that the sequential absorption of photons leads to the

100 emission of light at shorter wavelength than the excitation wavelength [36]. UCNPs possess a couple
101 of advantages compared to other types of fluorescent materials like organic dyes or fluorescent
102 proteins, including higher photostability, low toxicity, large Stokes shifts, high quantum yields and
103 the lack of both auto-luminescence and a light-scattering background [37, 38]. UCNPs do not undergo
104 photobleaching induced by UV or visible light, which is often a problem of common fluorophores.
105 Quantum dots (QDs), semiconductor nanoparticles, belong to the UCNPs. Due to their influenceable
106 optical and electronic properties, they are of interest for many applications and are applied as
107 alternative to molecular fluorophores in optical biosensors [39–41]. QDs are very small particles, with
108 good conductivity, a high extinction coefficient, high chemical stability, broadband optical
109 absorption, low toxicity and strong photoluminescence emission [42, 43]. In contrast, the
110 *chemiluminescence resonance energy transfer* (CRET) occurs by the oxidation of a chemiluminescent
111 substrate without an excitation source [44]. The quantum mechanical phenomenon of the *surface*
112 *plasmon resonance* (SPR, Figure 1(f)) is the fundamental principle behind many biosensor applications
113 and different lab-on-a-chip systems utilized for detecting molecular interactions [23]. Polarized light,
114 parallel to the incidence plane, strikes an electrically conducting surface. Often thin metal films or
115 semiconductor films like gold is used. At the interface between two media, occurs a resonance
116 interaction with oscillating electrons, generates electron charge density waves, so called surface
117 plasmons which are totally reflected. When an analyte is bound, the refractive index of the film and
118 consequently the resonance angle alters. Thus, the intensity of reflected light at a specific angle
119 (known as the resonance angle) is changed, proportional to the mass on a sensor surface [26]. SPR is
120 a versatile technique, in which no elaborate sample preparation and no radioactive or enzyme-
121 labelled reagents are necessary [45]. The *surface enhanced Raman scattering* (SERS, Figure 1(g)) is a
122 highly sensitive optical measurement method, that provides the signals based on the enhanced
123 inelastic scattering of light on atoms or molecules (Raman scattering) in the immediate near of a metal
124 surface, often Au or Ag, with nanoscale roughness [46].
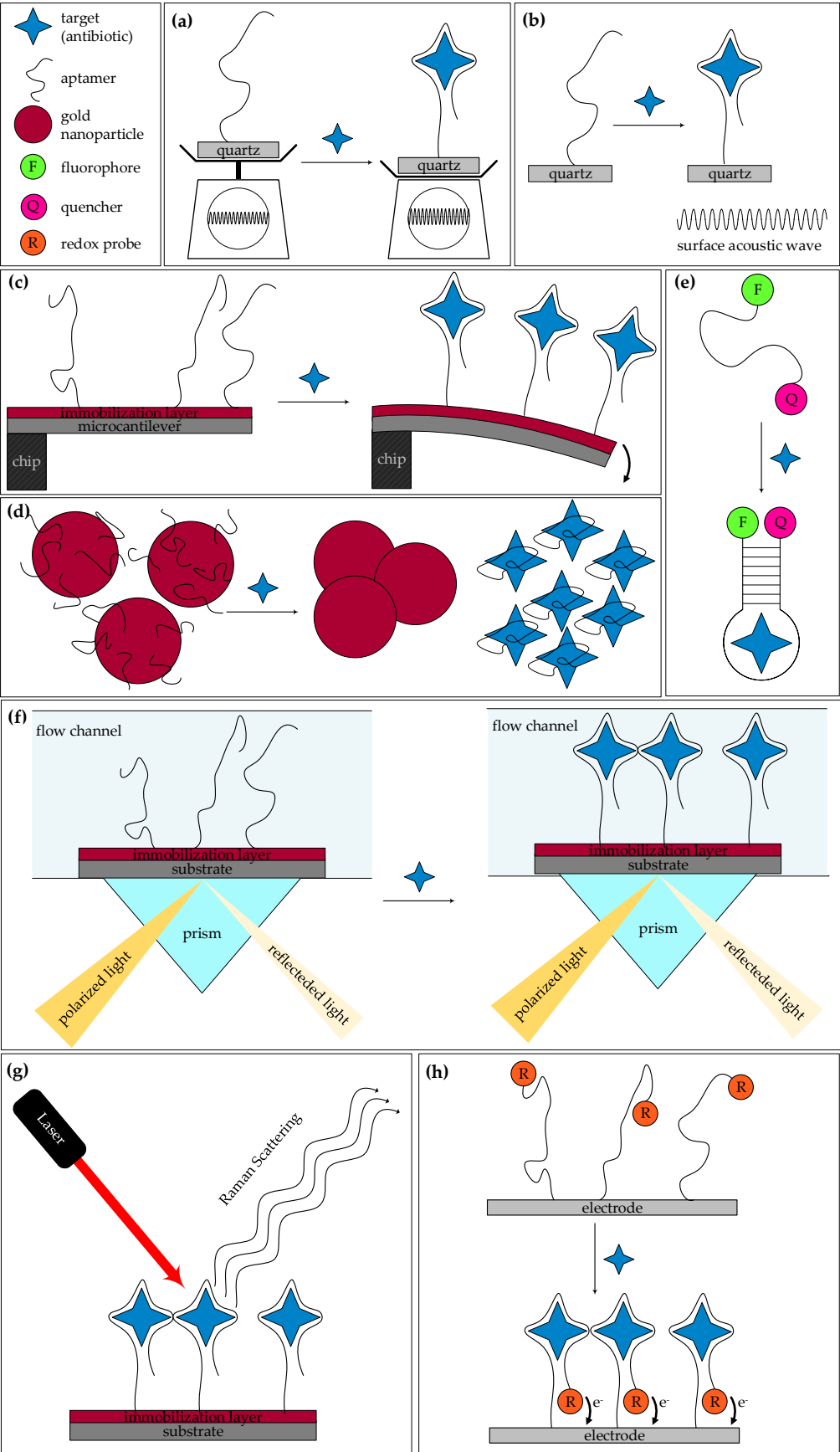
Figure 1. Working principles of the most widely used aptasensors. **(a)** quartz crystal microbalance, **(b)** surface acoustic wave, **(c)** micromechanical cantilever array, **(d)** AuNPs based colorimetric aptasensor, **(e)** fluorometric aptasensor, **(f)** surface plasmon resonance, **(g)** surface enhanced Raman scattering, **(h)** electrochemical aptasensor.

The principle of an aptamer-based electrochemical biosensor is the following (Figure 1(h)): The aptamer is immobilized onto an electrode surface and labelled with a redox probe (often ferrocene (Fc), methylene blue (MB), or Fe_3O_4 NPs). Upon target-binding the conformational change of the aptamer either brings the probe closer to the electrode surface. An electron transfer and thereby an electrochemical readout is possible [25], which is known as "signal on" mode. Alternatively the conformational change increases the distance between redox probe and surface electrode, resulting in an interruption of the previous electron transfer, designated as "signal off" mode [23]. A simultaneous detection of more than one target analyte is possible by using various metal ions e.g. Cd^{2+}, Pb^{2+}, Zn^{2+}, Cu^{2+} with diverse redox potentials to produce distinguishable electrochemical signals [47]. This kind of probes are designated as metal labelled biocodes [47]. Usually electrochemical measurements are carried out in a conventional three-electrode system, containing a working electrode (e.g. Au or glassy carbon), a reference electrode (e.g. Ag|AgCl or saturated calomel), an auxiliary electrode (e.g. platinum wire), and a redox probe in buffer solution (e.g. $[Fe(CN)_6]^{4-/3-}$). Four types of electrochemical sensors are distinguished by their measuring principle: (a) conductometric-based, which sense the change of electrical charge in a solution under constant voltage, (b) potentiometric-based, which sense changes in the electrical potential difference upon binding (c) amperometric-based, which sense the difference in current potentials during redox reactions when pairing occurs and (d) impedimetric-based, which sense changes in impedance upon interaction [15].

More methods for antibiotic detection based on the mentioned basic principles are described in detail in the appropriate section of the paper. Additionally, further detailed information about operating modes for aptamer-based biosensors can be read inter alia in reported review papers [48].

This systematical and comprehensive review discusses the application of aptamers in detection of different antibiotics groups. In this section, eight different groups of antibiotics and the designed aptasensors for their detection are discussed.

2. Aptasensors for different antibiotic classes

The various currently developed aptamer-based biosensors for antibiotic detection mentioned in the literature are ordered by antibiotics class and discussed below.

To compare the performance of aptasensors the following parameters or characteristics are important.

Affinity is a measure of the tendency of molecules to bind to other molecules [49]. The higher the affinity, the greater the *association constant K_A*. More common is the reciprocal value, the *dissociation constant K_D*. The higher the affinity of a target to its ligand, the lower the K_D of the complex, thus low K_D values are preferred.

Selectivity is the property to select multiple objects from a set of objects, while *specificity* is the property to select one object from a set of objects [50]. Thus, an analytical method is selective when different components of a mixture can be determined side by side and without interference. The method is specific when only one component of the mixture can be determined. Specificity tests are usually carried out by target detection in the simultaneous presence of the target and structurally similar substances. High specificity and selectivity is preferred.

The *limit of detection* (*LOD*) is the lowest quantity of a substance that can be distinguished from the absence of that substance (a blank value) within a stated confidence limit [51]. The maximum residue levels *MRL* is the highest concentration of an undesirable substance (impurity or pollutant), that is legally permitted in a food or commodity [52], defined by the European Union, e.g. in the Council Directive 96/23/EC [52] for antibiotic residues in live animals and animal products. The aim in the development of a biosensor is to achieve a low sensitivity, that the LOD is smaller than the MRL.

The *reproducibility* is the repeatability of scientific research results [53].

The *recovery* is determined by a standard addition method. Defined target concentrations are added to real samples and the recovery is detected. Furthermore, the results are compared to results with an alternative method, the enzyme-linked immunosorbent assay (ELISA).

180   The *applicability* of the proposed aptasensor for real-sample analysis is verified by the detection
181   of the target in real samples such as milk, honey, serum, water, and others.

182   The *stability* is the ability of the sensor to maintain its performance under the prevailing
183   conditions for a certain period of time [24]. It is tested by storing the sensor at defined conditions up
184   to several weeks, comparing the analytical performance before and after storage.

185   The most important data of the discussed aptasensors, including aptamer sequence, dissociation
186   constant (K_D), limit of detection (LOD), real sample analysis (RSA) and applied sensor type are
187   summarized in Table 1.

188   *2.1 β-lactams*

189   Because of their high efficacy, low toxicity and the possibility to derivatize them by means of
190   chemical and enzymatic methods, β-lactam antibiotics are considered to be the most important
191   antibiotic in terms of quantity and value [2]. Their mechanism of action is based on the prevention of
192   the formation of peptide cross-linking in the bacterial cell wall (murein) [1]. Therefore, they act
193   specifically on prokaryotes with a mureous cell wall. They are characterized by their representative
194   β-lactam ring (marked red in Figure 2).
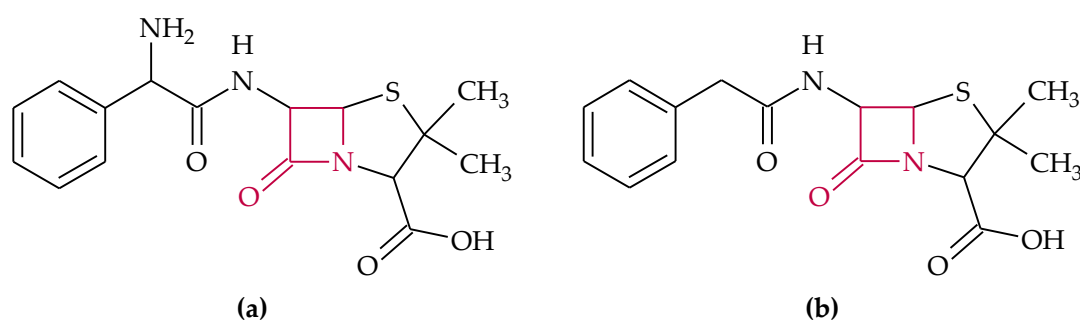
195
196   **Figure 2.**   Chemical structure of: **(a)** ampicillin and **(b)** penicillin G. The β-lactam ring
197   is marked red.

2.1.1 Ampicillin

199   The occurrence of penicillin resistant strains has stimulated the search for new antibiotics, from
200   which semi-synthetic penicillin, such as ampicillin, have been found [4]. Ampicillin (Figure 2(a)) is a
201   widely used broad spectrum antibiotic in veterinary medicine for the treatment and prevention of
202   primary respiratory, gastrointestinal, urogenital and skin bacterial infections in food-producing
203   animal and it has a low human toxicity [4].

204   Song et al. [54] reported the first aptasensor for ampicillin using AuNPs based dual fluorescence
205   colorimetric methods. They selected ampicillin specific aptamers by magnetic bead-based SELEX.
206   Three candidates showed similar intensity by conducting a fluorescence binding assay. Further
207   studies revealed that the aptamer has the highest affinity towards ampicillin as its target. Therefore,
208   it was selected for all subsequent measurements and was further used in other studies [55].
209   Measurements of antibiotics with similar structure like amicillin, amoxicillin, and penicillin G proved
210   the high specificity of the selected ampicillin aptamer. They investigated that fluorescence
211   measurements are more sensitive than colorimetric ones and the aptasensor can be used in milk as a
212   real sample.

213   Another fluorescent aptasensor for ampicillin detection was reported by Luo et al. [56] using
214   magnetic bead composites coated with AuNPs, nicking enzyme and taqman probes. The taqman
215   probe is a specific oligonucleotide containing a fluorophore covalently attached to the 5'-end of the
216   oligonucleotide and a quencher at the 3'-end. As long as the quencher and the fluorophore are in
217   proximity, the fluorescence is quenched due to FRET. Magnetic bead composites were modified with
218   the AuNPs with the help of polyethylenimine and then thiol-functionalized ampicillin specific
219   aptamers were immobilized on AuNPs via Au-SH interaction and complementary DNA (cDNA) was
220   added to hybridize with the aptamers. In the presence of the target ampicillin, the aptamers

221 preferentially bound to it, resulting in a conformational change and the release of cDNA and the
222 simultaneously formation an aptamer-target-complexes, which were magnetically separated. The
223 released cDNA hybridized with taqman probes to form a duplex-structure. The nicking enzyme
224 Nb. BbvCl cleaved the taqman probes into two fragments. As a result of the separation of the
225 fluorophore (5-hexachlorofluorescein) from the quencher (black hole quencher) the fluorescence
226 signal was recovered. Simultaneously the fragments of the taqman probe dissociated from the cDNA
227 and subsequently another taqman probe hybridized with the cDNA to initiate a new cycle of enzyme
228 assisted signal amplification. The fluorescence intensity increased in increment with the
229 concentration of ampicillin. The developed aptasensor showed the relatively high sensitivity and
230 specificity to amplicillin in complex water sample matrix.

231   Dapra et al. [55] designed an all-polymer impedimetric electrochemical microfluidic biosensor
232 for detection of ampicillin and kanamycin A. Cyclic olefin copolymer (Topas®) was used as substrate
233 on the top and bottom of the constructed chip. Because of their biocompatibility a conductive polymer
234 bilayer consisting of tosylate doped poly(3,4-ethylenedioxythiophene) (PEDOT) and the
235 hydroxymethyl derivate was used as electrode material. The covalent immobilization to the
236 electrodes with the selected target specific aptamers and formation of the aptamer-target conjugate
237 were examined by EIS. To validate the functionality of the label-free impedimetric aptasensor in real
238 samples, measurements of ampicillin in milk were successfully performed—. In a similar system
239 Rosati et al. [57] optimized the geometry of the electrodes and the microchannels (e.g. thickness,
240 width) and therefore the performance of the designed impedimetric aptasensor. Additionally the
241 ampicillin specific aptamer was equipped with an appended poly(T)-poly(C) sequence which allows
242 a direct immobilization on the electrodes applying UV irradiation [58].

243   An electrochemical aptasensor for ampicillin detection was reported by Wang et al. [59], by
244 coupling   polymerase-assisted   target   recycling amplification with strand displacement
245 amplification with the help of   polymerase   and   nicking   endonuclease. They used for the the first
246 time the target-aptamer binding triggered quadratic recycling amplification for electrochemical
247 detection of antibiotics. An Au working electrode was modified with cDNA, complementary to a
248 MB-labelled probe (MBP). A programmed hairpin probe (PHP) in the reaction solution contained the
249 ampicillin specific aptamer sequence. In the abscence of ampicillin, PHP was in a stabilized stem-
250 loop structure and coexisted with MBP in solution. The MBP is captured by the immobilized cDNA,
251 resulting in a strong electrochemical signal. The addition of ampicillin to the reaction solution led to
252 a conformational change of PHP, caused by aptamer-target binding. The now opened PHP associated
253 with MBP and formed dsDNA, wherein ampicillin was discharged. Thus, the released ampicillin was
254 able to combine to another PHP and initiated a new cycle (recycle I). Simultaneously the MBP worked
255 as a primer to initiate an extension reaction and to replicate the template part in the PHP in the
256 presence of polymerase and desoxyribinucleoside triphosphates (dNTPs). Moreover, in the dsDNA
257 of the first cycle a recognition sequence for nicking endonuclease (NE) was produced, so the NE
258 present in solution was able to nick the formed dsDNA and released an ssDNA fragment, which
259 initiated the next extension cycle. After some cycles a large amount of ssDNA was produced
260 (recycle II), which hybridized with MBP and formed duplex DNA. The duplex DNA could not be
261 captured on the Au electrode. In consequence the electrochemical signal was negligible. Excellent
262 specificity was proved by the addition of interfering antibiotics such as amoxicillin and penicillin G.
263 Moreover, measurements with spiked milk samples validated the application of the aptasensor in
264 real sample.

265   A further electrochemical method for ampicillin detection was developed by Wang et al. [60],
266 based on target-initiated T7 Exonuclease (Exo) assisted signal amplification. The proposed sensing
267 system showed that by using of the unique features of T7 exonuclease and hairpin probe, a large
268 amount of methylene blue-labelled mononucleotides are released through the cycling cleavage
269 processes, resulting in the amplified electrochemical signals. When ampicillin is added to the reaction
270 solution it forms a complex with the MB labelled hairpin probe containing the ampicillin recognition
271 sequence (aptamer). This leads to a release of a primer recognition fragment, which initiates the
272 elongation of duplex region under assistance of polymerase and dNTPs. The target ampicillin is
273 displaced and ampicillin recycling amplification is generated. Subsequently T7 Exo is able to

274 recognize and digest the polymerization-generated cDNA duplex. In consequence, a MB labelled
275 mononucleotide is produced, which possesses higher diffusivity toward the negatively charged
276 electrode than the hairpin probe and the electrochemical signal increases. The amplified signals were
277 detected by DPV. During the process a second recycling is initiated and the released complementary
278 strands can hybridize with a further hairpin probe. The obtained DPV response in the presence of
279 ampicillin and its analogues such as amoxicillin, penicillin, and penicillin G, verified the very high
280 ampicillin specificity. The assay was applied in milk to assess its functionality in real samples.
281   Wang et al. [61] presented another electrochemical aptasensor for the detection of ampicillin,
282 based on AuNPs and ssDNA binding protein (SSB) as electrochemical signal inhibition reagent. SSB
283 are proteins, which binds with high affinity to ssDNA, facilitate replication by allowing primer
284 hybridization, prevent premature hybridization of already separated complementary strands and
285 protect single strands from nucleases. Ampicillin specific thiol-modified aptamers were immobilized
286 on the GCE and thiol-modified cDNA was immobilized on AuNPs via Au-SH interaction. Through
287 hybridization between aptamer and a part of the cDNA, the modified AuNPs were assembled on the
288 surface of the GCE. The specific interaction between ssDNA-SSB and unhybridized cDNA led to the
289 loading of ssDNA-SSB on the elctrode surface, resulting in a increase of the steric hinerance effect,
290 blockation of the transfer of the redox probe $Fe(CN)_6^3$ to the electrode surface a weak electrochemical
291 signal. If ampicillin is present, the modified AuNPs are not able to assemble onto the GCE and in
292 consequence ssDNA-SB cannot hybridize, thus a strong electrochemical signal is occurs. The use of
293 the aptasensor for ampicillin detection in milk samples proved its applicability for real sample
294 analysis.
295   Yu et al. [62] developed a reagentless and reusable electrochemical aptasensor for ampicillin
296 detection in complex samplex. The response of presented sensor was based on changes in the
297 conformation and flexibility of the methylene blue (MB)-modified aptamer probe with binding the
298 ampicillin to the target, which leads to an increase in the MB current. The thiolated MB-labelled
299 ampicillin specific aptamer was immobilized onto the surface of the Au working electrode via Au-
300 SH interaction. In the absense of ampicillin, the aptamer is unstructured or partially folded, whereas
301 it is specifiically folded in the presence of the target, which brings the MB-label into close proximity
302 with the electrode surface, resulting in a strong electrochemical current. The results proved a high
303 selectivity towards ampicillin, by applying the aptasensor in bovine serum albumin (BSA), salvia and
304 milk as complex matrices.
305   In another study, Yu et al. [63] improved the analytical features of the first designed aptasensor.
306 They employed a displacement-based approach to the design of the new aptasensor. The aptamer
307 probe was first hybridized to a cDNA, the so-called displacement probe (DP) of a specific length
308 and/or melting temperature, then binding of ampicillin to the aptamer probe displaces the DP from
309 the DNA duplex resulting in a conformational change of the aptamer which finally caused a strong
310 electrochemical signal by means of MB. Selectvity and the practical use of the aptasensor for real
311 sample analysis was investigated, like described above [62].
312   Gai et al. [64] developed an aptasensor for ampicillin detection based on enzyme biofuel cell
313 (EBFC) and DNA bioconjugate. The DNA bioconjugates consisted of AuNPs modified on SiO_2 beads
314 and thiolated cDNA, which were immobilized on the AuNPs through Au-SH interaction. The amino-
315 functionalized ampicillin specific aptamers were immobilized on the glucoseoxidase- modified
316 bioanode. Glucoseoxidase is an enzyme, which catalyzes the oxidation of glucose to gluconolactone.
317 Subsequently, bioconjugate and bioanode were linked by double strand formation of aptamer and
318 cDNA. AuNPs modified carbon paper was used as substrate electrode to accelerate the electron
319 transfer and to promote the electrochemical conducting between enzyme and electrode. The
320 biocathode composed of a polydopamine film doped on the AuNPs modified carbon paper and
321 laccase attached to the modified carbon paper. Polydopamine acted as mediator for laccase (enzyme)
322 bioelectrocatalytic reduction of O_2 to H_2O. In the absense of ampicillin, the DNA bioconjugate blocks
323 the mass transport of the fuel glucose to the bioanode due to steric hindrance, resulting in a low open
324 circuit voltage (OCV) of EBFC. In the presence of ampicillin, the aptamer preferentially bound to it,
325 whereby the bioconjugate detaches from the bioanode and allows glucose to reach the active site of

glucoeoxidase. Thus, the biocatalytic oxidation of glucose could be realized, which caused a high OCV, whose amplitude was dependend on the ampicillin concentration.

The most important data of the discussed aptasensors, including aptamer sequence, dissociation constant (K_D), limit of detection (LOD), real sample analysis (RSA) and applied sensor type are summarized in Table 1.The comparison between the different aptasensors for ampicillin detection showed, that the electrochemical-based aptasensors [59-61] are elaborate and complex but also much more sensitive, as shown by the two to three magnitudes reduced LODs (Table 1).

2.1.2 Penicillin

Penicillin G (Figure 2(b)) is used for the production of 6-aminopenicillanic acid (6-APA), the main intermediate product for the synthesis of semi-synthetic penicillins and cephalosporins [2]. It is the most frequently used β-lactam antibiotic for the prevention and treatment of bacterial infections like scarlet, diphtheria, gonorrhoea, angina, tetanus. Penicillin is produced by the fungi *Penicillium notatum* and hardly humanly toxic [4].

The first aptasensor for detection of penicillin was reported by Zhao et al. [65]. They developed an electrochemical aptasensor using a composite film consisting of a magnetic graphene nanocomposite (GR–Fe3O4NPs) and a poly(3,4-ethylenedioxythiophene)–gold nanoparticles composite (PEDOT–AuNPs) for the modification of the electrode to assemble the penicillin aptamer on it. The proposed aptasensor showed good stability, and high specificity for detecting of penicillin in milk as a real sample.

Paniel at al. [66] described the selection of aptamers selective to penicillin G using the capture-SELEX process. The process is based on the selection of DNA aptamers using the ssDNA fixed on a support whereas the target is in solution. Eleven specific aptamers were selected and their binding capacity determined by affinity chromatography. This allowed the identification of the optimal penicillin G aptamer with highest retention capacity, which was selected for further characterization. Moreover, measurements using electrochemical impedance spectroscopy as detection technique were realised in milk to investigate the applicability of the sensor in real samples. Selectivity tests showed that the aptamer was able to bind other β-lactam antibiotics including amoxicillin and ampicillin, indeed with less affinity.

Lee et al. [67] identified ssDNA aptamers for the detection of penicillin G by reduced graphene oxide-SELEX (rGO-SELEX). Six different aptamers were found which specifically bound to penicillin G. The one of them with the highest binding energy was used for further experiments. rGO-SELEX is a method which uses the π-π stacking interaction between rGO and nucleic acids for an immobilization-free selection of aptamers. Furthermore, rGO is an effective fluorescene quencher through the FRET effect. Thus, the fluorescence recovery signal from the quenched FAM-labelled aptamer on the rGO surface can give information about the binding of a target to the aptamer. When a target molecule is catched by the aptamer, the conformational change leads to a removel of the quencher from the fluorophore, resulting in an increase of fluorescence. The fluorescence recovery assay with several antibiotics such as ampicillin, tetracycline, and kanamycin showed that the developed aptamer does not interact with the other antibiotics except of ampicillin. However, ampicillin has a nearly identical structure to penicillin except for one functional groups (see Figure 2), suggesting a high specificity of the aptamer for ß-lactams.

The comparison between the different aptasensors for penicillin G are showed in Table 1. Although penicillin is an important and widely used antibiotic, only a few aptamer-based biosensors exist for its detection. Hence there is still potential for research.

376   *2.2 Aminoglycosides*

377   Aminoglycoside antibiotics are the most commonly used antibiotics worldwide, with a broad
378   spectrum of activity – also against gram-negative bacteria [2]. Despite their relatively high toxicity
379   (especially on the ears and kidneys), they are the antibiotics of severe infections, which in turn leads
380   to an increase in resistance [2]. They exert their effect by binding to the 30S subunit of ribosomes,
381   which leads to reading errors during translation and ultimately inhibition of protein biosynthesis [2].
382   The basic structure of most aminoglycoside antibiotics consists of an aminocyclitol ring which is
383   linked glycosidically to other amino sugars (Figure 3) [4].

384
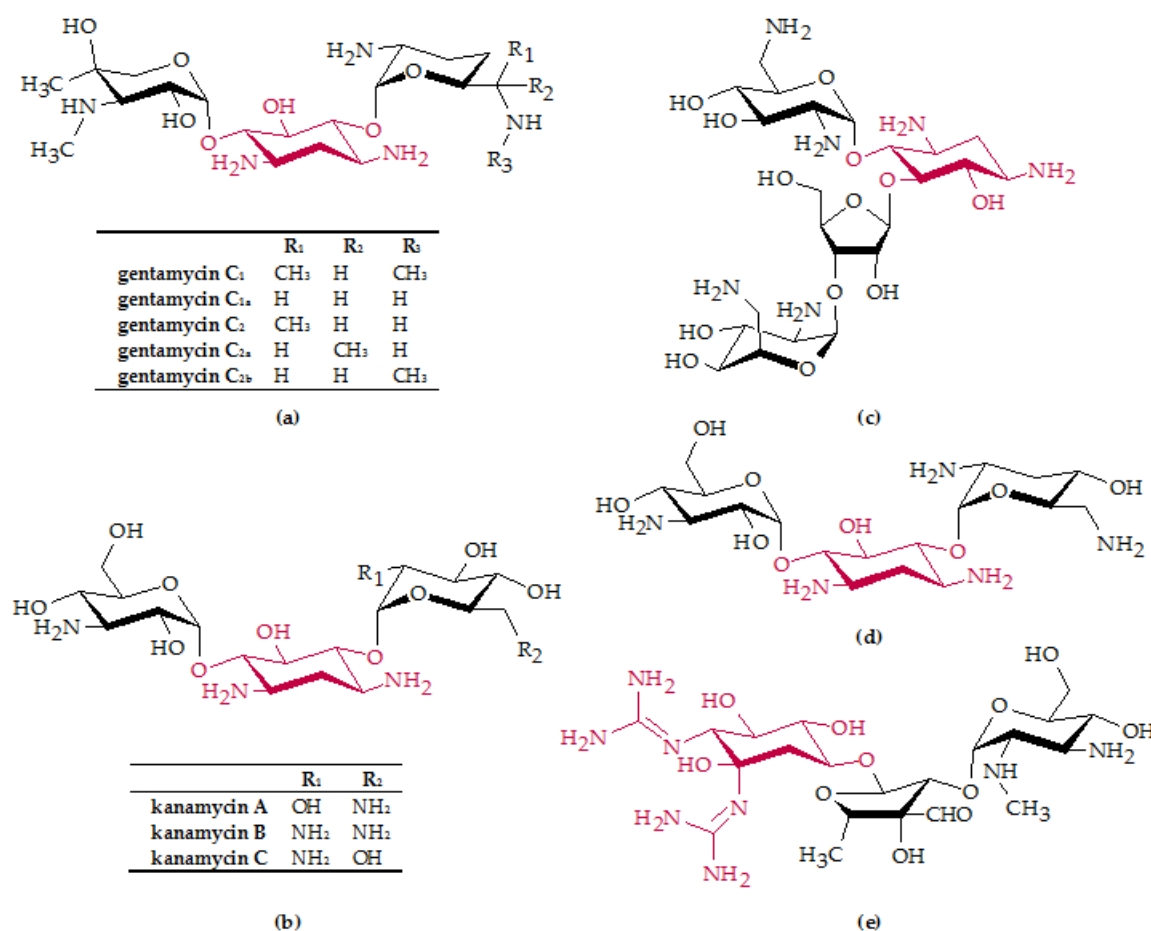
385   **Figure 3:** Chemical structure of: **(a)** gentamicin, **(b)** kanamycin, **(c)** neomycin B, **(d)** tobramycin and
386   **(e)** streptomycin. The basic structure of aminoglycoside antibiotics consists of an aminocyclitol ring
387   (marked in red) which is linked glycosidically to other amino sugars.

388   2.2.1   Gentamicin

389   The alkaline aminoglycoside antibiotic gentamicin (Figure 3(a)), isolated in 1963, is a broad-
390   spectrum antibiotic and acts bactericide against a large number of gram-positive and gram-negative
391   pathogens, such as *E. coli* and *Pseudomonas* [2]. It is used especially for severe wound infections and
392   accidental injuries, as well as secondary infections after burns [2]. Therapeutically used gentamicin
393   usually contains 70 % of the C_1 and 30 % of the C_2 component (Figure 3(a)) [2]. Gentamicin is less
394   toxic than kanamycin, neomycin and streptomycin. However, ototoxic and nephrotoxic damage have
395   been observed [2].
396   Rowe et al. [68] designed an electrochemical aptasensor for the detection of the aminoglycoside
397   antibiotics gentamicin, tobramycin, and kanamycin in blood samples in order to prevent overdosage
398   and side effects. Electrochemical measurements were conducted with a sensor chip containing an
399   integrated Au counter electrode and a Ag|AgCl reference electrode. The Au working electrode was

functionalized with aminoglycoside binding RNA-aptamers. The aptamer was modified by methylation of all 2'-hydroxyl groups outside the antibiotic binding pocket to avoid fast degradation during application in blood samples. As an alternative, more degradation-resistant DNA-aptamers were applied. Saturation curves showed that the aptasensor has a slightly higher affinity towards gentamicin and nearly equal affinity for tobramycin and kanamycin. Even if DNA aptamers are more stable, the SWV experiments showed a lower sensitivity of the DNA-aptamer based sensor to detect aminoglycosides in blood samples compared to RNA-based sensor. Upon target-binding the aptamer undergoes a significant conformational change, which could be followed via circular dichroism (CD). The original RNA-aptasensor could be used for antibiotic detection (tested with gentamicin) in human serum, after ultrafiltration of the serum by a low-molecular-weight-cut-off spin column, which efficiently removes the nucleases.

This work is the only aptasensor for gentamicin detection studied up to now in literature, therefore exits a great potential for more research.

2.2.2 Kanamycin

Kanamycin (Figure 3(b)) is a bactericidal antibiotic isolated from *Streptomyces kanamyceticus*, whose spectrum of activity comprises gram-positive and gram-negative bacteria [2]. It is widely used as a veterinary drug and as a second-line antibiotic to treat serious infections such as pneumonia, septicemia, urinary tract infections and intestinal infections [1]. If not explained in more detail kanamycin stand for a mixture of kanamycin A, B, and C, in which kanamycin A has the largest share [4]. Since sensitive and selective methods to detect kanamycin residues for food safety and clinical diagnosis are of great interest, there is more reports in kanamycin aptamer-based sensor in comparison to others antibiotics.

Song et al. [69] discovered the kanamycin specific aptamer, which was later used in a variety of other studies [70]. They selected the aptamer in vitro by SELEX using affinity chromatography with kanamycin-immobilized sepharose beads. The specific aptamers were immobilized onto the AuNPs to fabricate a colorimetric-based aptasensor. In the presence of kanamycin, the addition of salt leads to an aggregation of the modified AuNPs, which resulting a color change from red to purple.

Bai et al. [71] developed a label-free cantilever array aptasensor for kanamycin detection, composed of single side Au coated silicon cantilevers, functionalized with the kanamycin specific aptamer and 6-mercapto-1-hexanol (MCH) modified reference cantilevers. The change in compressive cantilever surface stress caused by aptamer-kanamycin binding results in different nanomechanical deflection between the cantilever pairs, which could be detected by the optical beam deflection system of the measureing platform.

Niu et al. (2014) [72] created an colorimetric aptasensor for multiplex detection of sulfadimethoxine, kanamycin and adenosine. Detailed information is described below in the appropriate chapter 2.8.1 of sulfadimethoxine.

Sharma et al. [30] designed a 'turn-off/turn-on' AuNPs based colorimetric aptasensor for kanamycin detction using the fact, that AuNPs are able to oxidise peroxidase substrates in presence of hydrogen peroxide (H_2O_2) to form colored reaction products, known as intrinsic peroxidase-like activity of AuNPs. Aptamers are able to inhibit this activity by adsorption onto the AuNPs surface. A shielding effect against interaction of AuNPs and peroxidase substrate is provided. This is referred to as a turn-off process. In the presence of kanamycin, the peroxidase-like activity can again be turned on, induced by desorption of the aptamer from AuNPs surface and high-affinity aptamer-target binding. Thus, tyrosine-reduced AuNPs were used as peroxidase nanozyme, which oxidises the colorless substrate 3,3′,5,5′-tetramethylbenzidine (TMB) to a purplish-blue product.

With regard to AuNPs-based colorimetric methods, Wang et al. [73] demonstrated, that the peroxidase-like activity of citrate-capped AuNPs could be enhanced by kanamycin. Two steps are involved: the attachment of kanamycin onto AuNPs by amino and carboxyl groups and the interaction of the glucoside section of kanamycin with AuNPs, leading to an increase of the hydroxyl radicals and Au^{3+} in solution, which catalyze the chromogenic reactions between TMB and H_2O_2. Finally, blue-colored species are produced. Based on the mentioned principle a colorimetric biosensor

451 for the detection of kanamycin was developed. Therefore, AuNPs were sequentially added to a TMB-
452 H_2O_2 solution, resulting in a visible color change of the solution.

453   A further colorimetric aptamer-based biosensor for the detection of kanamycin in milk was
454 introduced by Zhou et al. [74]. Different types of AuNPs were synthesized by self-assembly of two
455 different thiol-modified ssDNAs. One was complementary to the 3′-end of kanamycin aptamer and
456 the other one to the 5′-end. The thiol-modified ssDNAs were covalently linked to the surface of
457 AuNPs. AuNPs aggregates were formed due to hybridization between the aptamer and the ssDNAs-
458 functionalized AuNPs. The addition of kanamycin leads to competitive binding with the aptamer
459 and thus, triggered the disaggregation of AuNPs aggregates. Specificity of the proposed aptasensor
460 was verified by using the designed sensor in milk towards kanamycin.

461   Regarding to higher extinction coefficients of silver nanoparticles (AgNPs) than AuNPs, Xu et al.
462 created a colorimetric aptasensor for kanamycin detection based on unmodified AgNPs [75]. The salt-
463 induced aggregation of the AgNPs is protected in the presence of amino-functionalized kanamycin
464 due to their adsorption onto AgNPs surface via Ag-N binding and steric stabilization. Upon addition
465 of the kanamycin specific aptamer, kanamycin separates from the AgNPs surface and form a
466 kanamycin-aptamer conjugate, leading to an aggregation of the AgNPs. The result is a visible color
467 change of the AgNPs solution from yellow to ashy black, monitored by UV-Vis spectroscopy.

468   In 2017 Ha's team [76] described a paper chip-based colorimetric sensing assay for the detection
469 of residual kanamycin. The advantages of paper chip-based sensors are inter alia easy operation, low
470 cost, portability, disposability, simple fabrication and biocompatibility. The basic principle of the
471 presented aptasensor is the same as that of a standard colorimetric assay. AuNPs were synthesized
472 and modified with kanamycin specific aptamers. The paper chip out of lateral flow nitrocellulose
473 membrane was printed with a mask containing single circular wax-free hydrophilic regions and
474 surrounding regions with wax for constructing a hydrphobic barrier on the nitrocellulose membrane.
475 Each hydrophilic region was used independently.They adapted the colorimetric assay to a paper chip
476 system, which allowed to digitize colorimetric images and quantify the RGB color on the paper chip.

477   A colorimetric lateral flow strip aptasensor for one-site detection of kanamycin in food samples
478 was developed by Liu et al. [77]. The strip sensor consited of a sample pad, a conjugate pad, an
479 absorption pad, a PVC adhesive backing and nitrocellulose membrane, containing a test zone and a
480 control zone. Thiolized and biotin-modified aptamers and its thiolated cDNAs were immobilized on
481 AuNPs and AgNPs, respectively. AuNPs were used as color probes and AgNPs as signal
482 amplification element. Complexes were formed through the hybridization of the aptamers with their
483 cDNAs. A test zone strip was modified with biotin functionalized capture probes complementary to
484 the 3`end of cDNA, so that the complexes were captured in the test zone of the lateral flow strip. The
485 addition of kanamycin led to a competitive building of aptamer-target-complexes and the
486 accumulation of AuNPs on the test zone. Finally, the aptamer-target-complexes could be captured in
487 the control zone via biotin-streptavidin interaction. A qualitative detction of kanamycin was achieved
488 by observing the visible color change in the test zone by naked eye.

489   Wang et al. [78] designed a colorimetric aptasensor for the detection of kanamycin based on
490 liquid crystal film. Amino-functionalized kanamycin specific aptamers and *N,N*-dimethyl-*N*-(3-
491 (trimethoxysilyl)propyl)-1-octadecanaminiuchloride (DMOAP) were co-immobilized onto the
492 surface of a glas-slide, resulting in a homeotropic orientation of the liquid crystal film. The addition
493 of kanamycin resulted in the formtion of G-quadruplex structures, which destroyed the oriented
494 arrangement of the liquid crystals on the surface and caused a visible color change from pink to green.

495   Fluorescence as one of the most common optical techniques has been used in the fabrication of
496 aptasensors for kanamycin detection. In the work of Khabbaz et al. [79] a fluorometric aptasensor is
497 described based on streptavidin coated silica NP (SNPs). The functionalized SNPs were modified
498 with the dsDNA. Thus, the FAM-labelled cDNA is in close proximity to the surface of the SNPs,
499 resulting in a fluorescence signal. Upon addition of kanamycin the aptamer preferentially binds to it,
500 which causes the release of the cDNA from the aptamer and SNPs surface, resulting in a decrease of
501 fluorescence intensity. A high specificity towards kanamycin but also to the structurally similar
502 gentamicin was obtained. Therefore, the authors suggest that the sensor generally could be suited for
503 the detection of aminoglycoside antibiotics.

504   An aptamer-functionalized magnetic nanoparticles sensor based on multicolor fluorescence
505   labeling, for simultaneous detection of kanamycin and oxytetracycline is developed by Liu et al. [80].
506   Amino-Fe_3O_4 magnetic NPs were covalently coated with avidin using glutaraldehyde. Then the
507   target specific aptamers were immobilized onto the surface of the NPs via avidin-biotin binding. In
508   the presence of kanamycin and oxytetracycline, the aptamers preferentially bind their respective
509   target. In the absence, the aptamers bind to further added fluorescence labelled (FAM for
510   oxytetracycline and carboxy-X-rhodamine (ROX) for kanamycin) oligonucleotides, resulting in a
511   fluorescence emission of the modified NPs. Comparisons of the fluorescence signals, that were
512   induced by interaction with tetracycline, doxycycline, streptomycin, and ampicillin, indicated that
513   the aptasensor possess high specificity for kanamycin and oxytetracycline detection.

514   Generally, the binding affinity of an aptamer towards its target decreases by tagging the aptamer
515   with a fluorescent dye [81]. Therefore, Ramezani et al. [82] designed a fluorometric aptasensor for
516   kanamycin detection, based on catalytic recycling activity of exonuclease III (Exo III), AuNPs, and
517   FAM-labelled complimentary strand of the aptamer. Exo III is a sequence-independent enzyme
518   which selectively digests nucleic acids strands from 3′-end. In the absence of kanamycin, the added
519   aptamers bind to its FAM-labelled cDNA and form dsDNA. The dsDNA is not able to sorb onto
520   AuNPs. The addition of Exo III leads to the digestion of the cDNA and the aptamer is recycled from
521   dsDNA and the cycle continues. This results in a very strong fluorescence emission. In the presence
522   of kanamycin, an aptamer-kanamycin conjugate is formed. The cDNA remains onto the AuNPs and
523   the fluorescenec is quenched by the AuNPs. No dsDNA is formed and Exo III would not exhibit
524   activity. An excellent specificity towards kanamycin but also towards gentamicin was observed,
525   which is due to their very similar structure.

526   Xing et al. [83] designed a G-quadruplex aptamer-based fluorescent intercalator displacement
527   assay for kanamycin detection with thiazole orange as fluorescence probe. Kanamycin specific
528   aptamers are able to form stable parallel G-quadruplex DNA (G-DNA) from Guanosin-rich
529   sequences, built around tetrads of hydrogen-bonded guanine bases and stabilized by stacked tetrads
530   in monovalent cation-containing solution. The formation was obtained by nondenaturing
531   polyacrylamide gel electrophoresis (PAGE) and CD. Upon binding to G-DNA, thiazole orange
532   became strongly fluorescent. Addition of kanamycin indicates the displacement of thiazole orange
533   from G-DNA, resulting in a fluorescence signal, inversely related to kanamycin concentration.

534   Li et al. [84] developed a FRET aptasensor for kanamycin detection, using UCNPs as energy
535   donor and graphene as energy acceptor. The kanamycin specific aptamer was covalently conjugated
536   to hexanedioic acid modified UCNPs. In the absence of kanamycin, the aptamers are adsorbed onto
537   graphene surface. The UCNPs and graphene are in close proximity, resulting in a quenched UCNPs
538   fluorescence emission. Upon kanamycin addition, the aptamers bind preferably to kanamycin and
539   desorb from graphene. In consequence of the increased distance between UCNPs and graphene the
540   fluorescence emission is restored in dependence of the kanamycin concentration.

541   Moreover, Wang et al. [85] developed an aptamer-based fluorometric aptasensor for
542   kanamycin detection, based on novel FRET pair consisting of fluorescent carbon particles as energy
543   donor and layered MoS_2 as energy acceptor. The amino-functionalized aptamers were immobilized
544   on carbon particles, then the modified carbon particles assembled onto MoS_2 nanosheets surface via
545   van-der-Waals forces. Thus, due to energy transition the fluorescence of the carbon particles was
546   quenched. Upon kanamycin addition, aptamer-kanamycin complexes were formed and the carbon
547   particles separated from the MoS_2 nanosheets surface, leading to a strong fluorescence recovery. The
548   quenching ability of layered MoS_2 was tested and compared to that of GO and AuNPs and showed
549   comparable or even better values. The negligible fluorescence recovery of other aminoglycoside
550   antibiotics (e.g. streptomycin) and other veterinary antibiotics (e.g. sulfadimethoxine) demonstrated
551   the high specificity towards kanamycin.

552   Recently Ha et al. [86] selected kanamycin specific aptamers by the SELEX process and analyzed
553   the truncated variants for the optimal minimal sequence required for target binding. The aptamer
554   with highest binding specificity towards kanamycin and short sequence was selected for the further
555   study. The aptamer was labelled with FAM and adsorbed onto the surface of reduced graphene oxide
556   (rGO). Hence its fluorescence was quenched via FRET between the quencher rGO and the

557 fluorophore FAM. Kanamycin was immobilized on *N*-oxysuccinimide ester-coated plates. Upon
558 binding of kanamycin, the aptamer changed its conformation and desorbed from rGOs surface. The
559 fluorescence was no longer quenched and the signal increased.

560   Liao et al. [87] developed a fluorometric aptasensor for kanamycin detection, based on carbon
561 nanotubes (CNTs). Induced by π stacking of DNA bases on CNTs, dye-labelled sDNAs can be
562 noncovalent adsorbed on CNTs, resulting in the quenching of fluorescence. But CNTs were not able
563 to quench the fluorescence of dsDNAs formed through hybridization of aptamers and their FAM-
564 labelled cDNAs. The addition of kanamycin lead to the formation of aptamer-target complexes, the
565 dehybridization of dsDNAs, the adsorbtion of FAM-labelled cDNAs on CNTs and finally in a
566 quenched fluorescence.

567   A fluorescent evanescent wave aptasensor for continuous and online kanamycin detection was
568 presented by Tang et al. [88]. The basis for the detection of fluorescence signals was an optical fiber.
569 Guanine has been recognized as one of the efficient electron donors in photoinduced electron transfer
570 via formation of π-stacked complexes or transient collosion. The biunding of a target caused the
571 formation of a more complex structure and therefroe more efficient fluorescence quenching.
572 Guanosin-rich oligonucleotides tends to form multiple strand complexes (M-shapes) such a G-
573 quadruplexes. M-shapes of the aptamer (apt I, Table 1) can also be formed on the fiber surface by
574 interaction between the 5`Cy3-labbelled aptamer (apt II, Table 1) and a specific anchor (anchor apt,
575 (Table 1). Upon binding to kanamycin, the M-shape (apt I, Table 1) partially dissociated into
576 intramolecular hairpin structure and partially formed M-shapes (apt II, Table 1) with the anchor
577 aptamer (anchor apt, Table 1) immobilized on the optical fiber of the aptasensor. The amount of M-
578 shape aptamer (apt II, Table 1) on the fiber is indirectly proportional to the concentration of
579 kanamycin. Two different cDNAs (cDNA I and cDNA II, Table 1) of the anchor aptamer were
580 introduced into the system to investigate the affinity of the 5`Cy3-labelled aptamer towards the
581 anchor probe. They showed, that the affinity of 5`Cy3-labbeled aptamer was higher than that of
582 cDNA I but lower than that of cDNA II. Furthermore, the fluorescence quenching due to the
583 photoinduced electron transfer was determined, using 5`Cy5-labelled aptamer (apt III, Table 1) and
584 3′Cy5-labbeled aptamer (apt IV, Table 1). Addition of aminoglycosidic antibiotics, such as
585 kanamycin B and gentamicin, and other structurally different antibiotics, such as tetracycline and
586 sulfadimethoxine showed, that all the amino glycosidic antibiotics elicited a sensor response.
587 Therefore the proposed aptasensor is a group-specific one.

588   Chemiluminescence based aptasensor in comparison to other optical aptasensor like
589 fluorometric and colorimetric aptasensors has the lowest sensitivity [81]. However, there is a few
590 reports in aptamer based luminescence method for the detection of kanamycin [89].

591   Leung et al. [89] realized a oligonucleotide-based luminescence method for the detection of
592 kanamycin. A platinum (II) complex was used as signal transducer. In the absence of kanamycin, the
593 aptamer is present in random-coiled structure, whose interaction with the complex is only weak,
594 resulting in a low emission signal. Upon kanamycin addition, the aptamer changes its conformation
595 into a stem-loop structure, which interacts strongly with the complex, resulting in a strong
596 luminescence response.

597   Zhao et al. [90] developed a label-free electrochemiluminescence aptasensor for kanamycin
598 detection based on a novel "on-off-on" switch system towards $S_2O_8^{2-}$-O_2. A conventional three-
599 electrode cell, as well as $[Fe(CN)_6]^{3-/4-}$ as redox probe was used for electrochemical measurements.
600 The GCE was covered with prepared AuNP functionalized nano-C_{60} (inner layer). Poly-L-histidine
601 hydrochloride was covalently bound onto the modified electrode and formed a second inter layer,
602 which served as a novel co-reactant of the $S_2O_8^{2-}$ system. The third and outer layer was finally formed
603 by colloidal AuNPs. Capture probes were added. The capture probe contained the sequences of the
604 kanamycin specific aptamer and of the assistant probe, a guanine-rich nucleic acid. In the presence
605 of hemin, hemin-G-quadruplex DNAzymes (HQDs) were formed. In this "switch-off"state, the
606 electrochemiluminescence (ECL) is quenched by the HQDs, which catalyses the reduction of
607 dissolved O_2 of the $S_2O_8^{2-}$-O_2 system. In"switch-on" state upon formation of the kanamycin-aptamer
608 complex, the quencher HQD is released from the sensing interface, resulting in an increasing ECL.

Based on the developed chemiluminescence aptasensor for chloramphenicol detection by Hao et al. [91], the aptasensor was further developed by Hao et al. [92] for the simultaneous detection of kanamycin, oxytetracycline, and tetracycline. AuNPs were functionalized with *N*-(4-aminobutyl)-*N*-ethylisoluminol (ABEI) and cDNA to design a universal label, which showed excellent chemiluminescent properties. ABEI can be oxidized by H_2O_2 to the excited ABEI form, which decays to the ground state with simultaneous chemiluminescence emission. The modified AuNPs were added and bound covalently with the suitable aptamers. In the presence of the target the aptamers tend to bind, resulting in a dissociation of cDNA due to the stronger interaction between aptamer and target and in a decreasing chemiluminescence intensity. Addition of H_2O_2 and the chemiluminescence enhancer and stabilizer *p*-iodophenol leads to a steady-state chemiluminescence, which was negatively correlated with the logarithmic concentration of the target.

Electrochemical aptasensors compared to optical sensors are label free, more simple, practical and sensitive and have attained a great deal of attention in the detection of antibiotics [68].

Li et al. [93] developed a photoelectrochemical aptasensor for the detection of kanamycin. A Flour-doped SnO_2 electrode was gradually modified with graphene, graphite-like carbon nitride (a metal-free photoactive material), and the kanamycin specific aptamer. In the absence of kanamycin, the generated photocurrent was low. When kanamycin was added, it was trapped by the aptamers on the surface of the electrode. The captured molecules were oxidized by photogenerated holes. The recombination of photogenerated holes and electrons was inhibited, resulting in an amplified photocurrent.

In the work of Xin et al. [94] a photoelectrochemical aptasensor for kanamycin detection is presented. The core sensing unit of the photoelectrode consisted of AuNPs-functionalized self-doped TiO_2 nanotube arrays. Kanamycin specific aptamers were integrated into the photoelectrode by binding to the AuNPs. It was shown that kanamycin bound to the secondary structure of the aptamer. The SPR of the AuNPs and inter-bands from self-doped Ti^{3+} centre had synergistic effects and boosted the performance under visible light irradiation.

Lv et al. [95] developed a facile photoelectrochemical aptasensor for the detection of kanamycin, based on polypyrrole, CeO_2 and AuNPs. The semiconductor CeO_2, used as photoactive material, was deposited onto the surface of an indium tin oxide (ITO) working electrode, which enhances the photoelectric conversion efficiency. Thiolated kanamycin specific aptamers were immobilized on AuNPs via Au-SH interaction and subsequently the modified working electrode was functionalized with the prepared AuNPs. The addition of kanamycin led to a significant increase of the photocurrent, because recombination of photogenerated holes and electrons.

Zhou et al. [96] introduced a label-free impedimetric electrochemical aptasensor for kanamycin detection, in which the aptamer blocks the electron transfer between the redox probe $[Fe(CN)_6]^{3-/4}$ and the electrode. The addition of kanamycin leads to a conformational change (compact stem-loop structure) of the aptamer upon target-binding. The coverage of the aptamer on the electrode surface amplifies and further blocks the electron transfer efficiency.

An impedimetric disposable and portable aptasensor for the detection of kanamycin was designed by Sharma et al. [97]. Amino-functionalized kanamycin specific aptamers were immobilized onto the surface of the working SPCE via NH_2-COOH interaction. The interaction between the aptamers and kanamycin caused an inhibition in the Faradeic response and an increase in the electron transfer resistance.

Zhu et al. [98] developed a label-free biosensor for kanamycin detection based on aptamer-functionalized conducting polymer-Au nanocomposite. The disposable screen-printed electrode (SPE) was modified with a nanocomposite consisting of self-assembled 2,5-di-(2-thienyl)-1H-pyrrole-1-(p-benzoic acid) (DPB) on AuNPs by electro-polymerization. Kanamycin specific aptamers were covalently bound to the poly-DPB-AuNP nanocomposite after activation carboxylic acid groups by incubation in 1-ethyl-3-(3-dimethylamino-propyl) carbodiimide and *N*-hydroxysuccinimide ester solution. After addition of kanamycin an aptamer-kanamycin complex is formed, leading to current increase.

Sun et al. [99] introduced an electrochemical sensor for kanamycin detection based on synergistic contributions of chitosan-AuNPs (C-AuNPs), graphene-AuNPs (G-AuNPs), and multi-walled carbon

662   nanotubes (MWCNTs)-cobalt phthalocyanine composites (MWCNTs-CoPc). The nanocomposites
663   improve electron relay during electron transfer processes and the response speed of the aptasensor.
664   The electrode was sequentially modified by dripping C-AuNPs, G-AuNPs, and MWCNTs-CoPc onto
665   its surface. Song et al. [69] carried out mutation experiments, which revealed that the loop region of
666   the aptamer (GG sequence) is responsible for the binding to kanamycin. Based on this, Sun and
667   colleges suspected that two aptamers with equal sequence but different functionalization (amino and
668   biotin, Table 1) can combine different parts of one kanamycin molecule and form a double-aptamer
669   sandwich-complex, which was confirmed by experimental data. The modified working electrode was
670   further modified with the amino-aptamer and incubated with BSA to block possible remaining active
671   sites. The biotin-aptamer was labelled with streptavidin-horseradish peroxidase (HRP) and
672   subsequently conjugated to kanamycin. The prepared kanamycin-aptamer complex was added to the
673   modified electrode. The current response was measured in PBS containing hydroquinone and H_2O_2.
674   Upon binding to kanamycin, the kanamycin-aptamer complex leads to an increasing reduction
675   current of hydroquinone in the presence of H_2O_2.

676   An electrochemical aptasensor for kanamycin detection, based on thionine, graphene
677   polyaniline composite film (GPCF) and AuNPs, was developed by Li et al. [100]. GPCF enhance the
678   electron transfer between working electrode and the redox probe $[Fe(CN)_6]^{3-/4}$. Thionine shows
679   electrocatalytic activity towards small molecular compounds and AuNPs act as transducer between
680   aptamer and GPCF. An aptamer modified with different groups (Table 1) was used to recognize
681   kanamycin by forming a sandwich structure. The Au electrode was sequentially modified with
682   thionine, GPCF, AuNPs, and the 5′-amino-labelled aptamer I (Table 1) and was afterwards incubated
683   with BSA to avoid non-specific adsorption. The 5′-biotin-labelled aptamer II (Table 1) was bound to
684   streptavidin-HRP (S-HRP) and subsequently to kanamycin. Upon binding of the functionalized
685   kanamycin onto the modified electrode, the reduction current of hydroquinone increases in presence
686   of H_2O_2. Hydroquinone acts as mediator for electron transfer between the electrode surface and HP.
687   This is correlated to the amount of S-HRP and thus to the concentration of kanamycin.

688   Another sandwich-type electrochemical aptasensor for the detection of kanamycin was
689   developed by Xu et al. [101]. Graphene polyaniline and polyamidoamine dendrimer functionalized
690   AuNPs were assembled onto the working electrodes, which improved the charge-transport property
691   and loading capacity of the biomolecule. A kanamycin antibody was added and bound to the
692   modified AuNPs. Additionally, BSA and poly A_{10} oligonucleotides were self-assembled onto the
693   electrode surface to block active sites. In the presence of kanamycin, this was first captured by the
694   antibody. In a further step the biotinylated aptamer (present in solution) conjugates to kanamycin
695   and comes in close proximity to the electrode surface. Streptavidin-labelled HRP was introduced,
696   after the sandwich-type target identification and bound to the electrode surface, resulting in a strong
697   redox current signal due to the reduction reaction of H_2O_2 catalyzed by HRP.

698   In the work of Guo et al. [102] an electrochemical aptasensor for kanamycin detection is
699   presented. MWCNTs were prepared with ionic liquid (IL) of 1-hexyl-3-methylimidazolium
700   hexafluorophosphate, which could be used as an effective load matrix and showed synergic effects
701   regarding current response. Nanoporous platinum titanium alloy ($Pt_{10}Ti_{10}Al_{80}$) acted as
702   immobilization platform for the kanamycin specific aptamers. The working electrode was first
703   modified with MWCNTs-IL, second with $Pt_{10}Ti_{10}Al_{80}$ and third with the aptamers. Possible remaining
704   active sites of the $Pt_{10}Ti_{10}Al_{80}$ were blocked by incubating with BSA. Upon binding of kanamycin, the
705   aptamers switch from their random coiled to rigid folded structure, resulting in an increase of the
706   current intensity.

707   Qin et al. developed two different electrochemical aptasensors for kanamycin detection. One
708   based on multiwalled carbon nanotubes and graphene nanocomposites [103] and the other one on
709   hierarchical nanoporous PtCu and graphene nanocomposites [104]. The GCE was modified with
710   MWCNTs-1-butyl-3-methylimidazolium, amino-functionalized graphene, and the kanamycin
711   specific aptamer [103], or thionine functionalized graphene, H- nanoporous PtCu alloy, and the
712   aptamer [104], respectively. The formation of the kanamycin-aptamer complex impedes the
713   interfacial electron transfer, which results in a decrease of the measurable current.

Chen et al. [105] designed an electrochemical aptasensor for simultaneous detection of kanamycin and oxytetracycline based on metal ions doped nanoscale metal organic frameworks (MOFs) as signal tracers and Exo assisted targets recycling amplification. The two signal tags were synthesized by conjugating amine-functionalized nanoscale MOFs to the specific aptamers and to cadmium or lead for the detection of kanamycin and oxytetracycline, respectively. Superparamagnetic spherical polymer particles with a uniform size and surface, so called Dynabeads, were prepared with anti-ssDNA antibodies, to which the signal tracers could bind subsequently. In the present of the target the signal tracers are released from the dynabeads and the available aptamer binds to the respective target. The present enzyme RecJ$_F$ Exo decomposes the aptamer. RecJ$_f$ is a single-stranded DNA specific Exo that catalyzes the removal of deoxy-nucleotide monophosphates from DNA in the 5' to 3' direction. RecJf is a recombinant fusion protein of RecJ and maltose binding protein (MBP). It has the same enzymatic properties as wild-type RecJ. Fusion to MBP enhances RecJf solubility.   Releasing the target and the signal tracers, they generate remarkable enhanced electrochemical responses.

Song et al. [106] introduced an electrochemical aptasensor for the detection of kanamycin in which HRP acts as biocatalyst for signal amplification. AuNPs were modified with cDNA via Au-thiol bonds. Subsequently, HRP-AuNP-cDNA conjugates were prepared by the interactions between the positively charged amino groups of HRP and the negatively charged AuNPs. The kanamycin specific aptamers were assembled onto the Au working electrode by Au-thiol interactions. The functionalized electrode was immersed in a solution containing the HRP-AuNP-cDNA conjugates, hydroquinone (HQ), and H$_2$O$_2$. A hybridization reaction between cDNAs and aptamers took place. HRP catalyzes the oxidation of HQ to benzoquinone (BQ) and the simultaneous reduction of H$_2$O$_2$ to H$_2$O, which generates a voltammetric peak current signal. Upon addition of kanamycin, the cDNAs were displaced by the target and the HRP-AuNP-cDNA conjugates detached from the electrode surface resulting in a decrease of the current response.

In the studies of Wang et al. [107] two electrochemical aptasensors for kanamycin detection, based on an Exo III-assisted autocatalytic DNA biosensing platform, are presented. In the first work[107], the kanamycin specific aptamer and an universal primer sequence formed together the arched probe. When this was challenged with kanamycin, the recognition between aptamer and kanamycin leads to the release of the primer. The primer hybridized with a programmed hairpin probe (HP1), which functioned as template for Exo III. Mononucleotides were stepwise removed by Exo III, resulting in a release of primer and trigger. The released primer could bind another HP1 and triggered a new cleavage process and autonomous formation of free trigger, described as cycle 1. The trigger could act as secondary target, which replaced an assistant probe (named helper) from the MB-labelled hairpin probe (HP2). HP2 undergoes a conformational change and comes in close proximity to the electrode surface, which allows an efficient electron transfer. The Exo III cleavage process is triggered by the hybridization of trigger and helper, whereupon the trigger is recycled, named as cycle 2. In the absense of the target molecule, a negligible electrochemical response is obtained, known as signal-off behaviour. In the other work [108] the multiple recycling amplification is divided into polymerase-catalyzed taregt recycling amplification and Exo III-assisted secondary target recycling amplification. Here, HP1 contains the kanamycin aptamer, a specific recognition sequence for nicking endonuclease Nt.Alwl (enzyme that is able to cut the sugar-phosphate backbone of a nucleic acid), and a nucleic acid segment complementray to the 5´-end of the aptamer. By kanamycin binding to the aptamer, the triggered conformational change leads to an opening of the HP1 stem and HP1 hybridizes with the primer. The template part in HP1 is replicated in the presence of the polymerase and dNTPs. Kanamycin is displaced and can initiate a new cycle. A new HP1-template of dsDNA is synthesized, which contains inter alia the recognition sequence of Nt.Alwl, which cleaves one strand of the dsDNA. A new replication site for polymerase is generated and a short ssDNA fragment is released, which can hybridize with either another HP1 or the assistant probe (helper). The ssDNA can replace the helper from the 5´-MB labelled HP2, resulting in a conformational change of HP2, confining MB close to the elctrode surface and triggers an efficient electron transfer. Meanwhile, the hybridization between ssDNA and helper triggers the Exo III cleavage process. In the absense of kanamycin, HP1 coexists with the primer and the nicking

767 sequence remains as ssDNA, which is unsuitable for Nt.AlwI and no electrochemical signal is
768 generated. The Au electrode was modified with the HP2 and the helper.

769   Song et al. [109] developed an electrochemical aptasensor for the detection of kanamycin, using
770 cDNA and glucose oxidase modified AuNPs for signal amplification. Glucose oxidase (GlO)
771 catalyzes the reaction between glucose and dissolved oxygen to produce gluconic acid and H_2O_2.
772 AuNPs were functionalized with cDNA and subsequently with GlO. Furthermore, pure AuNPs were
773 growed in situ on the surface of molybdenum disulfide (MoS_2) nanosheets and then prepared with
774 hemin (H), resulting in a MoS_2-Au-H composite. In MoS_2-Au-H composites, MoS_2 nanosheets and
775 hemin showed high synergetic catalytic activity to the electro reduction of H_2O_2. The working
776 electrode was modified with the MoS_2-Au-H composite, the thiolated aptamer via Au-S bond, and
777 finally with MCH to prevent non-specific adsorption. The functionalized AuNPs bound to the cDNA
778 to form dsDNA. In the presence of kanamycin, the aptamer binds because of the stronger affinity of
779 the aptamer towards kanamycin. As a result, the cDNA-Au-GlO conjugate drops from the sensor and
780 leads to a decreasing current response measured. The amount of kanamycin captured on the
781 electrode surface is directly related to the current signal.

782   Huang et al. [110] designed an electrochemical aptasensor for multiplex antibiotics detection of
783 kanamycin and chloramphenicol. Detailed information is mentioned in the appropriated chapter
784 2.4.1 of chloramphenicol.

785   Nikolaus & Strehlitz [111] selected DNA-aptamers specific for binding of kanamycin A by
786 capture SELEX according to the work of Stoltenburg's team [112] . The derived aptamers also showed
787 binding to related aminoglycoside antibiotics. High specific aptamers for kanamycin A and group
788 specific aptamers for aminoglycoside antibiotics were differentiated and the region responsible for
789 aptamer binding (epitope-like region) could be estimated. Affinity and specificity of the kanamycin A
790 specific aptamers and of some truncated variants were performed using SPR and further tested in
791 bead based or microplate based assay by fluorescence detection of the 5′-FAM labelled aptamers. The
792 aptamers were immobilized on streptavidin coated magnetic beads modified with biotinylated
793 capture oligonucleotides or on streptavidin coated microplates modified with biotinylated capture
794 oligonucleotides, respectively. Upon addition of kanamycin A, the aptamers undergo a
795 conformational chance and leave the duplex, resulting in a reduced fluorescence signal.

796   In the study of Chen et al. [70] a fluorometric aptasensor for the detection of kanamycin A, based
797 on AuNPs, is presented. The AuNPs acts simultaneously as nanocarrier for the kanamycin specific
798 aptamers and as fluorescence quenchers. In the absence of kanamycin, the dye-labelled aptamers
799 could adsorb onto the AuNPs surface and thereby quenching the fluorescence signal. The addition
800 of kanamycin leads to a release of the aptamer from the AuNPs and to an increased measurable
801 fluorescence signal.

802   Ma et al. [113] developed a fluorescence displacement aptasensor for the detection of
803 kanamycin A, based on G-quadruplex. It is known, that the kanamycin A specific aptamer is able to
804 form G-quadruplex by the association of four separate aptamer strands. The dye, in this case
805 thioflavin T was chosen, can selectively bind to the G-quadruplex and thus causing a strong
806 fluorescence signal. In the presence of kanamycin A, thioflavin T is displaced, aptamer-target-
807 complexes are formed and the fluorescence signal is turned off. CD experiments were carried out to
808 invetsigate the conformation of Aptamer-target interactions. The scientists systematically mutated
809 guanosines to adenosines (mut I-mut IV, Table 1), to verify if the G-quadruplex started to collapse,
810 because the specific structure is mainly caused by the non-covalent bonding among guanine bases.

811   Dapra et al. [55] designed an impedimetric electrochemical aptasensor for the simultaneous
812 detection of kanamycin A and ampicillin. Detailed information is mentioned in the appropriate
813 chapter 2.1.1 of ampicillin.

814   Liu et al. [114] developed an impedimetric electrochemical aptamer-based biosensor for
815 kanamycin A detection, based on signaling probe displacement (SPD). The two types of probe,
816 thiolated aptamer capture probe (ACP) and its short complementary capture probe (CCP) were
817 immobilized onto the Au electrode by Au-S interactions. DNA duplexes were formed upon
818 hybridization of ferrocene tagged short complementary redox signaling probe to ACP and ferrocene
819 tagged aptamer redox signaling probe to CCP, resulting in a strong electrochemical signal. In the

820 presence of kanamycin A, a displacement of the signaling probe was induced, leading to a decrease
821 in current, which was quantitatively related to the concentration of kanamycin. For a direct
822 comparison, Liu and colleges fabricated an EIS aptasensor under the same conditions. The results
823 showed that the SPD aptasensor possessed better sensitivity, specificity, and tolerance to the
824 interference from non-specific adsorption. Amazing was the observation, that the aptasensor not only
825 showed high specificity to kanamycin A in the presence of antibiotics, such as ampicillin and
826 tetracycline, but also in the presence of the structural quite similar kanamycin B.

827 By the way, Robati et al. [81] authored a review about aptasensors for quantitative detection of
828 kanamycin and kanamycin A.

829 In summary, around half of all developed aptamer-based biosensors for the detection of
830 kanamycin and kanamycin A are based on electrochemical sensor principles (either impedimetric or
831 amperometric). Moreover, a comparatively large number of fluorometric aptasensors have been
832 developed. The most important data of the discussed aptasensors are summarized in Table 1. The
833 lowest LOD was reached with an amperometric aptasensor developed by Wang's team [108].

834 ### 2.2.3   Neomycin

835 The spectrum of activity of neomycin (Figure 3(c)) is mainly gram-negative bacteria including
836 *Salmonella* and *Shigella* [4]. Since it is hardly absorbed after oral administration, it is particularly
837 suitable for combating infections of the digestive tract [4]. It is also used for superficial skin and
838 mucous membrane infections [4]. A disadvantage is the high ear and kidney toxicity [4]. In general,
839 neomycin is an oligosaccharide mixture containing the three main components A, B, and C.
840 Commercially available neomycin consist of about 90 % neomycin B and 10 % neomycin A and B [4].

841 In 1995 Wallis et al. [115] selected RNA-aptamers for neomycin B recognition by *in vitro* selection
842 using SELEX. Most of the RNA molecules shared a region of nucleotide sequence homology, which
843 fold into a hairpin-structure. The stem-loop region was identified as neomycin B binding site. An
844 affinity study was carried out to determine the strongest binding aptamer, which was used in further
845 studies [116].

846 Ling et al. [116] present an fluorometric RNA-aptasensor for neomycin B detection based on
847 AuNPs. The RNA-aptamer was split between A14 and G15 (Table 1), because shorter RNA chains
848 show fewer interactions with nucleases, which could increase aptamers` stability in environment. A
849 high ribonuclease resistance of the unmodified RNA-aptamer could be established by incubation of
850 the aptamer with a ribonuclease (RNase I) and subsequent fluorescence measurements. The authors
851 exhibited that the splitting has no influence on its binding properties, because the splitting site on the
852 aptamer sequence is outside of the binding pocket. One fragment was conjugated to the AuNPs via
853 a polyA tail, the other one was labelled with FAM. In the presence of neomycin B the two individual
854 fragments self-assembled. The binding of neomycin B leads to a conformational change of the
855 fragments and they came into close proximity. Thus, results in measurable fluorescence quenching.

856 De-los-Santos-Alvarez et al. [117] developed an impedimetric electrochemical RNA-aptasensor
857 for neomycin B detection based on a competitive displacement assay. The aptamer was fully 2`-O-
858 methylated to gain endonuclease resistance, which avoids degradation during application and allows
859 measurements in real samples. Via carbodiimide chemistry the Au electrode was modified by a self-
860 assembled monolayer (SAM) of mercaptopropionic acid (MPA). Subsequent neomycin B was
861 immobilized onto the surface. The addition of the neomycin B specific aptamer leads to covalent
862 aptamer-target bindings. The incubation of the reaction solution with further neomycin B leads to
863 displacement of the aptamer from the surface bound neomycin B, resulting in a detectable signal,
864 which could be transduced by Faradaic impedance spectroscopy (FIS). Furthermore, it was shown,
865 that the aptasensor is capable of discriminating neomycin B from the structural very similar
866 paromomycin as well as from kanamycin and streptomycin.

867 In 2009 de-los-Santos-Alvarez et al. [118] studied how the modification of the RNA- aptamer
868 influences the affinity of the interaction between the aptamer and neomycin B. In general, the fully
869 2`-O-methylization of the RNA-aptamer should prevent the degradation by endonuclease. The
870 scientists were able to demonstrate, that this modification did not significantly alter the aptamer

871 affinity towards neomycin B. The procedure of electrochemical measurement was basically adapted
872 from their previously reported study [117]. Besides FIS, SPR was additionally used as transduction
873 technique because it is known as better suited method for the characterization of affinity events.
874   Although these modifications prevent digestion of RNA sequences by nucleases, they may result
875 in structural changes to the RNA sequences, which affect the binding affinity. In addition, the above
876 strategies can greatly increase the cost of potential applications. But De-los-Santos-Alvarez et al. [118]
877 could show that this must not be the case and Ling et al. [116] developed a stable biosensor based on
878 unmodified RNA-aptamer. The comparison of the obtained LODs (Table 1) showed that SPR [118] is
879 more sensitive than the optical [116] and the electrochemical [117] method.

880 ### 2.2.4 Tobramycin

881   Tobramycin (Figure 3(d)) is a semi-synthetic aminoglycoside antibiotic [2]. Its spectrum of
882 activity comprises numerous gram-negative pathogens, such as *Escherichia coli*, *Klebsiella*, *Proteu*s,
883 *Pseudomonas*, *Salmonell*a, and *Shigella,* as well as gram-positive *Staphylococci* and *Enterococci* [4]. It is
884 therapeutically effective for infections of the respiratory and the urogenital tract, the skin, bones, the
885 central nervous system (meningitis), and septicemia [4].
886   In 1995 Wang and Rando [119] selected RNA molecules that can specifically bind to the
887 aminoglycoside antibiotic tobramycin by *in vitro* selection using SELEX and investigated the
888 recognition process of aptamer-target binding. The RNAs that bind tobramycin with high affinity
889 contained consensus binding regions that may be confined to predicted stem-loop structures. The
890 binding behaviour was analyzed with a pyrene-butyramide-labelled fluorescent derivative of
891 tobramycin. Upon addition of the selected aptamer, the fluorescence emission intensity was
892 quenched. The selected aptamer found use in later studies [68].
893   Spiga et al. [120] introduced a DNA-based capture-SELEX coupled with in-stream direct-
894 specificity monitoring via SPR and high throughput sequencing for the selection of DNA aptamers
895 for small drugs, such as tobramyin. The aptamers were evaluated for their affinity to tobramycin via
896 direct immobilization onto a SPR chip, which was used in further studies [121].
897   Han et al. [122] developed a magnetic bead-based SELEX to identify thirtyseven ssDNA
898 aptamers specific for tobramycin using a fluorescent method based on the reported principle by Ma's
899 team [123].
900   A colorimetric aptasensor for the determination of tobramycin in milk and chicken eggs was
901 developed by Ma et al. [123]. The random coil ssDNA aptamers adsorbed on the surface of AuNPs
902 via van der Waals forces, hydrophobic interaction and attractive forces between N and O of the bases
903 and the AuNPs. At the proper salt concentration, the AuNPs kept distributed in solution. When
904 tobramycin was added, the aptamers changed from coil structure to folded rigid structure and
905 formed an aptamer-target complex. The complex detached from the AuNPs and the following
906 aggregation of the AuNPs led to a color change from red to purple blue.
907   In order to detect drug concentration in patient samples, which are much more complex matrices
908 than buffers, Cappi et al. [121] developed a portable, palm-sized transmission-localized SPR (TL-SPR)
909 system for tobramycin detection. Tobramycin specific aptamer (Table 1) was bound onto the surface
910 of Au nanoislands (AuNIs). Aptamer-functionalized Au-NIs were deposited on a glass slide covered
911 with fluorine-doped tin oxide. A white light LED was used as excitation source and a complementary
912 metal oxide semiconductor (CMOS) as light detector. The sensitivity of the CMOS image sensor was
913 matched to the localized plasmon resonance exhibited by the Au-NIs. Addition of tobramycin leads
914 to an increase of the local refractive index in the proximity of the Au-NIs, resulting in a shift of the
915 plasmon resonance wavelength and a redshift of the plasmon peak. For the first time it was shown,
916 that hue can be reliable used to measure and display real-time surface binding of small molecules
917 (here tobramycin) in SPR.
918   As mentioned, Rowe et al. [68] developed an electrochemical aptasensor for multiplex antibiotics
919 detection of the aminoglycoside antibiotics gentamicin, kanamycin, and tobramycin in blood
920 samples.

921   Gonzalez-Fernandez et al. [124] described an label-free impedimetric electrochemical aptasensor
922   for tobramycin detection in human serum. Two modified RNA-aptamers (Table 1), a partially and a
923   fully O-methylated one, were evaluated and compared in terms of affinity and analytical
924   characteristics. Beside the higher endonuclease resistance, the fully O-methylated aptamer had a
925   lower dissociation constant as well as a lower LOD than partially methylated aptamer (Table 1),
926   which was used in further experiments. The quite similar dose-response curves of tobramycin and
927   neomycin B indicated a high cross-reactivity. The authors declared that the (unexpected) interference
928   is clinically not relevant, because the antibiotics are rarely used in combined therapies.

929   In another study of Gonzalez-Fernandez et al. [125] an aptamer-based inhibition assay (indirect
930   competitive assay) for electrochemical detection of tobramycin was presented. Tobramycin was
931   immobilized onto the surface of carboxylated magnetic beads (MBs) using carbodiimide chemistry.
932   The tobramycin-modified microparticles (TMBs) were incubated with a fixed concentration of RNA-
933   aptamer and varying concentrations of tobramycin. Subsequently a streptavidin-alkaline
934   phosphatase conjugate (SC) was added, which could bind to the aptamer-TMB conjugate.
935   Furthermore, the electrochemically inactive substrate 1-naphthyl phosphate was added and covered
936   all electrodes. The SC catalyzes the hydrolysis of 1-naphthyl phosphate to α-naphthol. By addition of
937   tobramycin to the sample, the amount of aptamer available for surface interaction decreases, thus
938   leading to a smaller amount of enzymatic conjugate linked to the TMPs and in consequence to a
939   decreasing current.

940   The described aptamer-based inhibition assay [125] was further developed [126]. The main
941   principle was the same as mentioned, except that the monovalent labeling systems anti-fluorescein-
942   isothiocyantae-alkaline phosphatase Fab fragment (APhoF) or anti-fluorescein-isothiocyanate-
943   peroxidase Fab fragment (APerF) were used instead of SC to bind the aptamer-TMB conjugate,
944   respectively. APhoF and APerF catalyzed the hydrolysis of 1-naphthyl phosphate to α-naphthol,
945   which was detected using DPV in the case of APhoF and CA in the case of APerF. It could be noted
946   that the use of a monovalent labeling system to introduce an enzyme label significantly improves the
947   LOD and thus the sensitivity of the "signal-off" assay in comparison with the biotin-streptavidin
948   system.

949   Schoukroun-Barnes et al. [127] presented a systematic study of several approaches to develop
950   an electrochemical RNA aptamer-based biosensor for the detcetion of aminoglycoside antibiotics like
951   tobramycin. Electrochemical interrogation parameters and biomolecuar engeneering of the aptamer-
952   sequence were investigated and optimized.

953   In summary, there are just a few aptasensors developed for tobramycin detection and with the
954   exception of one, they are based on electrochemical principles. Almost all electrochemical sensors
955   used RNA aptamer sequences for the specific tobramycin recognition. The loweset LOD and
956   belonging K_D value was determined with the RNA aptamer sequence II (Table 1), mentioned by
957   Schoukroun-Barnes et al. [127]. An even higher affinity towards tobramycin was reached by Cappi
958   et al. [121] by using ssDNA aptamer sequence (Table 1).

959   2.2.5   Streptomycin

960   The discovery of Streptomycin (Figure 3(e)) from *Streptomyces griseus* by Selmon Waksman
961   (1943) allowed for the first time a therapy of the tuberculosis pathogen *Mycobacterium tuberculosis* [2].
962   However, due to the renal and ear-harming properties of streptomycin, other antibiotics (e.g.
963   rifampicin) are usually used today [2]. More frequently, it is used to combat penicillin-resistant
964   strains of *Neisseria gonorrhea* infections and still used for the treatment of tuberculosis [4].

965   The first streptomycin specific DNA-aptamers was screened by Zhou et al. [128] by affinity
966   magnetic beads-based SELEX. Streptomycin was detected by using label-free AuNPs-based
967   colorimetric method.

968   Liu et al. [129] developed an aptamer-based colorimetric sensor for the detection of
969   streptomycin. Different streptomycin specific aptamer sequences were obtained by SELEX. The
970   selected aptamer was used for all further experiments.

971   In the work of Luan et al. [130] a   point of care testing colorimetric aptasensor for streptomycin
972   detection was decribed. The capture probe was represented by SSB labelled on SiO_2 mikroparticles.
973   Thiol-modified streptomycin specific aptamers were immobilized on PowerVision (PV, special
974   dendrimer) doped AuNPs via Au-SH interaction to form the nanotracer. Additionally, the dendrimer
975   PV contained large quantities of HRP, which catalyzed the H_2O_2-TMB system and thus caused a color
976   change. In the presence of the target an Exo I, streptomycin and the nanotracer combined to a
977   complex. Exo I digested the aptamer from the nantracer, so that streptomycin was released again to
978   participate new cycling, more nanotracers were generated and released in the supernatant, which
979   improved the sensitivity. The feasability in real samples was verified by target detection in milk
980   samples and the results were compared to the referenced ELISA.

981   Zhao et al. [131] introduced a colorimetric detection of streptomycin in milk based on
982   peroxidase-mimicking catalytic activity of AuNPs. It is known, that AuNPs can easily oxidize
983   peroxidase substrate ABTS (2,2'-azino-bis(3-ethylbenzothiazoline-6-sulphonic acid)) in the presence
984   of H_2O_2, thus producing the green ABTS radical cation. In the absence of the target, the streptomycin
985   specific aptamer is adsorbed onto AuNPs and restrains its catalytic activity due to shield effect against
986   the substrate. In the presence of the target, an aptamer target complex is formed and the peroxidase
987   like activity oxidizes the substrate.

988   Emrani et al. [132] presented a colorimetric and fluorescence quenching aptasensor for
989   streptomycin detection, based on the specific aptamer and its FAM-labelled complementary strand
990   (cDNA) and aqueous AuNPs. For detection, the aptamer and its cDNA existents as FAM-labelled
991   dsDNA (FAM-dsDNA) in solution together with the AuNPs. In the absence of streptomycin, the
992   FAM-dsDNA is stable, resulting in a salt-induced aggregation of the AuNPs and thus in an obvious
993   color change from red to blue and simultaneously in a strong emission of fluorescence. In the
994   presence of streptomycin, the FAM-dsDNA decomposes. The aptamer binds to streptomycin and the
995   released cDNA adsorbs onto AuNPs surface. So AuNPs are stabilizes against salt-induced
996   aggregation and no color change can be observed. Simultaneously the fluorescence signal of cDNA
997   is quenched by the AuNPs. Comparisons between the pure colorimetric and the pure fluorometric
998   method showed higher sensitivity of the aptasensor by measuring with the fluorometric one,
999   displayed by the determined LODs (Table 1).

1000   In the work of Taghdisi et al. [133] a label-free fluorescent aptasensor for the detection of
1001   streptomycin is designed, based on Exo III, SYBR Au and aptamer complimentary strand. Exo III is
1002   an enzyme which selectively digests the 3´-end in dsDNA. For detection, the specific aptamer is
1003   conjugated to its complementary strand (cDNA). Upon streptomycin addition, the conjugate
1004   decomposes and the aptamer binds to its target. Thus, resulting in a higher protection from Exo III
1005   function. A strong fluorescence signal can be obtained by adding SYBR Au as the fluorescent dye to
1006   the reaction solution.

1007   Wu et al. [134] developed a fluorometric aptasensor for streptomycin detection in homogeneous
1008   media. The fluorescent probe was synthesized by labelling SSB, which specifically bind the aptamer,
1009   on QDs. The fluorescent probes were disperesed in solution and aggregated, which resulted in self-
1010   quenching of the fluorescence. In the presence of streptomycin and Exo I, the aptamer preferentially
1011   bound to its target. Exo I digested the aptamer-target complex, the target released and could
1012   participate in another cycle, which resulted in a strong fluorescence signal.

1013   In 2018 a point of care testing for the detection of streptomycin based on a fluorometric principle
1014   was introduced by Lin et al. [135] using digital image colorimetry for image aquistion and color
1015   readout. The streptomycin specific aptamer can hybridize with its cDNA to form dsDNA.
1016   Subsequently, the cyanine dye SYBR Green I can combine with the dsDNA and then emitte obvious
1017   green fluorescence. When streptomycin is present, the aptamer preferential forms a complex with its
1018   target, SYBR Green I cannot combine and the result is a decreased fluorescence signal. Instead of a
1019   fluorophotometer, a smartphone was construectd as a portable detection device to collect the
1020   fluorescence signals by photographing and read out the RGB values.

1021   Xu et al. [136] deveolped a photoelectrochemical aptasensor for streptomycin detection based
1022   on CdTe QDs single walled carbon nanohorns, synthetisized via one-pot method, which acted as
1023   photoactive species. These could inhibit electron-hole pair recombination, accelerate electron transfer

and improve the photocurrent intensity. A ITO electrode was modified with the photoactive species. The intrinsic hole oxidation reactions between the photoanode and the electrolyte interface was avoided, which resulted in a strong cathodic photocurrent under visible-light excitation. Afterwards amin-functionalized streptomycin specific aptamers were immobilized onto the electrode through interaction between amino and carboxyl groups. Occuring steric effects suppressed the photocurrent signal. The addition of streptomycin led to formation of aptamer-target complexs, so that the photocurrent signal recovered.

Ghanbari & Roushani [137] introduced an impedimetric electrochemical aptasensor for the detection of streptomycin. Thiol graphene QDs were immobilized onto the surface of a GCE, then AuNPs were bound to the modified QDs via Au-SH interaction and finally, thiolated streptomycin specific aptamers were immobilizes onto the AuNPs via Au-SH interaction, which blocked the electron transfer to the electrode surface. Upon addition of streptomycin, aptamer-target complexes were formed, causing an increase of the electrochemical signal.

Another electrochemical aptasensor for streptomycin detection, based on Exo I, arch-shape structure of aptamer-complimentary strand conjugate and screen-printed gold electrodes (SPGEs) electrode, was developed by Danesh et al. [138]. SPGEs were modified with the specific aptamer, the complementary strand of the aptamer (cDNA) and MCH. The arch-shape structure of the aptamer-cDNA conjugate is intact in the absence of streptomycin and the redox probe $[Fe(CN)_6]^{3-/4-}$ has no access to the electrode surface. Therefore, only a weak electrochemical signal can be measured. Upon addition of streptomycin the aptamer leaves the CS and binds to streptomycin. Subsequently, cDNA is degraded by added Exo I, leading to an access of redox probe to the electrode surface. Thus, resulting in a strong electrochemical signal.

As mentioned Xue et al. [39] developed an electrochemical aptamer-based biosensor for multiplex antibiotic detection of streptomycin, chloramphenicol and tetracycline, based on QDs as electrochemical tag. First three cDNA sequences (cDNA I) were designed, which were complementary to the corresponding target specific aptamers (apt), to part of the capture DNAs (cap) and part of cDNA sequences (cDNA II). Cap-DNAs were immobilized onto Au electrode surface by self-assembly. cDNA IIs were conjugated with streptavidin-modified lead sulfide (PbS), cadmium sulfide (CdS) and zinc sulfide (ZnS). When streptomycin, chloramphenicol or tetracycline were present they bound to their specific apt-DNA with high affinity. This resulted in a release of cDNA Is. Liberated cDNA IIs hybridized with their 3′-end with the corresponding cap. Then cDNA IIs hybridized with the 5′- end of corresponding cDNA Is on the electrode surface. Thus, a kind of sandwich complex was formed. Afterwards the surface captured quantum-dot tags were dissolved in HNO_3. Thus, leading to a release of Pb^{2+}, Cd^{2+} and Zn^{2+} which could be detected electrochemically. $[Fe(CN)_6]^{3-/4-}$ acted as redox probe. The different captured electrochemical signals, generated by the different QDs, reflects the type and concentration of the target antibiotic. PbS were used for streptomycin, CdS for chloramphenicol and ZnS for tetracycline. Additionally, the designed aptasensor was evaluated in milk.

Yin et al. [139–141] constructed three quite similar electrochemical aptasensors for the detection of streptomycin based on different modified electrodes. In the first work [139] porous carbon nanorods (PCNRs) were applied as core conductive material and a nanocomposite consisting of MWCNTs, copper oxide (CuO) a p-type semiconductor and AuNPs as electrode modifier. In another study [140] they presented an aptasensor based on AuNPs-functionalized magnetic MWCNTs and nanoporous PtTi alloy ($Pt_{10}Ti_{10}Al_{80}$). In the last work [141] a third electrochemical aptasensor utilizing a PCNRs and graphene-Fe_3O_4-AuNPs modified electrode was developed. Subsequently in each study the streptomycin specific aptamer was bound onto the surface of the modified electrode. Possible remaining active sites of the AuNPs were blocked by incubating with BSA. Upon binding the target the current response decreases. Comparisons of the current responses of the aptasensor to streptomycin and to a mixture of streptomycin and interfering substances (e.g. glucose, ascorbic acid, penicillin, the structurally very similar dihydrostreptomycin) confirmed an excellent specificity of the sensors towards streptomycin.

Summarized, there are only a few papers dealing with aptasensing of streptomycin. According to the data of Table 1, more than half of them are are based on electrochemical measurements. The

1077   up to five orders of magnitude lower LOD than those reached with the other sensors, could be
1078   determined by Luan et al. [130] using a colorimetric assay and was followed by Yin et al. [140] with
1079   an amperometric aptasensor.

1080   *2.3 Anthracyclines*

1081   Anthracyclines inhibit the replication of DNA by intercalation and inhibition of topoisomerases
1082   [142]. They are used clinically for the treatment of tumor, but they can cause heart damage in long-
1083   term medication [142]. The basic structure, which all anthracyclines exhibits, is marked red in Figure
1084   4.

1085
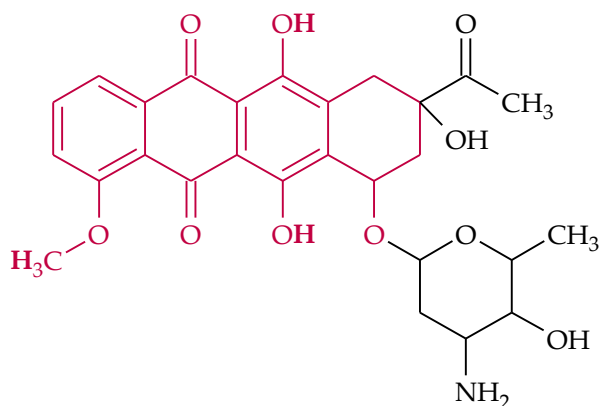
1086   **Figure 4:** Chemical structure of daunomycin. The basic structure of the anthracyclines is marked red.

1087   2.3.1   Daunomycin

1088   Daunomycin (Figure 4), the first discovered anthracycline, produced naturally by *Streptomyces*
1089   *peucetius*, acts as an intercalator whereat the intercalation between DNA bases leads to a local
1090   structural change in the DNA and thus to an inhibition of DNA replication and transcription [143].
1091   Therefore daunomycin has a growth inhibitory effect on gram-positive bacteria and fungi [4].
1092   Moreover an antiviral effect by inhibiting viral DNA replication in the host cell was obtained [4]. 1963
1093   an antileukemic activity was discovered [4]. Nowadays daunomycin is widely used for the treatment
1094   of breast tumors, lymphocytic and myeloid leukemia [144].
1095   In 2008 Wochner et al. [145] selected ssDNA aptamers, specific for daunomycin and tetracycline,
1096   which were used in further studies [146]. The aptamers were isolated from a pool of random
1097   sequences using a semiautomated procedure for magnetic beads. A fluorometric competition assay
1098   for daunomycin detection was established. Streptavidin coated microtiter plates were coupled with
1099   biotinylated daunomycin and subsequently blocked with biotin. Renatured aptamers were incubated
1100   with daunomycin, doxorubicin, tetracycline and chloramphenicol. The mixture was added to the
1101   microtiter plates. Upon aptamer-target binding the fluorescence intensity of OliGreen was increased.
1102   In the work of He et al. [144] a colorimetric aptasensor for daunomycin detection based on
1103   resonance scattering is described. A fluorescence spectrophotometer was used to record the
1104   resonance scattering intensity.
1105   Chandra et al. [146] developed an electrochemical biosensor for daunomycin using a specific
1106   aptamer and phosphatidylserine (PS) as bioreceptors, because maximum current response was
1107   obtained for PS-aptamer modified electrode. The bioreceptors were co-immobilized onto AuNPs
1108   modified and 2,2´:5´,2´´-terthiophene-3´-(p-benzoic acid) (TTBA) functionalized conducting polymer.
1109   Daunomycin was detected in human urine samples to verify the possible use of reported biosensor
1110   in real samples. So, in future the proposed methods could be useful for daunomycin detection in
1111   urine samples of cancer patients undergoing daunomycin chemotherapy.

1112   The features of discussed aptasensors are shown in Table 1. As seen, the electrochemical
1113 aptasensor [146] exhibited a higher sensitivity than the optical one [144]. Only a few studies have
1114 dealt with the aptamer-based daunomycin detection, so there is still potential for research.

2.4 *Chloramphenicol*

1116   Chloramphenicol is an antibiotic class of its own [2]. The chemical structure is shown in Figure 5
1117 [4]. It blocks the peptidyl transferase by binding to the 50S subunits of the 70S ribosomes [2].

1118
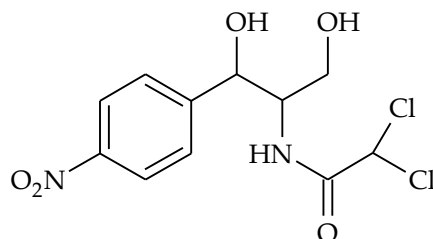
Figure 5. Chemical structure of chloramphenicol.

2.4.1   Chloramphenicol

1121   Chloramphenicol (Figure 5) was isolated in 1950 from *Streptomyces venezuelae*, but nowadays it
1122 is produced synthetically exclusively [2]. It is the first broad-spectrum antibiotic in history [4]. It acts
1123 against gram-positive as well as gram-negative pathogens, as well as against *Actinomycetes*, *Rickettsiae*
1124 and some large viruses [4]. Because of its serious side effects such as leukemia, aplastic anemia and
1125 the grey baby syndrom, it is only a reserve antibiotic used to treat typhoid, shigellosis and rickettsial
1126 infections [4, 91].
1127   In 2011 chloramphenicol specific aptamers were selected and characterized by Mehta et al. [147]
1128 using the SELEX procedure, which was used in further studies for chloramphenicol detection
1129 [109,110].
1130   HRP is one of the most widely used tracer in aptasensors, which catalyzes reactions of enzymes
1131 towards substrates, like TMB, to form colored products. The sensitivity of detection is often reduced
1132 by the amount of enzymes [105]. Therefore, the novel tracer power vision (PV) was investigated [105]
1133 for the utilization in a colorimetric aptasensor for chloramphenicol detection, based on the
1134 amplification of a nano-peroxidase-polymer. PV is composed of an enzyme-linker antibody
1135 conjunction, has a high enzyme-to-antibody ratio. PV and complementary strand (cDNA) were
1136 connected to AuNPs and formed a nano-peroxidase-polymer, acting as signal tag. Magnetic AuNPs
1137 were fabricated by assembling AuNPs onto Fe_3O_4 beads. Subsequently specific aptamers were
1138 immobilized onto AuNPs surfaces. Upon chloramphenicol addition, the signal tags could be
1139 dissociated. The PV on the signal tags catalyzed the oxidation of TMB, causing a color change and
1140 resulting in the change of UV-Vis absorbance. Additionally, comparisons between PV and HRB as
1141 signal labels showed that PV had higher catalytic response towards TMB with H_2O_2 than HRP.
1142   Miao and colleges developed seven different aptasensing strategies for chloramphenicol
1143 detection [148–152, 40, 41]. Two aptasensors based on a colorimetric [148, 149], one of them using an
1144 electrochemiluminescence [150] and four aptasensors based on fluorometric principle [40, 151, 41,
1145 152]. In each study the high specificity of the proposed sensor and possible cross-reactivities with
1146 interfering substances were demonstrated by measurements once in the presence of other antibiotics,
1147 such as kanamycin, tetracycline and oxytetracycline and further of a mixture containing
1148 chloramphenicol and various antibiotics.
1149   The colorimetric aptasensor for chloramphenicol detection introduced by Miao et al. [148] based
1150 on dsDNA antibody labelled enzyme-linked polymer nanotracers for signal amplification. For
1151 creating the capture probe, Fe_3O_4 magnetic NPs were first modified with AuNPs and subsequently
1152 with the dsDNA, consisting of the chloramphenicol specific aptamer and its complementary strand
1153 (cDNA). The enzyme-linked polymer nanotracer was fabricated by co-immobilization of HRP-

labelled AuNPs and dsDNA antibodies as signal tags on EnVision reagent, a kit containing about 100 HRPs and some anti-IgG antibody molecules. In the absence of chloramphenicol, the dsDNA antibodies bind to dsDNA onto the magnetic NPs. If chloramphenicol is present the aptamer preferentially binds to it, leading to a release of ssDNA, which cannot be recognized by the dsDNA antibodies in the nanotracers. After magnetic separation, the signal tag is substituted into supernatant. The supernatant contains numerous HRPs, which catalyse the H_2O_2 mediated oxidation of TMB, resulting in a visible color change, quantified. It was shown, that EV had higher catalytic response to the TMB-H_2O_2 system than HRP labelled nanotracers.

Based on magnetic aptamer-enzyme co-immobilization platinum nanoprobes and econuclease-assited target recycling, Miao's team [149] designed a triple amplification colorimetric aptasensor. The capture probes were formed by labelling dsDNA antibody on core-shell AuNPs modified Fe_3O_4NPs. The double stranded aptamer, composed of the aptamer hybrid and its cDNA, were immobilized on HRP-functionalized PtNPs and represent the nanotracers. A nanotracer-chloramphenicol complex was formed in the presence of the target, which then was released into the supernatant after magnetic separation. The Exo I in the supernatant digested the complex from the 3´-end of the aptamer and chloramphenicol was released and further participated in a new cycle. Pt and HRP in the nanotracers both catalysed the H_2O_2 mediated oxidation of TMB, resulting in color change of the reaction solution.

Abnous et al. [153] introduced a colorimetric sandwich type aptasensor for chloramphenicol detection, based on an indirect competitive enzyme-free method using AuNPs, biotin and streptavidin. First, 96-well plated were covered with chloramphenicol-BSA conjugates and casein. In the absence of additional free chloramphenicol, biotin-modified aptamers bound to the conjugate. Upon addition of streptavidin, the biotin modified aptamer attached on AuNPs, which were previously functionalized with a short 5´-biotinylated and 3´-thiolated DNA sequence. The formed sandwich complex leading to a visible sharp red color in the well, determined by recording the absorbance spectra. If chloramphenicol is present, biotin-modified aptamers bound to free chloramphenicol and subsequently are removed from the well by washing. So, streptavidin could not bound and hence functionalized AuNPs could not, too, resulting in a faint red color and so in a significantly reduction of the absorbance.

An fluorometric aptasensor for chloramphenicol detection, based on energy transfer of CdTE QDs to GO sheets was presented by Alibolandi et al. [154]. The GO sheets were modified with CdTe-QD-functionalized aptamers. Upon addition of the target chloramphenicol and therewith aptamer-target binding, the QD-aptamers released GO. The signal is no longer quenched and a strong excitation of fluorescence could be detected.

In the work of Wu et al. [155] a fluorometric aptasensor for the detection of chloramphenicol, based on UCNPs as signal labels, is presented. Near-infrared (NIR) light is used for UCNPs which results in a series of advantages compared to down-conversion fluorescent materials (e.g. organic fluorescent dyes, inorganic QDs). These include higher photostability, minimum photodamage to living organisms, low toxicity, large Stokes shifts, no induction of autofluorescence and light scattering background and a deeper light-penetration of tissues. Amino-functionalized silica-capped NaYF$_4$:Yb, Er UCNPs were modified with cDNA of the chloramphenicol specific aptamer. Biotinylated aptamers were immobilized onto the surface of avidin-conjugated Fe_3O_4 magnetic NPs, employed to capture and concentrate chloramphenicol. By hybridization of the prepared UCNPs with the magnetic NPs a DNA duplex was formed, wherein the maximum fluorescence signal was generated. The chloramphenicol-induced conformational change of the aptamer leads to a release of the UCNPs-cDNA and simultaneous to a substantially decreased fluorescence intensity.

A further fluorometric aptasensor with Exo-assisted target recycling was designed by Miao et al. [40]. The fluorometric assay based on FRET between CdSe QDs as donors and magnetic SiO$_2$ modified AuNPs as acceptor. The specific aptamer hybrid and its sequence (cDNA) were immobilized onto core-shell SiO$_2$ modified AuNPs and acted as signal probe. The capture probe was composed of antibody-labelled Fe_3O_4 modified AuNPs. By immunoreaction between capture and signal probe the composite probe for chloramphenicol was prepared. When chloramphenicol is added, the aptamer favours to bind it. The antibody cannot recognize ssDNA and therefore the

altered signal probe and the aptamer-target complex are released into the supernatant. Subsequently the supernatant is added into CdSe QD solution. The numerous SiO_2 modified AuNPs of the supernatant efficiently quench the fluorescence response of CdSe QDs by FRET. Exo I, which is also present in the supernatant, digests the aptamer from the 3′-end, resulting in free up of chloramphenicol, which could participate in further reactions with the probes.

Furthermore, Miao' team [152] established a "switch-on" fluorescence aptasensor based on hemin/G-quadruplex and nano-Pt-luminol as signal tracers. Dynabeads have been proved to be efficient fluorescent quencher for luminol by photo-induced electron transfer and were used for the "signal-off" state. Hemin/G-quadruplex and PtNPs are applied to catalyse H_2O_2, thereby producing reactive oxygen species, which promotes the emission intensity of luminol. The aptamer hybrid and its complementary sequence (cDNA) formed dsDNA, which was labelled with Pt-luminol and the hemin/G-quadruplex. The so designed signal probe was connected to anti-IgG-functionalized dynabeads by antigen antibody immune reaction. Upon chloramphenicol addition, it was captured by the aptamer. After magnetic separation, the nanotracer was released into the supernatant, resulting in a strong "switch-on" fluorescence signal, triggered by the catalysis of the H_2O_2-luminol system by PtNPs and the hemin/G-quadruplex.

Moreover, Miao's research group [151] developed a fluorometric aptasensor using 1,1`-dioctadecyl-3,3,3′,3′-tetramethyl-indocarbocyanineperchlorate (DIL)-encapsulating liposome as nanotracer. DIL, a lipophilic fluorescence dye, and SSB were co-immobilized on liposomes to prepare vesicle signal tracers. The chloramphenicol specific aptamer was labelled on amino-functionalized magnetic beads, employed as capture probes. The composite probe for detection was formed by SSB`s specific recognition towards the aptamer on the vesicle probe. Because of the still higher affinity of chloramphenicol towards the aptamer, a competition replacement reaction takes place, whereupon chloramphenicol is captures by the magnetic capture probe and the fluorescent vesicle signal tracer is replaced into the supernatant. The SSB and DIL functionalized liposomes generates fluorescence, which was analysed by fluorescence spectrometry.

Based on the mentioned aptasensor with DIL- encapsulating liposome as nanotracer, Miao et al. [41] introduced a "off-on" fluorometric aptasensor, using vesicle QD-Au colloid composite probes. Here, the vesicle nanotracer as signal probe consisted of liposome-CdSe/ZnS QD complex labelled with SSB. Aptamer-functionalized AuNPs acted as capture probe. The composite probe does not emit fluorescence signals, which represented the "off" state. Upon addition of chloramphenicol, the aptamer bound to it and the aptamer-target complex detaches from the composite probe. The result is a fluorescence signal, which represents the "on" state.

The detection of chloramphenicol residues in animal-sourced food was performed by Duan et al. [156] using fluorescent quantitative real-time polymerase chain reaction (qRT-PCR). The chloramphenicol specific aptamer was first partly hybridized with a biotin modified complementary probe and afterwards immobilized on streptavidin modified magnetic beads via biotin-streptavidin interaction. It was found that the length of the partly complementary probe influenced the binding affinity between aptamer and partly complementary probe. The longer the probe, the higher the binding strength and the more difficult for chloramphenicol to compete for the aptamer. The addition of chloramphenicol leads to the formation of a hairpin-structured aptamer-target complex and its release from the magnetic bead into the supernatant. The amount of enriched aptamer-target complex was dependent on the amount of added chloramphenicol. The fluorescence intensity for quantification of the apamer-target complex and chloramphenicol could be monitored by the addition of SYBR green and detection with a qRT-PCR system.

Wang's team [157] designed a ssDNA binding protein (SSB)-assisted fluorometric aptasensor for the detection of chloramphenicol in a homogenous solution. FRET was obtained between SSB-labelled core-shell QDs and aptamer-labelled AuNPs as donor and acceptor fluorophores, respectively. SSB could specifically bind ssDNA without using other coupling reagents. The prepared QDs and AuNPs were incubated together and hybridized via SSB-aptamer interaction, whereupon the fluorescence was quenched by the AuNPs. Upon addition of chloramphenicol the fluorescence was restored.

1259   In an unfavourable case, electrochemiluminescent aptasensors with "signal on" or "signal off"
1260   strategies can induce false-positive signals due to outside interferences such as environmental
1261   conditions [158]. Therefore, Feng et al. [158] developed a ratiometric electrochemiluminescent
1262   aptasensor for the detection of chloramphenicol, in order to circumvent mentioned problems. The
1263   ratiometric principle based on the ratio of cathode to anode electrochemiluminescent signal (which
1264   can eliminate most ambiguities by self-calibration of two emission bands). A SPCE, containing a two
1265   carbon working electrodes (W1 and W2), a carbon counter electrode and Ag|AgCl reference
1266   electrode, were utilized for electrochemiluminescent measurements in presence of H_2O_2. Luminol-
1267   functionalized AuNPs (L-AuNPs) acted as working signal tags and CdS QDs as internal reference
1268   tags, which were modified on W1 and W2, respectively. The ratio of working signal (W1) to internal
1269   reference signal (W2) as standard was determined. Chloramphenicol aptamer`s complementary
1270   strand (cDNA) and, subsequently the aptamer functionalized with chlorogenic acid as quencher of
1271   L-AuNPs, were immobilized onto the L-AuNPs. Chloramphenicol can induce the release of the
1272   aptamer, leading to a drift of chlorogenic acid from the surface of W1 and recovery of the
1273   electrochemiluminescence of the L-AuNPs. Simultaneously the CdS QDs on W2 emit a cathode
1274   signal, used as interference signal. The results showed no cross-reactivity and high specificity
1275   towards chloramphenicol.

1276   Based on the mentioned sensor principle [158], Feng's team refined the method further [159].
1277   Thereby a simultaneous detection of chloramphenicol and malachite green was realized. A malachite
1278   green specific aptamer and its complementary strand (cDNA) as well as cyanine dye as quencher for
1279   the CdS QDs and poly(ethylenimine) (PEI) as a bridging agent were additionally introduced in the
1280   sensor system, which was previously described by Feng and colleges [158]. PEI increases the loading
1281   of quenchers on aptamers, leading to an improved quenching efficiency. Interfering effects between
1282   chloramphenicol and malachite green were not determined, so finally a novel "dual potential"
1283   electrochemiluminescent aptasensor for the simultaneous detection of chloramphenicol and
1284   malachite green was developed.

1285   A chemiluminescent competitive-type aptasensor for the detection of chloramphenicol was
1286   developed by Hao et al. [91]. Chemiluminescence bioassays has the advantage of a simple sensor set-
1287   up and no requirement for an external light source. Biotinylated aptamers were directly immobilized
1288   on avidin-modified magnetic (Fe_3O_4) NPs and acted as capture probes. The signal probes were
1289   designed by functionalization of flower-like Au nanostructures with the aptamers complementary
1290   strand (cDNA) and ABEI. ABEI can be oxidized by H_2O_2 to the excited ABEI form, which decays to
1291   the ground state with simultaneous chemiluminescence emission. The capture probe can bind
1292   chloramphenicol and signal probes, but tend to competitively bind chloramphenicol due to the
1293   stronger interaction. Upon binding of chloramphenicol, signal probes are released and the unbound
1294   probes were removed in the external magnet, leading to a decreasing chemiluminescence signal. To
1295   establish a steady-state chemiluminescent system, the chemiluminescence enhancer and stabilizer *p*-
1296   iodophenol (PIP) was added to the $ABEI-H_2O_2$ system.

1297   The triple-amplification SPR electrochemiluminescence assay, presented by Miao et al. [150],
1298   based on polymer enzyme-linked nanotracers and Exo-assisted target recycling. The capture probe
1299   composed of the chloramphenicol specific aptamer and its partial complementary sequence (cDNA),
1300   immobilized onto CdS nanocrystals (CdS NCs), and connected to the working electrode.
1301   Semiconductor NCs are widely used for generating electrochemiluminescence signals. AuNPs are
1302   known to efficiently quench the CdS NCs electrochemiluminescence by resonance energy transfer
1303   (SPR). In combination with EnVision reagent (EV), an enzyme-linked dendrimer polymer reagent,
1304   AuNPs can further oxidize CdS NCs for electrochemiluminescence enhancement by catalysis of H_2O_2,
1305   which generates reactive oxygen species. That why AuNPs were labelled with HRP-functionalized
1306   EV and additionally ssDNA binding protein (SSB), which mediates the connection between capture
1307   and accrued signal probe via immunoreaction. In the presence of chloramphenicol, the aptamer
1308   preferentially binds to it and release the signal probe into the supernatant. As a result, the
1309   electrochemiluminescence signal decreases. Exo I, present in the solution, selectively digests the 3´-
1310   end of the aptamer. Thus, chloramphenicol detaches from the aptamer and can further participate in
1311   a new cycle to react with the probes.

Liu et al. [160] constructed a photoelectrochemical aptasensor using nitrogen-doped graphene QDs (NG-QDs) as transducer species for chloramphenicol detection. The F-doped SnO_2 glass working electrode was coated with NG-QDs and subsequently specific aptamer. When chloramphenicol is present, it can be captured by the specific aptamer and reacted with the photogenerated holes on NG-QDs, resulting in an enhanced photocurrent signal. The study verified the application of NG-QDs for photoelectrochemical sensing.

A photoelectrochemical aptasensor for chloramphenicol was designed by Wang et al. [161] using a TiO_2 based nanorod assay sensitized with Eu(III)-doped CdS QDs as the photoactive material. The TiO_2 nanorod assay absorbs visible light, depresses the recombination of photogenerated charges and improves the photo-to-current conversion energy. Eu(III)-doped CdS QDs extend the absorption of the assay into the visible light region and thus enhance the photoelectric properties. The modified nanorod assay was deposited on a fluorine-doped tin oxide electrode and subsequently amino-functionalized chloramphenicol specific aptamers were immobilized on the electrode via reaction between the amino groups of the aptamer and carboxy groups of the Eu(III)-doped CdS QDs. The addition of chloramphenicol led to the formation of the aptamer-target complex and a decreasing photocurrent.

Pilehvar et al. [162] developed an impedimetric electrochemical aptasensor for the detection of small molecules such as chloramphenicol. The Au electrode was modified with the specific aptamers by self-assembly. Upon binding of chloramphenicol, the aptamer undergoes a target-induced conformational change and forms a stem-loop structure. Chloramphenicol molecules are forced close to the electrode surface and blocks it from the redox active complex $[Fe(CN)_6]^{3-/4-}$, leading to an increase of the polarization resistance. The different subprocesses occurring during binding of chloramphenicol could be unravelled by electrical equivalent circuit (EEC).

Moreover, an amperometric electrochemical aptasensor for the detection of chloramphenicol was designed by Pilehvar et al. [163]. The aim of the study was to reach the maximum residue limit in the simultaneous presence of chloramphenicol and its structurally similar analogues thiamphenicol and florfenicol. The negligible influence of thiamphenicol and florfenicol showed that the proposed sensor discriminates chloramphenicol in complex matrixes from its analogues and proved the high specificity of the selected aptamer towards chloramphenicol. The thiolated chloramphenicol specific aptamers were immobilized onto the Au working electrode by self-assembly. Upon addition of chloramphenicol, the unfolded aptamers changed their conformation into hairpin structure. Thereby the target molecules are brought in close proximity to the electrode surface and an electron transfer was triggered. This is related to the irreversible reduction of the nitro group of chloramphenicol (Figure 5) with formation of hydroxylamine. Surprisingly, the same LODs were obtained for the measurement in water and milk, which suggests a very good applicability for real-sample analyzes in general. Almost simultaneously, the detailed electrochemical behaviour of chloramphenicol at biosensors was investigated by Pilehvar et al. [164]. The general approach and electrochemical measurements were the same, only the auxiliary electrode was different.

Yan et al. [165] introduced an electrochemical aptasensors for chloramphenicol detection in honey, based on target-induced strand-release. The Au working electrode was modified with chloramphenicol specific aptamer via Au-thiol interaction, which was subsequently hybridized with the complementary biotinylated detection probe (cDNA) and formed a DNA duplex. In the presence of chloramphenicol, the target-induced strand release resulted in the dissociation of biotinylated detection probe from the electrode. The remaining detection probe bound to streptavidin-alkaline phosphatase and thus catalyzed α-naphthyl sulfate (α-NP) substrate. As a result, the current response decreased.

An electrochemical aptasensor for *in vitro* chloramphenicol detection in *Haemophilus influenza* was developed by Yadav et al. [166]. The edge plane pyrolytic graphite EPPG as working electrode was modified with poly-(4-amino-3-hydroxynapthalene sulfonic acid) via electro-polymerization and subsequently specific aptamers were immobilized onto the surface of the working electrode. Upon binding of chloramphenicol, the aptamer undergoes a conformational change, bringing the target in close proximity of the electrode surface and finally triggers an electron transfer by reduction of the NO_2 group of chloramphenicol to hydroxyl amine. By using the bacterial strain of *H. influenza*,

a simultaneous *in vitro* chloramphenicol detection and bacterial resistant diagnosis was possible. In the case of chloramphenicol sensitive *H. influenza*, the concentration of chloramphenicol in the supernatant was much lower than in the case of chloramphenicol resistant *H. influenza*, because of chloramphenicol uptake. A significant accumulation in sensitive *H. influenza* was obtained, so resistant and sensitive *H. influenza* strain could be identified.

In the work of Bagheri Hashkavayi et al. [167] an electrochemical aptasensor for chloramphenicol detection, based on Au nanocubes-modified SPE is presented. The SPE was modified with Au nanocubes (AuNCs) using cysteine as cross-linker and in a second step with the chloramphenicol specific thiolated aptamer. The binding constant of the interaction of chloramphenicol and the aptamer was determined to be 2.9×10^6 M. The results indicated high specificity to chloramphenicol.

Hamidi-Asl et al. [168] introduced a electrochemical aptasensor for chloramphenicol detection based on aptamer incorporated gelantine. Gelantine, a physically cross-linked hydrogel, separated by partial hydrolysis of collagen, was investigated to be used as a biocompatible matrix for the chloramphenicol-specific aptamer, retaining aptamers bioactivity. The thiolated aptamer was mixed with different types of gelantine (A and B type) and dropped on the surface of a screen-printed Au electrode. The A type gelantine (gelA) derived from acid-treated and B type (gelB) from alkali-treated process. Upon chloramphenicol addition, the aptamer switched its structure and brought the analyte molecules in close proximity of the electrode surface, resulting in an enhanced electron transfer. The combination of the aptamer with gelB showed higher current signals than with gelA. Therefore, gelB was used for further experiments. Previously, a similar study by Pilehvar et al. [163] was performed in the same laboratory, but without gelantine. A higher LOD was determined in in the study here (Table 1), which implies that the gelantine increases the sensitivity of the aptasensor. This is presumably due to the fact that gelatine can hold the analyte molecules closer together and closer to the working electrode surface.

The presented aptasensor of Yadav et al. [166] was further developed by Rosy et al. [169], exploiting the cross linking properties of glutaraldehyde (GA). For sensor fabrication, first 1,5-diamoinonaphtalene was linked to the working electrode, consisting of edge plane pyrolytic graphite (EPPG), via electro-polymerization. Afterwards the chloramphenicol specific aptamer was immobilized on the amino-functionalized polymer modified EPPG surface using GA. GA covalently linked to the amino groups of the aptamer as well as to those present on the polymerized electrode. Compared to the previously reported aptasensor of Yadav et al. [166] without cross linking, the glutaraldehyde sandwiches aptasensor leads to tremendous increase of stability and sensitivity (23×10^{-9} μA/nM) due to the drastic increase of chloramphenicol binding, caused by covalent bonding of GA.

Yan et al. [170] introduced a "signal-on" electrochemical aptasensor for the simultaneous detection of chloramphenicol and polychlorinated biphenyl-72 (PCB72) using multi-metal ions encoded nanospherical brushes as tracers. For formation of the capture probe, the respective aptamers of chloramphenicol and PCB72 were labelled on magnetic AuNPs. Spherical hyperbranched polyethylene imine brushes (SPEIs) were conjugated with encoded metal-ions (Cd^{2+} and Pb^{2+}) by amino-groups and modified with cDNAs of the aptamers and acted as tracers. The capture probes and the tracers were connected via hybridization reaction. In the presence of the targets, the aptamers preferentially bind to them and thereby release the tracers into supernatant after magnetic separation. The tracers with metal ion could be directly detected by SWV, representing the "signal-on" state. The results delivered a high specificity of the aptasensor towards its two targets chloramphenicol and oxytetracycline. The number of targets that can be analysed in parallel is limited by the number of applicable metal ions which can be used as tracers. Thus, the proposed aptasensor can be extended to further biological detection by substitution of the appropriated metal tracers and aptamers.

Bagheri Hashkavayi et al. [171] developed an electrochemical aptasensor for chloramphenicol detection, based on dendric Au nanostructures on functionalized mesoporous silica. To improve the performance and the conductivity of the aptasensor, 1,4-diazabicyclo[2.2.2]octane-supported mesoporous silica (DB) was prepared onto the graphite SPE. Subsequently AuNPs were electrochemically deposited on the DB surface. Thereby dendritic Au nanostructures can be formed.

1418   Further, thiolated aptamers were immobilized onto the AuNPs-DB-SPE surface by Au-S bonds.
1419   Hemin was added, which is an electrochemical indicator that is reduced at carbon surfaces. Upon
1420   addition of chloramphenicol, the peak current for the hemin reduction increases, resulting from the
1421   closer proximity of hemin to electrode surface by aptamer-target binding. The LODs determined with
1422   the two different electrochemical aptasensor designed by Bagheri Hashkavayi and colleges achieved
1423   equal values (Table 1).
1424   An electrochemical aptasensor for the simultaneous detection of chloramphenicol and
1425   oxytetracycline was developed by Yan et al. [172]. The sensor based on high-capacity magnetic
1426   hollow porous NPs (MHNPs) coupling Exo-assisted cascade target recycling. The different signal
1427   tracers were designed by conjugating encoded metal-ions (Cd^{2+} and Pb^{2+}) by amino-groups to
1428   MHNPs and afterwards immobilizing the cDNA IIs (Table 1), which were complementary to the
1429   cDNA Is (Table 1). The cDNA Is were immobilized onto the AuNPs modified working electrode. By
1430   interaction of cDNA IIs with cDNA Is signal tracers and capture probes were connected. Specific
1431   aptamers were added and hybridized with the cDNA I-cDNA II conjugates, resulting in a SWV
1432   signal. In the presence of chloramphenicol and/or oxytetracycline, a target-induced strand release is
1433   triggered, the aptamers dissociated and accumulate in the supernatant. Thus, resulting in a decrease
1434   of the SWV current response. The enzyme Exo I, simultaneously present in supernatant, digested the
1435   3´-end of the aptamers, leading to a release of the targets for a further cycle, which amplifies the signal
1436   and improves sensitivity. In comparison to silica based nanotracers, the signals could be amplified
1437   for about 12 folds by the combination of coded nanotracers and Exo I assisted target recycling. This
1438   is partly due to the fact that MHNPs has highly density of loading sites at their surfaces, which can
1439   load more metal ions and thus leading to an amplification of the signal.
1440   Chen et al. developed two different electrochemical aptasensor for the simultaneous detection
1441   of chloramphenicol/kanamycin [47] and chloramphenicol/oxytetracycline [173]. Both based on
1442   aptamer-biocodes which were fabricated by co-immobilizing of aptamers and metal ions onto
1443   nanoscale MOFs (UiO-66). MOFs are featured by a large surface area, controllable pore structure,
1444   various functional groups and high thermal and chemical stability. The basic measuring principle
1445   was the following. The signal tags were formed by the modification of amine-functionalized
1446   nanoscale MOFs with different metal ions (Cd^{2+} and Pb^{2+}) and cDNA. The target specific aptamers
1447   were simultaneously immobilized onto amino-modified magnetic beads and formed the capture
1448   probe. Signal and capture probe can hybridize and generate an electrochemical signal. In the presence
1449   of the targets, the aptamers recognize and bind them specifically. The signal tags are replaced and
1450   released into the supernatant after magnetic separation. The peak current of the metal ions can be
1451   detected simultaneously by SWV. In the later work [173] they used circular strand-replacement DNA
1452   polymerization (CSRP) as signal amplification strategy to achieve maximal sensitivity of the sensing
1453   system. The analytical performance was further improved by the introduction of Y-shape DNA
1454   which possess structural flexibility and conformational stability. Y-shape DNA consisted of three
1455   overlapping DNA strands that are partially complementary to each other. Here, the Y-shape
1456   composed of assisted DNA (aDNA), capture-DNA (cap-DNA) and signal-DNA (sDNA). aDNA was
1457   immobilized onto magnetic AuNPs and hybridized with the cap-DNA, containing the target specific
1458   aptamers and the complementary sequence of the primer: sDNA was connected to different metal
1459   ions encoded nanoscale MOFs as signal tags. Bst DNA polymerase was introduced into the CSRP
1460   reaction to assist the target recycling amplification. Y-shape disassembled in the presence of the
1461   targets. The exposed primer recognition sequence of the cap-DNA hybridizes with the primer and
1462   initiates the polymerization in the presence of dNTPs. Thus, the released target triggered the
1463   successive polymerization reaction. As a result, the amount of signal tags in the supernatant after
1464   magnetic separation increased.
1465   Liu et al. [174] introduced an electrochemical aptasensor for chloramphenicol detection based
1466   on rGO and AgNPs. The GCE as working electrode was covered with AgNPs modified rGO.
1467   Subsequently the chloramphenicol specific aptamers were immobilized onto the surface of the
1468   modified electrode. Remaining active binding sites were blocked by MCH. Upon capturing of the
1469   target, chloramphenicol was electrocatalytically reduced by the rGO-AgNPs nanocomposite, which
1470   was detected by LSV.

1471   Huang et al. [110] designed an electrochemical aptasensor for multiplex antibiotics detection of
1472   kanamycin and chloramphenicol, based on endonuclease and exonuclease assisted dual recycling
1473   amplification strategy. AuNPs were syntehsized and decorated with the two kinds of restriction
1474   endonucleases EcoRI and BamHI to make them enrich and magnify and acted as signal transduction
1475   substances. Target specific thiolated aptamers were immobilized on bar A and their endonuclease
1476   labelled cDNAs were hybridized to form the enzyme-cleavage probes. Zi-MOF NPs with 1,4-
1477   benzene-dicyrboxylate were defined as UiO-66. The signal tags consisted of hierarchically porous
1478   aminomodified UiO-66 decorated with MB (for chloramphenicol) or Fc (for kanamycin) as
1479   electroactive components. The signal tags were immobilzed on bar B by two dsDNA stands. The
1480   dsDNA strands could be cleaved by the corresponding enzyme-cleavage probes on bar A. In the
1481   presence of the targets, the aptamers formed aptamer-target-complexes and the enzyme-cleavage
1482   probes departed into the reaction mixture. Exo I digested the aptamers from 3` to 5` end and the
1483   targets were released. The Exo I induced circulation achieved and the number of enzyme-cleavage
1484   probes increased. The enzyme-cleavage probes moved to bar B and cleavage the dsDNA strands on
1485   bar B, resulting in the reaese of the signal tags into the reaction mixture which caused a decrease of
1486   the electrochemical signal. The negligible interferenc between kanamycin and chlormphenicol
1487   proved the high specificity of the sensing system to the respective target.

1488   The most important data of the discussed aptasensors are summarized in Table 1. As seen, almost
1489   half of all developed aptamer-based biosensors for the detection of chloramphenicol are based on
1490   electrochemical sensor principles. Moreover, a comparatively large number of fluorometric
1491   aptasensors have been developed. Mehta et al. [147] identified and investigated the ssDNA aptamer
1492   sequence which was later used in numerous studies dealing with the aptasensing of chloramphenicol.
1493   The lowest LOD could be obtained by Chen et al. [173], followed by Rosy et al. [169] using
1494   amperometric aptasensors.

1495   *2.5   (Fluoro)Quinolones*

1496   (Fluoro)Quinolones have a very broad spectrum of action thus they act against gram-positives,
1497   gram-negatives, *Mycobacteria*, *Chlamydia* and anaerobes and are just a little humanly toxic. Their
1498   mechanism of action based on the inhibition of DNA-gyrase, which belongs to the group of
1499   topoisomerases II. Inter alia DNA-gyrase is responsible for the derivatization of the DNA.
1500   Structurally quinolones are derived from quinolone (marked red in Figure 6) [2]. The efficacy of the
1501   quinolones was further enhanced by the introduction of an additional fluorine atom, resulting in a
1502   whole series of fluoroquinolones.
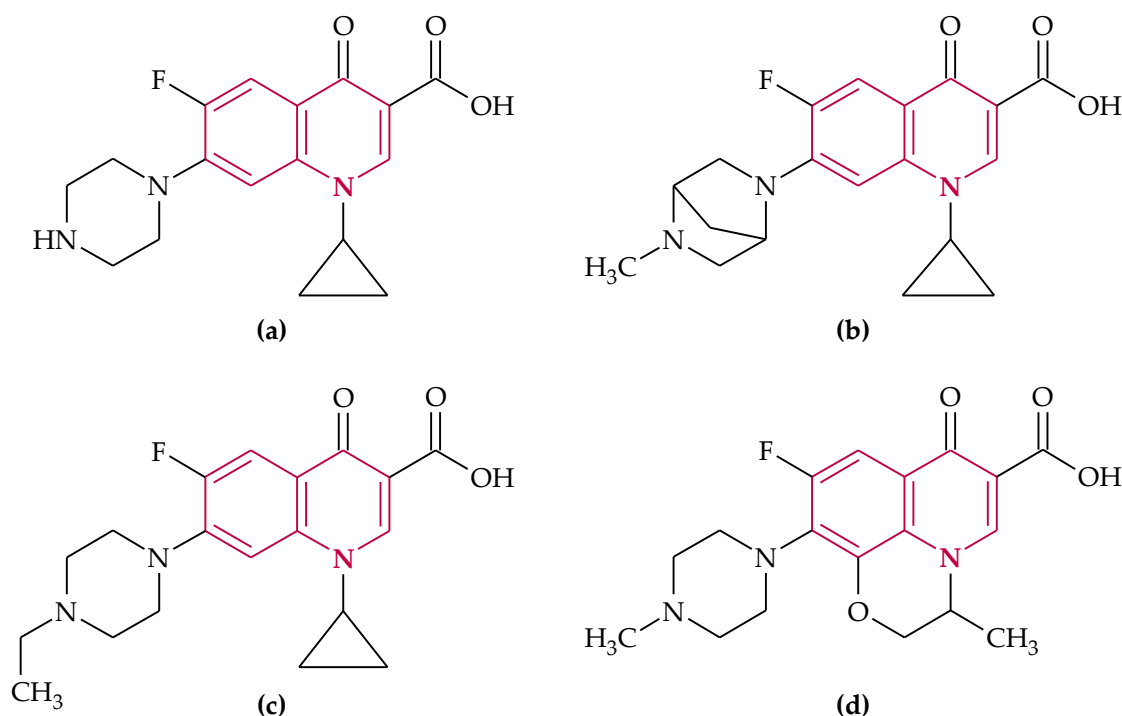
Figure 6. Chemical structure of: **(a)** ciprofloxacin, **(b)** danofloxacin, **(c)** enrofloxacin and **(d)** ofloxacin. The structure of quinolone is marked red.

2.5.1 Ciprofloxacin

Ciprofloxacin (Figure 6 (a)), a second-generation fluoroquinolone, acts against *Bacillus anthracis*, the causative agent of the anthrax and is one of the most used quinolones nowadays [1, 2].

In 2017 Lavee et al. [175] developed for the first time a colorimetric aptamer-based assay for the determination of ciprofloxacin. AuNPs possess enzyme-like activity that can catalyse the reduction of 4-nitrophenol to 4-aminophenol by sodium borohydride ($NaBH_4$). The AuNPs were modified with the ciprofloxacin specific aptamer and two partly cDNAs (cDNA I, cDNA II, Table 1). In the absence of the target, the reduction of 4-nitrophenol was prevented by the flower-shape coating. The addition of enrofloxacin leads to the detachment of the aptamer-cDNA conjugate, an aptamer-target-complex was formed and the AuNPs exerted their catalytic activity. As a result the color changed from yellow to colorless. The highest LODs were observed in the milk samples (Table 1), which indicates that interferences of complex matrices in the milk disturb the signal.

In the study of Abnous et al. [176] an electrochemical aptasensor for ultrasensitive detection of fluoroquinolones, especially ciprofloxacin, is presented. As a physical barrier for the access of redox probe ($[Fe(CN)_6]^{3-/4-}$) to the surface of SPGE single-stranded DNA-binding protein was used..

The electrochemical aptasensor [176] possess 1.5 fold lower LOD than the colorimetric one [175] (Table 1). No further published studies about an aptasensing of ciprofloxacin were reported. Here is still potential for research.

2.5.2 Danofloxacin

Danofloxacin (Figure 6(b)) acts against gram-positive and gram-negative bacteria and is often used for the treatment of respiratory diseases of cattle and pigs [177]. It is exclusively used in animal husbandry, not least because of its toxicity to humans [177].

By the application of SELEX, Han et al. [177] selected specific and high-affinity RNA aptamers with 2'-fluoro-2'-deoxyribonucleotide modified pyrimidine nucleotides bound to danofloxacin. In their work the scientists truncated the selected aptamers to the motif necessary for binding of danofloxacin, which leads to an improved affinity. In consequence, Han and colleges employed an optical aptasensor for the detection of danofloxacin in buffer.

1533   There are no other reports about investigations for danofloxacin detection by an aptasensor
1534   mentioned in the literature.

1535   2.5.3   Enrofloxacin

1536   Enrofloxacin (Figure 6(c)) is a high-potency antibacterial agent which is widely employed for
1537   disease prevention and therapy in poultry and livestock breeding and aquaculture practice [178, 179].
1538   For the detection of enrofloxacin, Liu et al. [178] designed a fluorometric aptasensor. Yb, Er ion-
1539   pair doped magnetic Fe_3O_4 UCNPs and amino-functionalized silica-modified (NH_2-Si) UCNPs were
1540   produced and further modified with streptavidin via classical glutaraldehyde method. Biotinylated
1541   enrofloxacin specific aptamers were immobilized onto the surface of the Fe_3O_4 UCNPs and
1542   biotinylated cDNAs onto NH_2-Si UCNPs. The two kinds of functionalized UCNPs were mixed and
1543   formed hybridization probes by the formation of duplex structures between the aptamers and the
1544   cDNAs. As long as enrofloxacin was absence, the hybridization probe exhibits a background
1545   fluorescence signal. Upon enrofloxacin addition, the aptamer-modified UCNPs preferentially bound
1546   to the target and some of the duplex structures dissociated, resulting in a decrease of the fluorescence
1547   signal, after magnetic separation.
1548   Moreover, Liu's group [179] developed a fluorometric "double recognition" aptasensor for the
1549   detection of enrofloxacin. The potential promising idea was to build a hybrid synergistic
1550   identification system by integrating two antibiotic recognition elements. Aptamers and fully
1551   synthetic molecularly imprinted polymers (MIPs) were chosen. MIPs are one of the most suitable
1552   alternative for biological molecular recognition instead of ligand-receptor, antigen-antibody and
1553   substrate-enzyme. Molecular imprinting is a strategy, where a molecular recognition unit is prepared
1554   by polymerizing functional monomers in the presence of template molecules. MIPs exhibit excellent
1555   specificity to substrates, compared to traditional molecular-recognition-based separation techniques.
1556   Biotinylated enrofloxacin specific aptamers were immobilised on $NaY_{0.78}F_4:Yb_{0.2},Tm_{0.02}$ UCNPs via
1557   biotin-avidin reaction. The modified UCNPs were suspended in a solution, containing enrofloxacin
1558   templates, and a "pre-polymerization complex" was formed, whereat the aptamer was folded into
1559   the desired (correct) shape. The complex acted as polymerization centre for the subsequent NP
1560   formation. The commonly used monomers of methacrylic acid in molecular imprinting technique
1561   were introduced into the system and interacted with the residual functional groups of enrofloxacin
1562   templates (not embedded in aptamer). Thus, in the polymerization process enrofloxacin molecules
1563   were immobilized with aptamers and further with a polymer matrix. It was shown, that the
1564   recognition ability of the NPs was enhanced by the combined characteristics of the specific molecular
1565   recognition properties of aptamers and MIPs. The enrofloxacin templates were removed by a
1566   washing procedure. The ultimately arising imprinting cavities were complementary to target
1567   enrofloxacin and possessed high affinity and specificity towards it. The LOD of the proposed
1568   aptasensor [179] was about five times lower than the previously presented "simple" one [178] (Table
1569   1), which presumably is related to the improved recognition ability of the NPs by the use of aptamers
1570   in combination with MIPs.
1571   The two described are the only paper which deal with the aptamer-based detection of
1572   enrofloxacin, so here exists potential for further research.

1573   2.5.4   Ofloxacin

1574   Ofloxacin (Figure 6(d)) is a second-generation fluoroquinolone, used in bacterial infections of
1575   the respiratory tract and the gastrointestinal tract [180].
1576   Reinemann et al. [181] searched for aptamer sequences specific for ofloxacin and furthermore
1577   determined the dissociation constant (K_D value) of the aptamer-target system.
1578   In 2017 Pilehvar et al. [180] developed a rapid and sensitive label-free electrochemical aptasensor
1579   for ofloxacin detection. For the immobilization of the specific aptamer a covalently attached AuNPs
1580   modified GCE was used. Another GCE acts as counter and a Ag|AgCl electrode as reference
1581   electrode. A high specificity, besides good reproducibility and stability, was achieved. To verify the

1582　application in environmental monitoring the aptasensor was tested in real samples such as effluent
1583　of sewage treatment plant and tap water.

1584　*2.6 Lincosamide*

1585　　　Lincosamide, called acylaminopyranosides due to their chemical structure, bind to the 50S
1586　subunit of the bacterial ribosomes and block the enzyme peptidyltransferase, resulting in a
1587　interrupted chain elongation during protein biosynthesis [2]. Lincosamide are frequently used in the
1588　case of staphylococcal, streptococcal, and pneumococcal infections [4]. Three representatives exist:
1589　the natural lincomycin (Figure 7) and two semi-synthetic derivates clindamycin and pirlimycin [1].
1590　The structure, which is common to all anthracyclines, is marked red in Figure 7. Anthracyclines are
1591　applied especially if a penicillin allergy exists [4].

1592
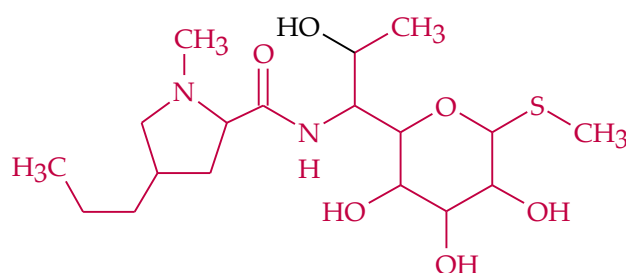
1593　　　**Figure 7.** Chemical structure of lincomycin. The basic structure of the anthracyclines is marked red.

1594　2.6.1　Lincomycin

1595　　　Lincomycin was the first discovered lincosamide, isolated from *Streptomyces lincolnensis* in a soil
1596　sample from Lincoln (Nebraska) [1, 4]. It is preferably for the treatment of bone marrow inflammation
1597　and wound-and respiratory infections [4].
1598　　　To best of our knowledge, there is just a report of aptasensor for lincomycin by Li et al. [182].
1599　They developed an aptamer-MIP biosensor for lincomycin detection based on electrogenerated
1600　CRET. A AuNP-functionalized GO nanocomposite was used for signal amplification. C-dots, which
1601　were modified onto the lincomycin specific aptamers, served as signal indicator and exhibited
1602　enhanced signal intensity in the absence of lincomycin. Electrogenerated CRET was observed
1603　between Au-GO nanocomposite and the C-dots. In the presence of lincomycin, it competitively
1604　bound to the aptamers and the MIPs and thus the energy transfer was blocked, resulting in a decrease
1605　of the electrochemical signal. Lincomycin templates were added to an aptamer containing solution
1606　to form aptamer-target complexes. The MIP was prepared on the Au-GO-modified GCE via
1607　electropolymerization. The lincomycin templates were removed by a washing procedure and the
1608　aptamer-MIP sensor was obtained with the imprinting cavities. For a contrast-test, non-MIP was
1609　fabricated by the same method but without using the lincomycin template. Besides, a random DNA
1610　sequence was used instead of the aptamer. In the contrast-test, lincomycin was neither captured by
1611　the aptamer-non-MIP sensor, nor by the random DNA-MIP sensor. The results confirmed, that the
1612　combined characteristics of the specific molecular recognition properties of aptamers and MIPs
1613　enhance the recognition ability and cause a high specificity towards their target.

1614　*2.7 Tetracyclines*

1615　　　Tetracyclines are the most widely used antibiotics besides penicillines which are of great
1616　economic importance due to their broad-spectrum activity (acting against gram-positive, gram-
1617　negative bacteria, *Rickettsiae*, *Mycoplasmas*, *Leptospira* and some large viruses) and their low toxicity
1618　[2, 4]. In some countries, they are widely used as nutritive antibiotics in poultry and pig fattening,
1619　which encourages resistance development. Tetracyclines inhibit protein biosynthesis by binding to
1620　the 50S subunit of the ribosomes. They are formed exclusively by *Streptomyces*. Their name derives
1621　from their basic structure, which consists of four linearly arranged six rings (marked red in Figure 8).
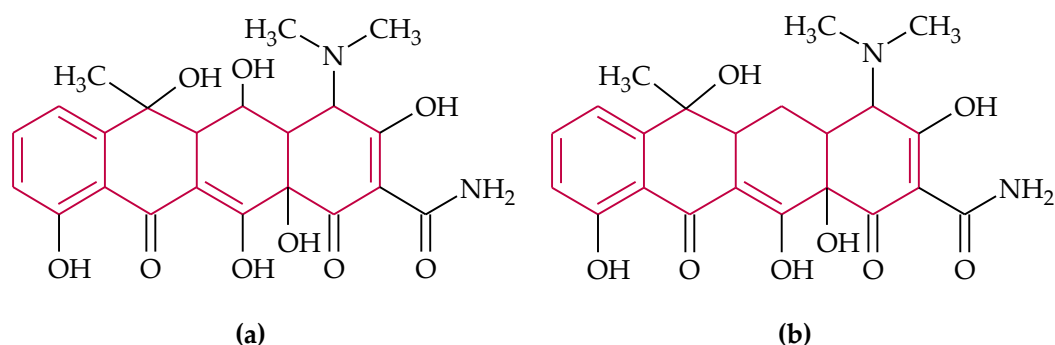
Figure 8. Chemical structure of: **(a)** oxytetracycline and **(b)** tetracycline. The basic structure of the tetracyclines is marked red.

2.7.1   Oxytetracycline

Oxytetracycline (Figure 8(a)) is the primary product in the formation of tetracyclines by *Streptomyces* [4].

Niazi et al. [183] selected oxytetracycline specific ssDNA aptamers by Flu-Mag SELEX and investigated their affinity, specificity and specificity. The one with best affinity (lowest K_D, Table 1) was later used in a variety of studies which deal with oxytetracycline detection [184–188]. In the Flu-Mag SELEX method fluorescent labels for DNA quantification and magnetic beads for target immobilization are used for aptamer selection [189]. In further investigation they   selected ssDNA aptamers specific for tetracycline, oxytetracycline and doxycycline [190].

Kwon et al. [191] truncated 76-mer ssDNA aptamers with high affinity and specificity for oxytetracycline, selected by SELEX, to a unique shortened 8-mer ssDNA, by selection of the nucleotide bases which exhibit high homogeneity in accordance to their conserved regions. The shortened aptamer was found to exhibit a very high binding affinity (K_D, Table 1), determined by isothermal titration calorimetry, and specificity to oxytetracycline, tetracycline, doxycycline and chlortetracycline. By utilization of the shortened aptamer, an ultra-sensitive (Table 1) colorimetric oxytetracycline detection based on unmodified AuNPs was possible. The truncated aptamer was used in other studies [192].

An aptamer-based cantilever array sensor for the detection of oxytetracycline was introduced by Hou et al. [193]. Cantilever sensors offers improved dynamic response, reduced size, increased reliability and high precision, compared to more conventional sensors. Molecular recognition can be directly and specifically transduced into nanomechanical response. The cantilever array consisted of silicon cantilevers coated with a 20 nm layer of Au. The sensing cantilevers were functionalized with SAMs of the oxytetracycline specific aptamers by Au-S bond binding while the reference cantilevers were modified with MCH to eliminate the influence of environmental disturbances, such as temperature and non-specific adsorption. Sensing and reference cantilever were arranged alternately in the array. When oxytetracycline bound to the aptamer onto the cantilevers surface, a difference in surface stress is generated between functionalized and non-functionalized side of the cantilever, resulting in a bending. The nanomechanical deflection of each cantilever was determined in real time by monitoring the position of a laser beam reflected from the cantilever onto a position sensitive detector with a four-quadrant photodiode.

Kim et al. [185] introduced a combination of light scattering particle immunoagglutination assay (LSPIA) with a microfluidic device for oxytetracycline detection. Light scattering offers advantages such as low cost, small size and ease of integration. A portable miniature spectrometer was used for forward light scattering intensity measurements, collected by multi-mode fiber. Highly carboxylated polystyrene submicron latex microspheres were coated with the aptamers by covalent coupling method. The aptamer conjugated microsphere and the target solution were injected into the Y-shaped microfluidic channel by a syringe pump. Aptamer-target binding causes the microspheres to form agglutination complexes, which can be detected by static or DLS method. In the proposed assay, an increase in the oxytetracycline concentration can be interpreted with an increase in the aggregated

particle size, resulting in an increased light scattering intensity. A mixture of gentamicin, penicillin G, enrofloxacin and sulfamethazine was used as negative control which simultaneously implies a high specificity of the designed aptasensor towards oxytetracycline.

Moreover, Kim's team [188] developed an indirect competitive assay-based aptasensor for oxytetracycline detection in milk. Oxytetracycline specific aptamers were selected by SELEX and identified by ELAA. The one with strongest affinity (Table 1) was used for further investigations. The selected aptamer showed highest specificity to oxytetracycline, even in the presence of the structurally similar antibiotics tetracycline and chlortetracycline, no cross-reactivities could be observed in the indirect competitive ELAA. Biotinylated aptamers and oxytetracycline were added into microtiter plates. After competitive reaction a streptavidin-HRP solution and subsequently a TMB solution were added and the absorbance was measured. The results validated the proposed ELAA as satisfactory screening method for oxytetracycline detection in milk.

Meng et al. [192] designed an ultrasensitive surface enhanced Raman scattering (SERS) aptasensor for the detection of oxytetracycline. Advantages of SERS, a molecular fingerprint spectrum, are amongst others ultrasensitive and non-invasive probing, compatibility with aqueous solution, minimal sample preparation and label-free monitoring of analytes in complex matrices. Thiolated stem-loop DNA, containing the oxytetracycline specific aptamer, was immobilized onto the surface of 80 nm AuNPs by forming Au-S bonds. A monolayer of MCH was self-assembled to prevent non-specific adsorption and to improve the capture efficiency of the aptamers. Avidin was added, which bound specifically to the biotin modified 5´ end of the DNA. 13 nm AuNPs attached to the avidin modified DNA strand by the electrostatic subsequently effect (avidin positively charged, AuNPs negatively charged). Subsequently, the 13 nm AuNPs were functionalized with the Raman reporter molecule 4-mercaptobenzoic acid (MBA). Between the 80 nm AuNPs and the 13 nm AuNPs a SERS hot spot was formed, which is a highly-localized regions of intense local field enhancement. In the presence of oxytetracycline, the aptamer preferentially bound to it, leading to a partial dehybridization of the DNA. In consequence, the 13 nm AuNPs approach the 80 nm AuNPs more closely and the Raman intensity increased significant.

A colorimetric aptasensor for the detection of oxytetracycline was presented by Kim et al. [186]. Oxytetracycline specific aptamers are immobilized onto AuNPs surfaces and stabilize them, even if salt is added. Upon addition of oxytetracycline, aptamers detach from the surfaces and conjugates with their target. Thus, the AuNPs are no longer stabilized by the aptamers and aggregates after addition of salt, resulting in a visible color change from red to purple, monitored by UV-Vis spectrophotometry. Supplementary Kim's group [187] investigated the affinity-ratio and its pivotal role in AuNP-based competitive colorimetric aptasensor.

In the work of Seo et al. [194] a reflectance-based colorimetric aptasensor using AuNPs for oxytetracycline detection is presented. Oxytetracycline specific aptamers are immobilized onto AuNPs surfaces. Upon addition of oxytetracycline, the aptamers detach from the AuNPs and bind to their targets. After adding salt, the AuNPs aggregated. The result is a visible color change from red to purple (absorbance peak shifts from 520 nm to 650 nm), because the localized SPR is changed. The absorbance can be detected indirectly from the spectrum transmitted using a spectrophotometer. Alternatively, the reflected spectrum from the SPR of the AuNPs can be measured directly. Two types of reflection exist: the specular and the diffuse reflection. The diffuse reflection was of primary interest for the mentioned experiment. So, in order to minimize the specular reflection, the incidence angle was optimized. The reflectance-based measurements at two wavelengths (650 and 520 nm) were found to generate more sensitive and stable signals than absorbance-based sensors. Besides, small amounts of samples can be directly measured and the use of different loading platform with various shapes, such as well plates, disc plates and microfluidic channels, is possible, since the measurement can be configured with flexible optical fibers.

Zhao et al. [32] designed a fluorometric assay for oxytetracycline detection based on an fluorescein-labelled long-chain aptamer assembled onto rGO. The efficient quenching ability of rGO and the different interaction intensity of the aptamer and the aptamer-oxytetracycline complex with rGO are used for fluorometric detection. Compared with GO, rGO possess more crystalline graphene regions on the sheet, which improves the quenching ability. Via hydrophobic and π-π stacking

interactions between the ring structures in the nucleobases of the aptamers and the hexagonal cells of rGO, the FAM-modified long-chain (76-mer) aptamers were adsorbed onto the surface of rGO. Thereby the FRET proximity was induced, leading to fluorescence quenching of dyes by rGO. In the presence of oxytetracycline, a well-folded aptamer-oxytetracycline complex was formed. The exposure of nucleobases decreased and the dyes remove from the rGO surface, resulting in a hindered FRET process and ultimately in a restoration of fluorescence.

Yuan et al. [195] designed a fluorometric aptasensor for oxytetracycline detection using an indirect labelled long-chain aptamer, which based on the work of Zhao et al. [32]. It was established, that the secondary structure of long-chain aptamers causes indistinctive structural transformation after binding of oxytetracycline, resulting in a hindering of an effective desorption from the graphene sheet and thus to a hindered fluorescence restoration. To avoid the mentioned negative effects, a novel recognition probe for oxytetracycline detection based on an indirectly fluorescence amidite labelled aptamer was designed. The recognition probe consisted of the long-chain (76-mer) aptamer and a FAM-labelled short-chain (11mer) ssDNA (cDNA I), which was hybridized with the 5′-end of the aptamer. The oxytetracycline specific aptamers were adsorbed onto the surface of GO via strong π-stacking interaction between the hexagonal cells of graphene and the ring structure of the nucleobases. Due to the FRET proximity, the FAM on the probe was quenched by the GO. Upon addition of oxytetracycline, cDNA I was released, because the aptamer preferentially binds to its target. Upon addition of the short-chain (11mer) ssDNA (cDNA II), which was complementary to cDNA I, the originally adsorbed cDNA I hybridized with cDNA II and formed dsDNA. The dsDNA escaped from the graphene sheet to the solution, resulting in a hindered FRET process and in a restoration of fluorescence.

During the last several years the formation of GO hydrogel by self-assembly of GO sheets and influence of different parameters onto the gelation process has been systematically investigated [196]. Tan et al. [197] introduced a fluorometric aptasensor based on target-responsive GO hydrogel for the detection of oxytetracycline. The hydrogel was prepared by mixing GO sheets, adenosine and oxytetracycline specific aptamers together. The strong hydrogen bonding and electrostatic interactions between adenosine and the GO nanosheets are most likely responsible for the fast gelation. The FAM-labelled aptamers adsorbed on the GO sheets via the strong π-π stacking interactions and the fluorescence of FAM was quenched by GO due to FRET. If the functional hydrogel is immersed in the oxytetracycline containing solution, the aptamers prefer to capture the antibiotic molecules to form an aptamer-target complex. The conformational change induces a steric hindrance and the complex desorbs from the GO surface to the supernatant. The increasing distance between FAM and the GO sheets results in a recovery of fluorescence. In general, the developed aptasensor is distinguished by a facile and fast gelation, soaking and fluorescence detection process and thermal and chemical stability.

In the work of Fang et al. [38] a luminescent aptasensor for oxytetracycline detection, based on UCNPs and magnetic NPs, is presented. UCNPs possess a couple of advantages compared to other types of fluorescent materials (e.g. organic dyes, fluorescent proteins, AuNPs, QDs), including higher photostability, low toxicity, large Stokes shifts, high quantum yields and the lack of both auto-luminescence and a light-scattering background. The signal probes composed of amino-functionalized NaYF4:Yb, Er UCNPs modified with amino-functionalized cDNA. Capture probes were formed by immobilizing oxytetracycline specific amino-functionalized aptamers onto the surface of amino-functionalized Fe_3O_4 magnetic NPs via classical glutaraldehyde method. By hybridization of capture and signal probes poly-network structures were generated, leading to a maximum luminescence emission, after magnetic separation by an external magnet. Upon addition of oxytetracycline, the signal probes were replaced, since the affinity of the aptamers to their target is higher than to the cDNA, resulting in a decrease of luminescence intensity.

A aptasensor for the detection of oxytetracycline, based on luminescence resonance energy transfer (LRET) from UCNPs to SYBR green, was developed by Zhang et al. [198]. SYBR green is a label-free indicator, making a very simple and convenient detection possible. The oxytetracycline specific amino-functionalized aptamers were covalently linked to NaYF4:Yb,Tm UCNPs via classical glutaraldehyde method and hybridized with their amino-functionalized complementary strands.

1770   The subsequent added SYBR green inserted into the formed dsDNA and brings energy donor and
1771   acceptor in close proximity to each other. Thus, leading to a LRET from UCNPs to SYBR green and a
1772   quenched luminescence. When oxytetracycline was present, the aptamers dehybridized from their
1773   cDNA and preferentially bound to the target molecules. Thereby SYBR green was liberated and the
1774   luminescence recovers.

1775   A „signal-off" photoelectrochemical aptasensor for oxytetracycline detection was developed by
1776   Yan et al. [199]. A p-type semiconductor BiOI doped with graphene (G) acted as photoactive species.
1777   The doping with graphene promoted the cathodic photocurrent response of BiIO under visible light
1778   irradiation. Amino-functionalized oxytetracycline-binding aptamers were immobilized on the BiIO-
1779   G modified electrode using glutaraldehyde as cross-linking. In the absence of oxytetracycline, BiOI-
1780   G efficiently converts visible light irradiation to cathodic current. When oxytetracycline was added,
1781   the photocurrent response of the photocathode decreased. Obviously, the diffusion of electron
1782   acceptor to electrode surface is sterically hindered by the formation of the aptamer-oxytetracycline
1783   complex. The applicability for real sample analysis was verified by assaying oxytetracycline in a
1784   commercial tablet and compare the results to this obtained by the additionally performed HPLC.

1785   Li et al. [200] constructed a photoelectrochemical aptasensor for the detection of oxytetracycline
1786   based on signal „switch off-on" strategy. Electrochemical impedance and photoelectrochemical
1787   measurements were carried out in an electrochemical workstation, containing a four-electrode
1788   configuration. TiO_2 nanorods (semiconductor) were uniformly prepared on an indium tin oxide
1789   conducting glass. Subsequently AuNPs were electrodeposited on the surface of the TiO_2 film. CdTe
1790   QDs were conjugated to hairpin cDNAs, which were than immobilized onto the working electrode
1791   by Au-S bonds. The CdTE QDs came in close proximity to the electrode surface and generate a strong
1792   photocurrent under visible light irradiation, with ascorbic acid as electron donor. After immersion
1793   into aptamer solution, the aptamers and the cDNAs hybridize and the photocurrent decreases,
1794   because the cDNA changed into a rod-like double helix and CdTE QDs were far away from electrode
1795   surface. The decrease value varied with the cDNA chain length. In the presence of oxytetracycline,
1796   the aptamer preferentially binds to its target instead of the hairpin cDNA and detaches from the
1797   electrode. The cDNAs regained their original hairpin forms and the photocurrent signal was
1798   recovered. The recovery value increases with increasing oxytetracycline concentration. Different
1799   types of hairpin cDNAs (I, II and III) were investigated with regard to their effects on the detection
1800   performance. Their sequences are listed in Table 1. cDNA I was complementary to the whole
1801   sequence of the aptamer and cDNA II and III were complementary to part of the sequence. cDNA III
1802   showed higher stability and a lower signal background and hence it was selected for the final
1803   construction of the aptasensor.

1804   Kim et al. [184] introduced an electrochemical sensing system for oxytetracycline detection,
1805   using a single glass chip, containing an interdigitated array (IDA) Au electrode, a reference and a
1806   counter electrode. Thiol-modified aptamers were immobilized onto the IDA Au electrode. The
1807   binding of oxytetracycline leads to a conformational change of the aptamer. Thus, the target is close
1808   to the electrode surface and an electron transfer is triggered. Ferricyanide solution was used as a
1809   mediator for electron flow between bulk solution and working electrode.

1810   Zheng et al. [201] developed an electrochemical aptasensor for direct detection of oxytetracycline
1811   in mouse blood, serum and urine. First, the working electrode was incubated with ferrocene-
1812   functionalized cDNA of the aptamer and these formed a SAM onto the surface of the electrode via
1813   Au-S bonding. Then the electrode was passivated with MCH to reduce non-specific between the
1814   DNA probe and the surface as well as to stabilize the monolayer. The aptamer was added and formed
1815   dsDNA with its cDNA. A partial hybridization of the aptamer and its target was induced, when
1816   oxytetracycline was introduced. Thereby the cDNA self-fold into a hairpin structure and brings the
1817   redox-active electrochemical probe ferrocene in close proximity of the electrode surface, resulting in
1818   a current response. The aim of the study was to quantify oxytetracycline in mouse blood, serum and
1819   urine, which succeeded well. Comparisons to an additionally carried out ELISA showed almost
1820   identical results.

1821   A competitive aptasensor for the detection of oxytetracycline based on HRP and GO-polyaniline
1822   (GO-PANI) composites as signal amplifiers was introduced by Xu et al. [202]. GO-PANI composites

1823   exhibit obviously higher electrical conductivity than the pure GO or PANI. The prepared GO-PANI
1824   was immobilized onto the surface of the GCE via electrostatic adsorption force. The electrodes were
1825   immersed into $HAuCl_4$, AuNPs were electrodeposited onto the surface of the GCE. The complete
1826   antigen oxytetracycline-BSA was fixed on the electrodes, based on the binding between the amino
1827   group of BSA and AuNPs. The GCE was incubated in BSA to block non-specific binding sites. Finally,
1828   oxytetracycline samples and HRP-labelled aptamers were added simultaneously. The oxytetracycline
1829   in the samples competed with those on the electrode to bind the aptamer. The more oxytetracycline
1830   was added, the less HRP combined with oxytetracycline-BSA conjugate on the electrodes, resulting
1831   in a current decrease, which indicated the quantity of oxytetracycline. The electrochemical
1832   measurements were carried out in PBS containing $K_3[Fe(CN)_6]$, hydroquinone (HQ) and H_2O_2. HQ is
1833   oxidized to benzoquinone (BQ) and simultaneously H_2O_2 is reduced to H_2O. Based on their similar
1834   structure and type of interaction, tetracycline and chlortetracycline were used as interfering
1835   substances for evaluation of the specificity of the aptasensor to oxytetracycline, which can be
1836   estimated as good.

1837   The electrochemical aptasensors for simultaneous detection of kanamycin/oxytetracycline [105]
1838   and chloramphenicol/oxytetracycline [173] were reported, as mentioned in the previous sections.

1839   Zhang et al. [203] developed an electrochemical aptasensor for the simultaneous detection of
1840   tetracycline and oxytetracycline. Detailed information is mentioned in the section of tetracycline.

1841   A sandwich-type electrochemical aptasensor for oxytetracycline detection based on graphene-
1842   three-dimensional nanostructure Au nanocomposites (Gr-3D Au) was introduced by Liu et al. [204].
1843   Compared to a pure graphene film, conductivity and surface area of Gr-3D Au are significant
1844   improved. A Gr-3D Au film was modified on the working electrode by one-step electrochemical co-
1845   reduction with graphite oxide and $HAuCl_4$ at cathodic potentials. This enhanced the electron transfer
1846   and the loading capacity of biomolecules. The antibodies of oxytetracycline were attached to the
1847   electrode surface via electrostatic interaction. To avoid non-specific interactions BSA was added.
1848   Oxytetracycline was captured by the antibodies. AuNPs were modified with HRP and the
1849   oxytetracycline specific aptamer and formed the nanoprobes. The addition of the nanoprobes leaded
1850   to the formation of a sandwich-type system, resulting in an electro-reduction of H_2O_2 (present in
1851   solution), enhanced by HRP. The current response corresponded to the oxytetracycline concentration.
1852   Measurements in the presence of structural analogues, e.g. tetracycline, doxycycline and
1853   chlortetracycline, revealed the high selectivity of aptasensor towards oxytetracycline.

1854   In summary, most of the aptamer-based biosensors for the detection of oxytetracycline are
1855   amperometric ones. Moreover, colorimetric and fluorometric aptasensors were developed
1856   frequently, i. a. due to their simplicity. Niazi et al. [183] selected and investigated a ssDNA aptamer
1857   sequence (Table 1), which was further used in almost all studies about aptasensing of oxytetracycline.
1858   But the ssDNA aptamer with highest affinity, and thus lowest K_D value, was proposed by Kwon et
1859   al. [191] (Table 1). As seen, Meng et al. [192] reached the lowest LOD by using a SERS based
1860   aptasensor for oxytetracycline detection, followed by Chen et al. [173] with an amperometric one
1861   (Table 1).

1862   2.7.2   Tetracycline

1863   Tetracycline (Figure 8(b)) is used in veterinary medicine and treatment as well as prevention of
1864   microbial infections such as respiratory tract infections, arthritis and severe acne [205]. In particular
1865   it has been used as a feed additive to promote the growth of livestock in agriculture sector [206].

1866   In 2008 Niazi et al. [190] identified tetracycline group specific ssDNA aptamers by modified
1867   SELEX (Toggle-SELEX combined with Flu-Mag SELEX). Tosyl-activated magnetic beads coated
1868   oxytetracycline, tetracycline and doxycycline, respectively, were employed as targets and counter
1869   targets. Twenty aptamers were selected whereof seven showed high affinity to the basic backbone of
1870   the tetracycline group. Aptamers which fail to bind specific to all tested target molecules were
1871   eliminated during counter selection steps. The specificity to the structural analogues followed the
1872   order oxytetracycline > tetracycline > doxycycline. A consensus sequence motif was found in most of
1873   the selected aptamers, which was predicted to be essential for target binding. The selected aptamer

1874 sequence was used in almost every aptamer based study, which is mentioned below, for tetracycline
1875 detection by a biosensor.
1876   Kwon et al. [191] truncated 76-mer ssDNA aptamers with high affinity and specificity for
1877 oxytetracycline to a unique shortened 8-mer ssDNA with selectivity to oxytetracycline, tetracycline,
1878 doxycycline and chlortetracycline. Detailed information is mentioned once in the section of
1879 oxytetracycline.
1880   The ligand binding properties of a synthetic tetracycline binding RNA aptamer were
1881 thermodynamically characterized by Müller et al. [207]. The dissociation constant was determined
1882 by a fluorometric assay. Functional groups crucial for the aptamer-target interaction and their
1883 respective enthalpic and entropic contributions were investigated for proposing detailed structural
1884 and functional roles for certain groups.
1885   Aslipashaki et al. [205] developed an aptamer-based extraction followed by electrospray
1886 ionization-ion mobility spectrometry (ESI-IMS) for tetracycline detection in biological fluids.
1887 Aptamer-based solid-phase extraction was used to separate tetracycline from the complex matrix.
1888 Therefore, the tetracycline specific aptamers were covalently bound onto CNBr-activated sepharose.
1889 To prove the applicability of the proposed method for real sample analysis and for investigation of
1890 the matrix effects, tetracycline was detected in human urine and plasma samples.
1891   Jeong & Rhee Paeng [208] introduced a competitive ELAA for the determination of tetracycline
1892 residue in bovine milk using two different aptamers individually, one 76mer DNA and a 57mer RNA
1893 aptamer. The RNA aptamer featured a lower K_D and thus a higher affinity to tetracycline than the
1894 DNA aptamer (Table 1). The ELAA was carried out in polystyrene immuno microplates. The
1895 biotinylated aptamer was immobilized onto microplate via avidin-biotin interaction. Tetracycline
1896 was conjugated to HRP and formed the competitor. The ELAA was utilized for tetracycline detection
1897 in tetracycline spiked, pretreated (protein, fat carbohydrate cations were removed) milk samples. The
1898 LODs obtained for the RNA aptamer were lower than the one for the DNA aptamer, as well as in
1899 buffer as in milk (Table 1). The specificity of aptamer was evaluated by a cross-reactivity study, by
1900 addition of structurally similar antibiotics like oxytetracycline, chlortetracycline and doxycycline. All
1901 of the tested antibiotics showed high cross-reactivity with tetracycline. Consequently, the ELAA
1902 showed no superior specificity. This was confirmed again by comparing the results to an additionally
1903 performed ELISA, which exhibited high specificity to tetracycline. Therefore, the use of aptamers
1904 does not necessarily lead to a better selectivity and sensitivity even if aptamers have several
1905 advantages over antibodies.
1906   Two different colorimetric aptasensors for tetracycline detection were presented by Wang's team
1907 based on an indirect competitive ELAA (icELAA) [209] and a direct competitive ELAA (dcELAA)
1908 [210]. The ELAAs were performed in flat-bottom immuno plates. In the icELAA, the microtiter plates
1909 were coated with BSA-functionalized tetracycline. The plated were blocked with Hammerstein
1910 bovine casein to prevent non-specific adsorption. Biotinylated aptamer was added and bound to its
1911 target. Streptavidin-HRP conjugate was added and bound to the aptamer [209]. In the dcELAA,
1912 streptavidin was coated on the microtiter plates. The plates were blocked against non-specific
1913 adsorption with casein or BSA. Biotinylated aptamer was added and bound to streptavidin. HRP-
1914 labelled tetracycline was added and bound to the aptamer [210]. In both assays, the TMB solution
1915 changed from colorless to blue, until the reaction was stopped by the addition of H_2SO_4, whereat the
1916 color turned to yellow. Cross-reactivity studies were performed with oxytetracycline and
1917 doxycycline, which indicated a high specificity towards tetracycline. Comparing the applied sensing
1918 systems, significantly lower LODs were obtained with the icELAA (Table 1).
1919   Luo et al. [211] designed resonance scattering (RS) method to for the detection of tetracycline
1920 using aptamer-coated AuNPs as catalyst. In the absence of tetracycline, the tetracycline specific
1921 aptamers adsorb onto the surface of the AuNPs and keep the AuNPs distributing evenly in solution.
1922 Thus, the AuNPs catalyse the Fehling reaction to yield a bigger Cu_2O cubic and obtain a high RS
1923 signal. If tetracycline is present, aptamer-tetracycline conjugates are formed and the AuNPs
1924 aggregate under NaCl existence. Less AuNPs catalyse the Fehling reaction, yielding a smaller Cu_2O
1925 cubic, leading to a lower RS signal. The RS intensities are linear to the diameter of the particle.
1926 Catalytic reaction conditions, such as reagent concentration, reaction time and reaction temperature,

were adjusted to achieve the optimal RS signal. Addition of a variety of foreign substances, such as antibiotics (e.g. kanamycin) and organic molecules (e.g. L-lysine) into the assay verified its selectivity, and specificity towards tetracycline.

Another SERS apatsensor for tetracycline detection was developed by Li et al. [212]. By loading the Raman reporter *p*-aminothiophenol (PATP) onto AuNPs, a nanocarrier was formed, which acted as signal probe. Subsequently, the nanocarrier was functionalized with Na_2SiO_2 to immobilize cDNA to produce a large amplification factor for Raman signal. The recognition probe was formed by immobilizing tetracycline specific aptamers on polymethacrylic acid-functionalized magnetite colloid nanocrystal clusters via condensation reaction. The incurred magnetic nanospheres possessed a high saturation magnetization value and excellent biocompatibility, which enables a rapid and easy magnetic separation. In the absence of the target, signal and recognition probe hybridizes via aptamer-cDNA interaction. In the presence of tetracycline, the aptamer preferentially binds to its target, leading to a diverge of signal and recognition probe and a release of some signal probes into bulk solution. The result is a strong SERS signal after magnetic separation. Negligible changes in the SERS intensity were obtained for the possible interfering antibiotics whereas a greatly change was monitored for tetracycline, indicating a high specificity of the sensor for tetracycline.

Two different colorimetric aptasensor for the detection of tetracycline were presented by He et al. [213]. For both, the tetracycline specific aptamers were immobilized onto AuNPs via electrostatic interactions. TEM and CD were used to characterize this modification. In the one colorimetric assay hexadecyltrimethylammonium bromide (CTAB) [213] was used and in the other one poly(diallyldimethylammonuim) (PDDA) [214]. CTAB, a cationic surfactant, is able to assemble DNA to form supramolecules and could imply the aggregation of AuNPs due to the electrostatic attraction between CTAB and AuNPs. PDDA, a cationic polyelectrolyte, could generate and stabilize AuNPs and interacted with aptamers as they were negatively charged to form a counterpart macromolecule. When CTAB bound to the aptamers, the aptamers are sequestered from the AuNPs, resulting in an aggregation of the AuNPs and a visible color change. In the presence of tetracycline, the aptamers bound to it and CTAB cannot assemble aptamers to form supramolecules [213]. On the other hand, when PDDA bound to the aptamers to form a complex structure, AuNPs did not aggregate, because they are stabilized by the complex structures. Upon addition of tetracycline, a aptamer-target complex is formed and the PDDA lose their ability to protect the AuNPs, resulting in an aggregation of the AuNPs and a visible color change [214].

Furthermore, Luo et al. [215] introduced a colorimetric aptasensor for tetracycline detection, based on cysteamine-stabilized AuNPs (CS-AuNPs). The aggregation of the positively charged CS-AuNPs can be induced by electrostatic attraction between CS-AuNPs and the added tetracycline specific aptamers. The result is a visible color change from red to blue, detected by UV-Vis spectrophotometry. In the presence of tetracycline, the aptamer-target interaction, which is stronger than the electrostatic one, causes a conformational change of the aptamer from G-quadruplex into hairpin structure. Therefore, the aptamer CS-AuNPs interaction, and thus the color change, holded of.

Ramezani et al. [216] developed a colorimetric aptasensor for the detection of tetracycline, based on triple-helix molecular switch (THMS) and AuNPs. The THMS consisted of the label-free tetracycline specific aptamer sequence with two arm segments and a label-free oligonucleotide as signal transduction probe (STP). In the absence of tetracycline, THMS is stable and cannot protect the AuNPs against salt-induced aggregation, owing to its rigid structure. Thus, the addition of salt leads to a visible color change from red to blue. If tetracycline is present, THMS is disassembled. The aptamer forms a complex with its target, while STP adsorbs onto the surface of the AuNPs. Thus, the dispersed AuNPs remains stable against salt-induced aggregation.

Wang et al. [217] found that some antibiotics can absorb directly on unmodified AuNPs, regardless of the presence of aptamers, which can lead to false positive colorimetric signals. The scientists established two rational screening criteria for antibiotic targets qualified for unmodified AuNPs based colorimetric assay, relying on the oil-water partition coefficients (log P > 0) and net physiological charges (≤ 0) of the antibiotics.

1979   A GO based colorimetric aptasensor for the detection of tetracycline was presented by Tang et
1980   al. [218]. In the absence of tetracycline, the aptamers were adsorbed onto the surface of GO via
1981   hydrophobic and π-π stacking interaction and thus, GO was protected from aggregation, which
1982   otherwise occurs in the salty solution. Upon tetracycline addition, the aptamer preferentially binds
1983   to it and does not stabilize GO any longer, which leads GO aggregates and the solution color changes.

1984   Jalalian et al. [219] introduced a fluorometric aptasensor for the detection of tetracycline based
1985   on THMS. The tetracycline specific aptamer possessed two arm segments, which bound to the loop
1986   sequence of a FAM-labelled complementary signal transduction probe (cDNA) and formed an open
1987   THMS configuration, whereby a strong fluorescence emission was induced. In the presence of
1988   tetracycline, the THMS complex was disassembled and the free cDNA folded to a stem loop structure,
1989   which brought the fluorophore on the 5′-end and the black hole quencher on the 3′-end in close
1990   proximity. As a result, the fluorescence signal decreased. The arm segment length (6-8 bp) of the
1991   aptamer (Table 1) was investigated regarding the formation of a stable THMS. The best results could
1992   be achieved with the longest one, so this was selected for further investigations.

1993   A label-free fluorescent strategy for tetracycline detection based on THMS an G-quadruplex was
1994   presented by Chen et al. [220]. A shortened 8-mer tetracycline specific aptamer sequence and two
1995   flanked arm segments, which can bind to the signal transduction probe, formed the THMS. The signal
1996   transduction probe consisted of thioflavin T and Guanosin-rich oligonucleotides. If no target was
1997   available, the THMS remained stable and the fluorescent background vanishingly low. The addition
1998   of tetracycline led to the formation of aptamer-target complexes, the disassembling of the THMS and
1999   the release of the signal transduction probe, which self-assembled into G-quadruplex, specifically
2000   bound to thioflavin T, resulting in a strong fluorescence signal.

2001   Ouyang et al. [221] developed a lanthanoide-doped UCNPs based aptasensor for the detection
2002   of tetracycline in food samples. The tetracycline specific aptamers were immobilized onto magnetic
2003   NPs via classical glutaraldehyde crosslink method and formed the capture probe. The signal probe
2004   consisted of cDNA modified ($NaY_{0.48}Gd_{0.3}F_4:Yb_{0.2}$, $Ho_{0.02}$) UCNPs. In the presence of tetracycline, the
2005   aptamer preferentially bound to it, resulting in the decay of the hybridized complex and the
2006   fluorescence signal caused by the UCNPs increased.

2007   Sun et al. [222] introduced a label-free fluorescent aptasensor for tetracycline detection based on
2008   thiazole orange as intercalated dye, according to the work of Xing et al. [83]. Essentially thiazole
2009   orange is no fluorescent in aqueous solution, but it shows high fluorescence emission intensity upon
2010   interaction with nucleic acids without regard to base composition. Thus, thiazole orange was
2011   intercalated into G-quadruplex structure of the tetracycline specific aptamers, resulting in a strong
2012   fluorescence signal. The addition of tetracycline resulted in the conformational change of the
2013   aptamers from G-quadruplex to hairpin structure, the formation of aptamer-target-complexes, the
2014   release of thiazole orange and finally a reduced fluorescence intensity.

2015   A chemiluminescent aptasensor for the simultaneous detection of kanamycin, oxytetracycline
2016   and tetracycline was developed by Hao et al. [92], as mentioned in the section of kanamycin.

2017   Liu et al. [206] presented a photoelectrochemical aptasensor for tetracycline detection. Graphitic
2018   carbon nitride (G-C_3N_4), a semiconductor, coupled with CdS QDs was used as transducer. The UV-
2019   Vis diffuse reflection spectra verified that the CdS QDs enhanced the absorption of G-C_3N_4 in the
2020   visible region and thus, dramatically promote the photocurrent response. A fluorine-doped tin oxide
2021   electrode was modified with the G-C_3N_4-CdS nanocomposite. The specific aptamer was anchored
2022   onto G-C_3N_4 surface via π-π stacking interaction between the nucleobases G-C_3N_4. The photocurrent
2023   increased, when tetracycline was added. In the presence of other antibiotics (e.g. chlortetracycline,
2024   doxycycline, kanamycin) no obvious responses were detected, revealing that the proposed
2025   aptasensor had a high specificity towards tetracycline, due to its specific aptamer-target recognition.

2026   A label-free "signal-off" photoelectrochemical aptasensor for the detection of tetracycline was
2027   introduced by Li et al. [223], based on localized SPR of AuNPs and dual-function quercetin. Quercetin
2028   is an electron donor, which can efficiency promote the separation of photonic carriers. A triple signal
2029   amplification has been applied to improve the sensitivity. Plasmonic AuNPs can convert collected
2030   light into electrical energy by generating hot electrons, which can be injected in the conduction band
2031   of TiO_2NPs by visible light irradiation. Moreover, the recombination of photonic carriers is reduced

by the rapid electron communication between AuNPs and TiO$_2$NPs. Furthermore, quercetin was chosen as both photosensitizer and electron sacrificial agent for enlarged photocurrent. The working electrode was first modified with a nano-TiO$_2$ film and then with AuNPs and acted as photoanode. Tetracycline specific aptamers were added and self-assembled onto the surface. The modified photoanode was covered with MCH to block nonspecific sites. With the addition of tetracycline, the photocurrent decreases due to the formation of an aptamer-tetracycline complex, which subsequently closed the entrance of long passageways and resulted in a hindered electron transfer.

Zhang et al. [224] developed a photoelectrochemical aptasensor for the detection of tetracycline. Spindle-like ZnO nanorods closely anchored to CdSNPs placed on AuNPs were synthesized and used as photoactive material by efficiently absorbing light and promoting electron transfer. A ITO electrode was modified with the prepared nanocomposite and tetracycline specific aptamers. In the presence of tetracycline, the aptamers capture their targets and a restored photocurrent signal is produced through the reaction between captured tetracycline and photogenerated holes.

Le et al. [225] presented an impedimetric electrochemical aptasensor for the detection of tetracycline. Tetracycline specific amino-modified aptamers were immobilized onto the surface of the Au electrode and subsequently tetracycline was added. Oxytetracycline, streptomycin and neomycin were introduced into the sensing system to verify the specificity towards tetracycline, which was found to be high.

Xu et al. [226] developed an impedimetric electrochemical aptasensor for tetracycline detection based on interdigitated array microelectrodes. SbZnNPs, which improves the electrochemical conductivity, were conjugated to chitosan and formed a SbZnNPs-chitosan nanocomposite. The microelectrode was modified with the nanocomposite by electrostatic adsorption of the Au-amino non-covalent bond. Subsequently thiolated aptamer was assembled onto the surface of the modified electrode. The addition of tetracycline caused an increase in the resistance response, because the response compound of tetracycline and the probe hindered the electron transfer. A comparison between the aptasensor with and without the nanocomposite proved the improving effect of the modification regarding to the sensitivity.

Another impedimetric electrochemical aptasensor for tetracycline detection was introduced by Zhao et al. [227], using interdigitated array microelectrodes and ionic-liquid-ferroferric oxide nanocomposite. Ferroferric oxide has a good electrochemical conductivity (electrons can quickly shift between two kinds of oxidation states) and formed a film on the microelectrode surface, resulting in an increased electrode area. The stability of the sensor was improved by adding ionic liquid, a biocompatible material. The aptamer was immobilized onto the modified microelectrode. The proposed aptasensor was successfully applied for tetracycline detection in milk samples.

A very similar aptasensor based on the same sensing principle of Zhao's work [227] was described by Hou et al. [228]. An interdigital array microelectrode was used to miniaturize the conventional electrode system, enhance the sensitivity, shorten the detection time and minimize interfering effects. Measurements of tetracycline in real milk samples demonstrated the possible use of the aptasensor for real sample analysis.

For tetracycline detection an electrochemical aptasensor was developed by Kim et al. [229], based on the modified screen-printed Au working electrode. Biotinylated and thiolated aptamers were compared regarding to their coverage ability of the SPE and the resulting higher sensitivity. The biotinylated variant showed better results and therefore was used for further investigations. In the presence of tetracycline, the electron transfer was hindered by the formed aptamer-tetracycline complex and the current response decreased.

Zhang et al. [203] described an label-free electrochemical aptasensor for the detection of tetracyclines. The tetracycline and oxytetracycline specific aptamer was selected by SELEX and coupled on a GCE via EDC/NHS-chemistry. The affinity constant was determined to be 218 mol^{-1}. The high specificity was verified by measurements in the presence of penicillin as an interference.

Zhou et al. [230] developed an electrochemical aptasensor for tetracycline detection with MWCNTs amplification. Ferricyanide solution acted as mediator to generate electron flow between bulk solution and working electrode. The GCE was modified with carboxyl-functionalized MWCNTs. MWCNTs are employed as the carriers of the electrochemical capture probe for an

amplified current upon target binding. The tetracycline specific amino-modified aptamer was added and self-assembled onto the electrode surface. Ethanolamine was used to remove non-specific adsorption. In the absence of tetracycline, a strong Faradaic current is observed. In the presence of tetracycline, the formation of an aptamer-target complex hinders the electron transfer, resulting in a decrease of the electrochemical signal.

A label-free aptasensor for electrochemical detection of tetracycline was designed by Chen et al. [231]. The tetracycline binding aptamer with highest affinity was screened out from a 13 bp ssDNA random sequence by isothermal titration calorimetry (ITC) and selected for further experiments. The aptamer was immobilized onto the surface of the working electrode. The interaction between the aptamer and tetracycline was investigated by the ferricyanide generated electron flow between bulk solution and working electrode and monitored by EIS. By initially addition of a mixture of possible interferents, the current response changed not until tetracycline was added, which proved the high specificity for tetracycline.

For tetracycline detection Shen et al. [232] introduced an electrochemical aptasensor, using an indicator consisted of prussian blue (PB), chitosan (CS) and glutaraldehyde (GA). The as-prepared CS-GA conjugate and subsequently PB were immobilized onto the GCE via electrodeposition. AuNPs were added and bound to the abundant primary amino-groups of CS. The tetracycline specific amino-functionalized aptamers covalently attached on the modified GCE. Finally, ethanolamine was used to remove non-specific adsorption on the functionalized electrode surface. The addition of tetracycline led to a decreased current response, because the formation of the aptamer-target complex hindered the electron transfer between PB and prussian white.

Another label-free electrochemical aptasensor for the detection of tetracycline was developed by Guo's team [233]. The GCE was modified with AuNPs by one-step electrodeposition method. Subsequently the tetracycline specific aptamer was immobilized onto the modified electrode via Au-S bonding and MB was dripped onto the electrode. The formation of an aptamer tetracycline complex hinders the electron transfer, resulting in a decrease of the redox peaks (CV) and an increase of the impedance (EIS), because of the nonconductive properties of the biomacromolecule.

Benvidi et al. [234] presented an electrochemical aptasensor for the detection of tetracycline. The GCE was modified with GO nanosheets. Via π-π stacking interactions between the ring structures in the nucleobases of the aptamers and the hexagonal cells of GO, the tetracycline specific aptamers were adsorbed onto the surface of GO. If tetracycline is added, the formation of the tetracycline-aptamer triggers an interfacial electron transfer to the electrode surface, resulting in an increased current.

Moreover, Guo et al. [235] introduced an electrochemical aptasensor for tetracycline detection, based on signal amplification MWCNTs and Fe_3O_4 dispersed in chitosan (CS). MWCNTs and Fe_3O_4 possess high electrical conductivity and CS can keep the biological activity of the biomolecules that immobilized on CS, because of its large amount of amino and hydroxyl groups. MWCNTs-CS, Fe_3O_4-CS and the tetracycline specific aptamer were immobilized onto the surface of the SPE. The CV current response decreased in the presence of tetracycline, because of the hindering of the electron transfer process. The applicability of the aptasensor in real samples was proved by tetracycline detection in milk.

Jahanbani & Benvidi [236] fabricated two similar electrochemical aptasensors and compared their performances for determination of tetracycline. The first aptasensor (aptasensor I) based on oleic acid modified carbon paste electrode (CPE). Oleic acid is able to react with the amine- aptamers after activation of its carboxyl group to form an amine-reactive ester. The second aptasensor (aptasensor II) based on magnetic bar inserted into CPE (MBCPE), which was further modified with Fe_3O_4 NPs and oleic acid. A free carboxyl group is provided on the surface of the Fe_3O_4 NPs by depositing a double layer of oleic acid, which improved the number of active groups. Subsequently the aptamers were immobilized onto the surface of the electrodes. For both aptasensors, lower LODs were obtained using EIS than using DPV (Table 1). The aptasensors II showed a wider dynamic range and lower LODs as well with EIS as with DPV than aptasensor I (Table 1). The higher sensitivity of aptasensor II is due to the fact, that the number of active groups (carboxylic acid) on the surface of aptasensor II is

higher than that on aptasensor I and furthermore due to the presence of magnetic bar, which adsorbs a high amount of NPs at the electrode surface and thus increases the effective electrode area.

A M-shape electrochemical aptasensor for the detection of tetracycline was developed by Taghdisi et al. [237]. The M-shape structure was constructed by immobilization of three partially complementary strands (cDNA I, II and III; Table 1) of the aptamer onto the surface of the SPGE and subsequently partially binding of the aptamer to each of the strands. The M-shape acts as a gate and barrier for the access of redox probe to the electrode surface. In the absence of tetracycline, the M-shape remains intact, leading to a weak electrochemical signal, monitored by DPV. Upon addition of tetracycline, the M-shape structure disassemble, because the aptamer leaves the cDNAs to form an aptamer-target conjugate. Exo I is introduced and degrades cDNA I and cDNA II from their 3´-terminus, resulting in more access of redox mediator to the electrode surface and thus to an increase of the electrochemical signal. DPV measurements in the simultaneous presence of doxycycline, amoxicillin, ciprofloxacin, chloramphenicol and clindamycin showed that doxycycline, which belong to the class of tetracyclines, caused an increased electrochemical signal. Therefore, the M-shape structure seems to be selective to more than representative of the tetracycline class.

A label-free electrochemical aptasensor for tetracycline detection was presented by Zhan et al. [238]. A nanocomposite was formed out of Fe_3O_4, rGO and sodium alginate, which was then modified the surface of a SPCE. Fe_3O_4 modified rGO possess high specific capacitance and stable cycling performance and sodium alginate is a biocompatible polymer, used for the immobilization of biomolecules. The tetracycline binding aptamer was immobilized on the modified electrode. Thionine acted as electrochemical redox probe for the investigation of the interaction between the aptamer and tetracycline, monitored by DPV. The long flexible aptamer chain prevents electrical contact of the redox probe with the electrode. Upon tetracycline addition, aptamer-target complex is formed, making the aptamer configuration rigid, resulting an orientation of the redox probe towards the electrode and an electron-transfer. In order to evaluate the specificity of the aptasensor towards tetracycline, were tested to be detected. In the presence of possible interfering substances (e.g. ampicillin, anthramycin, meropenem), only tetracycline triggered an increase of the electrochemical current response, indicating a high specificity to tetracycline.

Xu et al. [239] integrated two different aptasensors to construct a ratiometric electrochemical aptasensor for tetracycline detection based on ferrocene and carbon nanofibers. For the fabrication of sensor 1, ferrocene-labelled thiol-functionalized aptamers were immobilized onto surface of the AuNPs-chitosan nanocomposite modified SPCE via Au-SH interaction. For the fabrication of sensor 2, thiol-functionalized aptamers were immobilized onto the surface of the carbon nanofibers-AuNPs modified SPCE. The addition of tetracycline caused an increase of the electrochemical current. The tetracycline detection results of sensor 1 and sensor 2 were calculated by ratio. Thus, the problem of low accuracy and large differences between batches were solved.

Summarized, around half of all developed aptamer-based biosensors for the detection of tetracycline are based on electrochemical sensor principles (either impedimetric or amperometric). Colorimetric aptasensors are frequently used, mainly due to their simple handling and evaluation. In almost all of the mentioned studies, the same tetracycline specific ssDNA aptamer was used, which selected and investigated by Niazi et al. [190]. The summarised data in Table 1 shows, in comparison between the RNA aptamer [208] and the ssDNA aptamers applied for tetracycline detection, the RNA aptamer featured a lower K_D and thus a much higher affinity to tetracycline than the DNA aptamers [208]. By shortening the ssDNA sequence to the possible minimum with sufficient affinity, Kwon et al. [191] managed to achieve a similar high affinity of the ssDNA aptamer to the target, as Jeong et al. [208] reached with the RNA aptamer. The lowest LOD was obtained by Jahanbani's team [236] with the constructed impedimetric aptasensor II, followed by the amperometric one of Benvidi et al. [234]. Directly thereafter (before other developed electrochemical aptasensors) follows the colorimetric aptasensor of Tang et al. [218] and the SERS based one of Li et al. [212] which achieved similar sensitivity.

2.8 Sulfonamides

2188   Sulfonamides were the first synthetic antibiotics [143]. As the name suggests they are
2189   characterized by their sulfonamide group (marked red in Figure 9). As analogues of *p*-aminobenzoic
2190   acid they interfere with the synthesis of folic acid [1]. Sulfonamides acts against enterobacteria like
2191   *Escherichia coli* or *Salmonella* and are mainly used to treat urinary tract infection and pneumonia.

2192
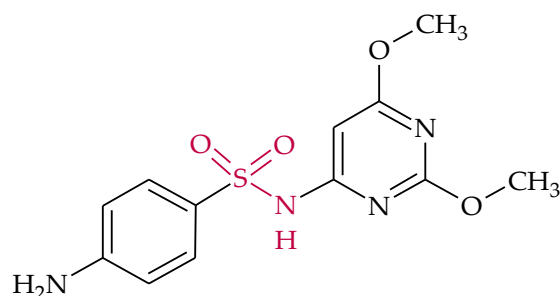
2193   **Figure 9:** Chemical structure of sulfadimethoxine. The sulfonamide group is marked red.

2194   2.8.1   Sulfadimethoxine

2195   Sulfadimethoxine (Figure 9) is a cheap broad-spectrum antibiotic, which is effective against
2196   bacterial and coccidial infections and used for treatment (and prevention) of poultry diseases [240,
2197   241].
2198   Song et al. [240] selected aptamers specific for sulfadimethoxine by magnetic bead-based SELEX
2199   and identified the one with highest affinity towards its target. Therefore, they applied a fluorescence
2200   binding assay wherein the different FAM-labelled aptamers were added to sulfadimethoxine-
2201   immobilized beads and the amount of each eluted aptamer sample was measured by fluorescence.
2202   Coordination polymer nanobelts acts as fluorescent quenchers, thus the aptamer is quenched due to
2203   its adsorption on the coordination polymer nanobelt in the absence of sulfadimethoxine and the
2204   fluorescence intensity decreases. Not even the derivates (sulfathiazole and sulfaquinoxaline) bound
2205   to the aptamer, which verified the high specificity of the aptamer. The developed aptamer was
2206   utilized in various further work [242].
2207   In the work of Liu et al. [249] actually two aptasensing procedures are applied: a fluorescence
2208   quenching one and a colorimetric one, similar to the system mentioned by Song et al. [61] for
2209   ampicillin detection. This fluorescence quenching and colorimetric aptasensors in general based on
2210   target-induced release of complimentary strand from aptamer, strong interaction of ssDNA and
2211   water resuspended AuNPs and less/no interaction of dsDNA and AuNPs. Liu and colleges were
2212   interested in the unknown effects of remnant non AuNPs in the colloid Au solution and therefore
2213   they examined sodium citrate, sodium acetate, sodium chloride, citric acid, ketoglutaric acid,
2214   hydrochloric acid with regard to an effect. The authors were able to demonstrate that sodium citrate
2215   and three acids influences both, fluorescent quenching and colorimetric aptasensor sensitivity. By the
2216   removal of them by using water resuspension AuNPs the sensitivity could improve by 10-folds.
2217   Chen et al. [241] developed a label-free colorimetric aptasensor for sensitively detection of
2218   sulfadimethoxine based on unmodified AuNPs. To improve the sensitivity of the aptasensor, the
2219   amount of aptamer adsorbed to AuNPs, the concentration of salt and the NPs pH value were
2220   optimized.
2221   Niu et al. [72] report the development of a AuNPs based colorimetric multiplex aptasensor
2222   wherein more than one aptamer serves the stability of the AuNPs. The principle of the aptasensor
2223   was first tested for each target itself and subsequent the multiplex aptasensor was developed.
2224   Sulfadimethoxine, kanamycin and adenosine were used as targets. Their specific aptamers were
2225   mixed at a volume ratio 1:1:1 and adsorbed directly onto the AuNPs surface. The addition of one,
2226   two or three targets lead to a conformation change of each corresponding aptamer from random
2227   coiled to rigid folded structure. Thus, the affected aptamers were no longer able to stabilize the
2228   AuNPs and finally the AuNPs aggregated (in a specific reaction buffer) which lead to a detectable
2229   (UV-Vis) color change of the solution. A series of experiments were performed to detect one, two or

three of the targets. With the mentioned homogenous multiplex system, a simultaneous detection of three targets was possible. However, when a sample gives a positive result it is not possible to determine which of the targets triggered the signal.

In the work of Yan et al. [243] an aptamer-based colorimetric biosensor for sulfadimethoxine detection is presented, which is practicable for fast-screening food analysis because of its high sensitivity with simultaneous short analysis time (about 15 min). The photometric assay based on inhibition and reactivation of the peroxidase-like activity of AuNPs. By the adsorption of target-specific ssDNA on the surface of AuNPs they are shielded and in consequence the peroxidase-like activity is inhibited. In the presence of its target (in this case sulfadimethoxine) the aptamer desorbs from the AuNPs surface which results in a reactivation of AuNPs catalytic property. Thus, TMB is oxidized by H_2O_2, resulting in a color change of the solution (from purple to blue) which is related to the analyte concentration and could be observed by bare eye or UV-Vis spectrometry.

Wang et al. [244] developed a colorimetric aptasensor for sulfadimethoxine detection based on peroxidase-like activity of graphene-Ni-Pd hybrids. The hybrids themselves could cause a visible color change in the reaction solution by oxidizing TMB in the presence of H_2O_2. The catalytic activity of the hybrids can be controlled by the aptamer through occupation in the active interface via π-π-stacking interaction between the bases of the aptamer and the graphene surface. In the presence of sulfadimethoxine, aptamer-target complexes are formed and due to the decrease of exposed base groups, the complex release from the surface of the hybrid. The peroxidase-like catalytic activity recovers with increasing amount of sulfadimethoxine, which at the end influences the color change of TMB.

Liu et al. [245] used magnetized UCNPs to design a fluorometric aptasensor for sulfadimethoxine detection. The $NaYF_4$:Yb, Tm UCNP acted as internal fluorophore signals and were modified with ssDNA strands complementary to the sulfadmethoxine specific aptamer (cDNA) via biotin-streptavidin interaction. In turn, magnetic nanoparticles were modified with the aptamer via biotin-streptavidin interaction, too. Then the prepared UCNPs and magnetic NPs were hybridized by attaching the aptamer to its cDNA. A part of the UCNPs dissociated from the surface of the magnetic NPs in the presence of sulfadimethoxine, whereby the fluorescence signal decreased. The magnetic property improved the efficiency of the process by using an extern magnetic to rapidly separate the bound targets. The quantification of the target in spiked perch and catfish samples prove the possible use of the aptasensor for real sample analysis.

For sulfadimethoxine detection Okoth et al. [246] constructed a photoelectrochemical aptasensor based on aptamer-chitosan-graphene-Bi_2S_3 modified electrode, in which bismuth sulfide (Bi_2S_3) nanorods doped with graphene were used as photoactive material. The effect of graphene doping on the performance of the sensor was determined by photoelectrochemical measurements. The influence of the amount of graphene on the electrical conductivity of the as-prepared material was conducted by EIS, using $[Fe(CN)_6]^{3-/4-}$ as redox probe.

According to the data of Table 1, most of the aptasensors developed for sulfadimethoxine detection were colorimetric ones. The ssDNA aptamer sequence with the corresponding K_D value, selected by Song et al. [240], was used in all above mentioned studies. As seen, Song et al. [240] and Yan et al. [243] reached the same LODs with the different systems. On the other hand, the PEC sensor of Liu et al. [245] showed a much higher (factor 92) sensitivity.

3. Summary

In recent years widespread and uncontrolled usage of antibiotics and accordingly their resistance has emerged as a serious problem. Therefore, simple, sensitive, robust and rapid methods for evaluation of antibiotic and their residues are needed for an on-site screening analysis. Among different analytical methods, the aptamer-based biosensors (aptasensors) are promising tools with notable recognition capabilities because of good selectivity, specificity, and sensitivity. This review describes various developed aptasensors for detection of eight different groups of antibiotics.

Electrochemical aptamer biosensors compared to other developed aptasensors are the most common used ones for antibiotic detection, because of their operational simplicity, high sensitivity, portability and low costs. Because antibiotics are most often not electrochemically active by themselves, redox tags like MB, Fc or the commonly used Fe^{2+}/Fe^{3+} system must be added. Target induced strand displacement is one of the most widely used signal transduction strategy in aptamer-based biosensors for antibiotic detection. The challenge in replacement reactions is that the affinity of the aptamer towards the target must be stronger than to the cDNA. The described indirect measuring methods, in which the target is immobilized, are usable for the proof of the function of the developed measurement method, but irrelevant for practical application.

Often a once established aptamer sequence, specific for a target, is used for almost all further studies. In general, the 5´-end of the aptamer-sequence is preferred for immobilization and the 3´-end for labeling (e.g. with FAM) of the aptamer. To evaluate the specificity of the used aptamer towards its target, structural similar derivates and possible interfering substances are introduced into the sensing system and their influence onto the signal and the detection of the actual target are investigated. In most of the developed aptasensors DNA-aptamers were used, just a few of the mentioned papers dealt with RNA-aptamers. RNA aptamers featured lower K_D values and thus a higher affinity to their target than DNA aptamers, but RNA is attacked and degraded faster. As shown in the table, and also compared with the standard HPLC or ELISA methods, sensitivity and selectivity of many aptasensors are acceptable.

The most commonly investigated antibiotics detected by an aptasensor are kanamycin, chloramphenicol, tetracycline and oxytetracycline. Therefore, a great potential for developing of aptamers for other antibiotics with high affinity and specificity exits.

2304   **Abbreviations**

2305	ABEI	*N*-(4-aminobutyl)-*N*-ethylisoluminol
2306	AC	alternating current
2307	AFM	atomic force microscopy
2308	AuNPs	gold nanoparticles
2309	BSA	bovine serum albumin
2310	CA	chronoamperometry
2311	CC	chronocoulometry
2312	CD	circular dichroism
2313	cDNA	complementary DNA
2314	CMOS	complementary metal oxide semiconductor
2315	CNT	carbon nanotube
2316	CRET	chemiluminescence resonance energy transfer
2317	CSRP	circular strand-replacement DNA polymerization
2318	CV	cyclic voltammetry
2319	Cy3/Cy5	cyanin 3, cyanin 5
2320	dNTPs	desoxyribinucleoside triphosphates
2321	DLS	dynamic light scattering
2322	dsDNA	double stranded DNA
2323	DPV	differential pulse voltammetry
2324	EDX	energy dispersive X-ray spectroscopy
2325	EEC	electrical equivalent circuit
2326	EIS	electrochemical impedance spectroscopy
2327	ELAA	enzyme-linked aptamer assay
2328	ELISA	enzyme-linked immunosorbent assay
2329	ELONA	enzyme-linked oligonucleotide assay
2330	EPR	electron paramagnetic resonance
2331	ESI-IMS	electrospray ionization-ion mobility spectrometry
2332	Exo	exonuclease
2333	FAM	carboxyfluorescein
2334	Fc	ferrocene
2335	FESEM	field emission scanning electron microscopy
2336	FIS	Faradaic impedance spectroscopy
2337	FRET	fluorescence resonance energy transfer
2338	FTIR	Fourier transform infrared spectroscopy
2339	GCE	glassy carbon electrode
2340	GO	graphene oxide
2341	HRP	horseradish peroxidase
2342	ITO	indium tin oxide
2343	K_D	dissociation constant
2344	LOD	limit of detection
2345	MB	methylene blue
2346	MBA	4-mercaptobenzoic acid
2347	MCH	6-mercapto-1-hexanol
2348	MIP	molecularly imprinted polymer
2349	MOF	metal organic framework
2350	MWCNTs	multi-walled carbon nanotubes
2351	NPs	nanoparticles
2352	OCPVD	open-circuit photovoltage decay
2353	OCV	open circuit voltage
2354	PAGE	polyacrylamide gel electrophoresis

2355	PCR	polymerase chain reaction
2356	QCM	quartz crystal microbalance
2357	QD	quantum dot
2358	rGO	reduced graphene oxide
2359	ROX	carboxy-X-rhodamine
2360	SAM	self-assembled monolayer
2361	SAW	surface acoustic wave
2362	SCE	saturated calomel electrode
2363	SELEX	systematic evolution of ligands by exponential enrichment
2364	SEM	scanning electron microscope
2365	SERS	surface-enhanced Raman scattering
2366	SPCE	screen-printed carbon electrode
2367	SPGE	screen-printed gold electrode
2368	SPE	screen-printed electrode
2369	SPR	surface plasmon resonance spectroscopy
2370	SSB	ssDNA binding protein
2371	ssDNA	single stranded DNA
2372	SWV	square wave voltammetry
2373	TEM	transmission electron microscopy
2374	THMS	triple-helix molecular switch
2375	TMB	3,3′,5,5′-tetramethylbenzidine
2376	PEDOT	poly(3,4-ethylenedioxythiophene)
2377	UCNPs	upconversion nanoparticles
2378	XPS	X-ray photoelectron spectroscopy
2379	XRD	X-ray diffraction

2380

2381   **Acknowledgments:** This work was funded by the European Social Fund (ESF) in Germany.

2382   **Author Contributions:** Yvonne Joseph and Asol Mehlhorn contributed to the design and implementation
2383   of the research. Asol Mehlhorn wrote the manuscript and Parvaneh Rahimi worked on the manuscript. All
2384   authors provided critical feedback and helped shape the research and manuscript.

2385   **Conflicts of Interest:**   The authors declare no conflict of interest.

2386

References

1. *Antibiotics. Targets, mechanisms and resistance;* Gualerzi, C.O.; Brandi, L.; Fabbretti, A.; Pon, C.L., Eds.; Wiley-VCH Verl.: Weinheim, 2014.

2. Schmid, R.D.; Hammelehle, R. *Taschenatlas der Biotechnologie und Gentechnik*, 2. Aufl.; Wiley-VCH: Weinheim, 2006.

3. Clara, M. *Antibiotika im Grundwasser*. *Sondermessprogramm im Rahmen der Gewässerzustandsüberwachungsverordnung;* Umweltbundesamt: Wien, 2010.

4. Onken, D. *Antibiotika*. *Chemie und Anwendung;* Akad.-Verl.: Berlin, 1985.

5. Briscoe, S.E.; McWhinney, B.C.; Lipman, J.; Roberts, J.A.; Ungerer, J.P.J. A method for determining the free (unbound) concentration of ten beta-lactam antibiotics in human plasma using high performance liquid chromatography with ultraviolet detection. *J. Chromatogr. B* **2012**, *907*, 178–184, doi:10.1016/j.jchromb.2012.09.016.

6. Dai, X.-h.; Xue, Y.-g.; Liu, H.-j.; Dai, L.-l.; Yan, H.; Li, N. Development of Determination Method of Fluoroquinolone Antibiotics in Sludge Based on Solid Phase Extraction and HPLC-Fluorescence Detection Analysis. *Huan Jing Ke Xue* **2016**, *37*, 1553–1561.

7. van den Meersche, T.; van Pamel, E.; van Poucke, C.; Herman, L.; Heyndrickx, M.; Rasschaert, G.; Daeseleire, E. Development, validation and application of an ultra high performance liquid chromatographic-tandem mass spectrometric method for the simultaneous detection and quantification of five different classes of veterinary antibiotics in swine manure. *J. Chromatogr. A* **2016**, *1429*, 248–257, doi:10.1016/j.chroma.2015.12.046.

8. Yu, Y.-J.; Wu, H.-L.; Fu, H.-Y.; Zhao, J.; Li, Y.-N.; Li, S.-F.; Kang, C.; Yu, R.-Q. Chromatographic background drift correction coupled with parallel factor analysis to resolve coelution problems in three-dimensional chromatographic data: Quantification of eleven antibiotics in tap water samples by high-performance liquid chromatography coupled with a diode array detector. *J. Chromatogr. A* **2013**, *1302*, 72–80, doi:10.1016/j.chroma.2013.06.009.

9. Yang, S.; Zhu, X.; Wang, J.; Jin, X.; Liu, Y.; Qian, F.; Zhang, S.; Chen, J. Combustion of hazardous biological waste derived from the fermentation of antibiotics using TG-FTIR and Py-GC/MS techniques. *Bioresource technology* **2015**, *193*, 156–163, doi:10.1016/j.biortech.2015.06.083.

10. Berendsen, B.J.A.; Wegh, R.S.; Memelink, J.; Zuidema, T.; Stolker, L.A.M. The analysis of animal faeces as a tool to monitor antibiotic usage. *Talanta* **2015**, *132*, 258–268, doi:10.1016/j.talanta.2014.09.022.

11. Martinez-Carballo, E.; Gonzalez-Barreiro, C.; Scharf, S.; Gans, O. Environmental monitoring study of selected veterinary antibiotics in animal manure and soils in Austria. *Environmental pollution* **2007**, *148*, 570–579, doi:10.1016/j.envpol.2006.11.035.

12. Haller, M.Y.; Müller, S.R.; McArdell, C.S.; Alder, A.C.; Suter, M.J.-F. Quantification of veterinary antibiotics (sulfonamides and trimethoprim) in animal manure by liquid chromatography–mass spectrometry. *J. Chromatogr. A* **2002**, *952*, 111–120, doi:10.1016/S0021-9673(02)00083-3.

13. Gbylik-Sikorska, M.; Posyniak, A.; Sniegocki, T.; Zmudzki, J. Liquid chromatography-tandem mass spectrometry multiclass method for the determination of antibiotics residues in water samples from water supply systems in food-producing animal farms. *Chemosphere* **2015**, *119*, 8–15, doi:10.1016/j.chemosphere.2014.04.105.

14. Koyun, A.; Ahlatcolu, E.; Koca, Y. Biosensors and Their Principles. In *Medical Technology Management and Patient Safety;* Mana Sezdi, Ed.; INTECH Open Access Publisher, 2012.

15. Mungroo, N.A.; Neethirajan, S. Biosensors for the detection of antibiotics in poultry industry-a review. *Biosensors* **2014**, *4*, 472–493, doi:10.3390/bios4040472.

16. Ellington, A.D.; Szostak, J.W. In vitro selection of RNA molecules that bind specific ligands. *Nature* **1990**, *346*, 818–822, doi:10.1038/346818a0.

17. Stoltenburg, R.; Reinemann, C.; Strehlitz, B. SELEX- A (r)evolutionary method to generate high-affinity nucleic acid ligands. *Biomol. Eng* **2007**, *24*, 381–403, doi:10.1016/j.bioeng.2007.06.001.

18. Wang, R.E.; Wu, H.; Niu, Y.; Cai, J. Improving the stability of aptamers by chemical modification. *Curr. Med. Chem.* **2011**, *18*, 4126–4138.

19. Jayasena, S.D. Aptamers: an emerging class of molecules that rival antibodies in diagnostics. *Clin. Chem* **1999**, *45*, 1628–1650.

20. Tuerk, C.; Gold, L. Systematic evolution of ligands by exponential enrichment: RNA ligands to bacteriophage T4 DNA polymerase. *Science* **1990**, *249*, 505–510, doi:10.1126/science.2200121.

21. Song, K.-M.; Lee, S.; Ban, C. Aptamers and their biological applications. *Sensors* **2012**, *12*, 612–631, doi:10.3390/s120100612.

22. Potyrailo, R.A.; Conrad, R.C.; Ellington, A.D.; Hieftje, G.M. Adapting Selected Nucleic Acid Ligands (Aptamers) to Biosensors. *Anal. Chem.* **1998**, *70*, 3419–3425, doi:10.1021/ac9802325.

23. Song, S.; Wang, L.; Li, J.; Fan, C.; Zhao, J. Aptamer-based biosensors. *Trends Anal. Chem.* **2008**, *27*, 108–117, doi:10.1016/j.trac.2007.12.004.

24. Gründler, P. *Chemical sensors. An introduction for scientists and engineers ; with 25 tables;* Springer: Berlin, Heidelberg, 2007.

25. Pfeiffer, F.; Mayer, G. Selection and Biosensor Application of Aptamers for Small Molecules. *Front Chem* **2016**, *4*, 25, doi:10.3389/fchem.2016.00025.

26. Hall, E.A.; Hummel, G. *Biosensoren. Mit 24 Tabellen;* Springer: Berlin u.a., 1995.

27. Anderson, M.L.; Morris, C.A.; Stroud, R.M.; Merzbacher, C.I.; Rolison, D.R. Colloidal Gold Aerogels: Preparation, Properties, and Characterization. *Langmuir* **1999**, *15*, 674–681, doi:10.1021/la980784i.

28. Mayer, K.M.; Hafner, J.H. Localized surface plasmon resonance sensors. *Chemical reviews* **2011**, *111*, 3828–3857, doi:10.1021/cr100313v.

29. Liu, S.; Leech, D.; Ju, H. Application of Colloidal Gold in Protein Immobilization, Electron Transfer, and Biosensing. *Analytical Letters* **2003**, *36*, 1–19, doi:10.1081/AL-120017740.

30. Sharma, T.K.; Ramanathan, R.; Weerathunge, P.; Mohammadtaheri, M.; Daima, H.K.; Shukla, R.; Bansal, V. Aptamer-mediated 'turn-off/turn-on' nanozyme activity of gold nanoparticles for kanamycin detection. *Chem. Commun.* **2014**, *50*, 15856–15859, doi:10.1039/c4cc07275h.

31. Wang, E., R.; Zhang, Y.; Cai, J.; Cai, W.; Gao, T. Aptamer-Based Fluorescent Biosensors. *Curr. Med. Chem* **2011**, *18*, 4175–4184, doi:10.2174/092986711797189637.

32. Zhao, H.; Gao, S.; Liu, M.; Chang, Y.; Fan, X.; Quan, X. Fluorescent assay for oxytetracycline based on a long-chain aptamer assembled onto reduced graphene oxide. *Microchim. Acta* **2013**, *180*, 829–835, doi:10.1007/s00604-013-1006-7.

33. Swathi, R.S.; Sebastian, K.L. Resonance energy transfer from a dye molecule to graphene. *J. Chem. Phys.* **2008**, *129*, 54703, doi:10.1063/1.2956498.

34. Swathi, R.S.; Sebastian, K.L. Long range resonance energy transfer from a dye molecule to graphene has (distance)(-4) dependence. *J. Chem. Phys.* **2009**, *130*, 86101, doi:10.1063/1.3077292.

35. Förster, T. Zwischenmolekulare Energiewanderung und Fluoreszenz. *Ann. Phys.* **1948**, *437*, 55–75, doi:10.1002/andp.19484370105.

36. Zhou, B.; Shi, B.; Jin, D.; Liu, X. Controlling upconversion nanocrystals for emerging applications. *Nat. Nanotechnol.* **2015**, *10*, 924–936, doi:10.1038/nnano.2015.251.

37. Wang, F.; Liu, X. Recent advances in the chemistry of lanthanide-doped upconversion nanocrystals. *Chem. Soc. Rev.* **2009**, *38*, 976–989, doi:10.1039/b809132n.

38. Fang, C.; Wu, S.; Duan, N.; Dai, S.; Wang, Z. Highly sensitive aptasensor for oxytetracycline based on upconversion and magnetic nanoparticles. *Anal. Methods* **2015**, *7*, 2585–2593, doi:10.1039/C4AY03035D.

39. Xue, J.; Liu, J.; Wang, C.; Tian, Y.; Zhou, N. Simultaneous electrochemical detection of multiple antibiotic residues in milk based on aptamers and quantum dots. *Anal. Methods* **2016**, *8*, 1981–1988, doi:10.1039/C5AY03136B.

40. Miao, Y.; Gan, N.; Li, T.; Cao, Y.; Hu, F.; Chen, Y. An ultrasensitive fluorescence aptasensor for chloramphenicol based on FRET between quantum dots as donor and the magnetic SiO2@Au NPs probe as acceptor with exonuclease-assisted target recycling. *Sens. Actuators, B* **2016**, *222*, 1066–1072, doi:10.1016/j.snb.2015.09.049.

41. Miao, Y.-B.; Ren, H.-X.; Gan, N.; Zhou, Y.; Cao, Y.; Li, T.; Chen, Y. A homogeneous and "off-on" fluorescence aptamer-based assay for chloramphenicol using vesicle quantum dot-gold colloid composite probes. *Anal. Chim. Acta* **2016**, *929*, 49–55, doi:10.1016/j.aca.2016.04.060.

2491   42. Namdari, P.; Negahdari, B.; Eatemadi, A. Synthesis, properties and biomedical applications of
2492   carbon-based quantum dots: An updated review. *Biomed. Pharmacother.* **2017**, *87*, 209–222,
2493   doi:10.1016/j.biopha.2016.12.108.
2494   43. Walling, M.A.; Novak, J.A.; Shepard, J.R.E. Quantum dots for live cell and in vivo imaging. *Int.*
2495   *J. Mol. Sci.* **2009**, *10*, 441–491, doi:10.3390/ijms10020441.
2496   44. Feng, C.; Dai, S.; Wang, L. Optical aptasensors for quantitative detection of small biomolecules:
2497   a review. *Biosens. Bioelectron.* **2014**, *59*, 64–74, doi:10.1016/j.bios.2014.03.014.
2498   45. Nguyen, H.H.; Park, J.; Kang, S.; Kim, M. Surface plasmon resonance: a versatile technique for
2499   biosensor applications. *Sensors* **2015**, *15*, 10481–10510, doi:10.3390/s150510481.
2500   46. Schlücker, S. Surface-enhanced Raman spectroscopy: concepts and chemical applications.
2501   *Angew. Chem. Int. Ed* **2014**, *53*, 4756–4795, doi:10.1002/anie.201205748.
2502   47. Chen, M.; Gan, N.; Zhou, Y.; Li, T.; Xu, Q.; Cao, Y.; Chen, Y. A novel aptamer- metal ions-
2503   nanoscale MOF based electrochemical biocodes for multiple antibiotics detection and signal
2504   amplification. *Sens. Actuators, B* **2017**, *242*, 1201–1209, doi:10.1016/j.snb.2016.08.185.
2505   48. Hayat, A.; Marty, J.L. Aptamer based electrochemical sensors for emerging environmental
2506   pollutants. *Front Chem* **2014**, *2*, 41, doi:10.3389/fchem.2014.00041.
2507   49. Nelson, D.L.; Cox, M.M.; Lehninger, A.L. *Lehninger Biochemie. Mit 131 Tabellen*, 4., vollst. überarb.
2508   u. erw. Aufl.; Springer: Berlin u.a., 2009.
2509   50. Schwedt, G. *Analytische Chemie. Grundlagen, Methoden und Praxis*, 1. Nachdr; Wiley-VCH:
2510   Weinheim, 2004.
2511   51. Armbruster, D.A.; Pry, T. Limit of Blank, Limit of Detection and Limit of Quantitation. *Clin*
2512   *Biochem Rev.* **2008**, 49–52.
2513   52. *Council Directive 96/23/EC of 29 April 1996 on measures to monitor certain substances and residues*
2514   *thereof in live animals and animal products and repealing Directives 85/358/EEC and 86/469/EEC and*
2515   *Decisions 89/187/EEC and 91/664/EEC. CD 96/23/EC*, 1996.
2516   53. Eggins, B.R. *Chemical sensors and biosensors;* Wiley: Chichester, 2002.
2517   54. Song, K.-M.; Jeong, E.; Jeon, W.; Cho, M.; Ban, C. Aptasensor for ampicillin using gold
2518   nanoparticle based dual fluorescence-colorimetric methods. *Anal. Bioanal. Chem.* **2012**, *402*, 2153–
2519   2161, doi:10.1007/s00216-011-5662-3.
2520   55. Dapra, J.; Lauridsen, L.H.; Nielsen, A.T.; Rozlosnik, N. Comparative study on aptamers as
2521   recognition elements for antibiotics in a label-free all-polymer biosensor. *Biosens. Bioelectron.*
2522   **2013**, *43*, 315–320, doi:10.1016/j.bios.2012.12.058.
2523   56. Luo, Z.; Wang, Y.; Lu, X.; Chen, J.; Wei, F.; Huang, Z.; Zhou, C.; Duan, Y. Fluorescent aptasensor
2524   for antibiotic detection using magnetic bead composites coated with gold nanoparticles and a
2525   nicking enzyme. *Anal. Chim. Acta* **2017**, *984*, 177–184, doi:10.1016/j.aca.2017.06.037.
2526   57. Rosati, G.; Daprà, J.; Cherré, S.; Rozlosnik, N. Performance Improvement by Layout Designs of
2527   Conductive Polymer Microelectrode Based Impedimetric Biosensors. *Electroanalysis* **2014**, *26*,
2528   1400–1408, doi:10.1002/elan.201400062.
2529   58. Sun, Y.; Perch-Nielsen, I.; Dufva, M.; Sabourin, D.; Bang, D.D.; Hogberg, J.; Wolff, A. Direct
2530   immobilization of DNA probes on non-modified plastics by UV irradiation and integration in
2531   microfluidic devices for rapid bioassay. *Anal. Bioanal. Chem.* **2012**, *402*, 741–748,
2532   doi:10.1007/s00216-011-5459-4.
2533   59. Wang, H.; Wang, Y.; Liu, S.; Yu, J.; Xu, W.; Guo, Y.; Huang, J. Target-aptamer binding triggered
2534   quadratic recycling amplification for highly specific and ultrasensitive detection of antibiotics
2535   at the attomole level. *Chem. Commun.* **2015**, *51*, 8377–8380, doi:10.1039/c5cc01473e.
2536   60. Wang, X.; Dong, S.; Gai, P.; Duan, R.; Li, F. Highly sensitive homogeneous electrochemical
2537   aptasensor for antibiotic residues detection based on dual recycling amplification strategy.
2538   *Biosens. Bioelectron.* **2016**, *82*, 49–54, doi:10.1016/j.bios.2016.03.055.
2539   61. Wang, J.; Ma, K.; Yin, H.; Zhou, Y.; Ai, S. Aptamer based voltammetric determination of
2540   ampicillin using a single-stranded DNA binding protein and DNA functionalized gold
2541   nanoparticles. *Microchim. Acta* **2018**, *185*, 589, doi:10.1007/s00604-017-2566-8.

62. Yu, Z.-g.; Lai, R.Y. A reagentless and reusable electrochemical aptamer-based sensor for rapid detection of ampicillin in complex samples. *Talanta* **2018**, *176*, 619–624, doi:10.1016/j.talanta.2017.08.057.

63. Yu, Z.-g.; Sutlief, A.L.; Lai, R.Y. Towards the development of a sensitive and selective electrochemical aptamer-based ampicillin sensor. *Sens. Actuators, B* **2018**, *258*, 722–729, doi:10.1016/j.snb.2017.11.193.

64. Gai, P.; Gu, C.; Hou, T.; Li, F. Ultrasensitive Self-Powered Aptasensor Based on Enzyme Biofuel Cell and DNA Bioconjugate: A Facile and Powerful Tool for Antibiotic Residue Detection. *Anal. Chem.* **2017**, *89*, 2163–2169, doi:10.1021/acs.analchem.6b05109.

65. Zhao, J.; Guo, W.; Pei, M.; Ding, F. GR–Fe 3 O 4 NPs and PEDOT–AuNPs composite based electrochemical aptasensor for the sensitive detection of penicillin. *Anal. Methods* **2016**, *8*, 4391–4397, doi:10.1039/C6AY00555A.

66. Paniel, N.; Istamboulie, G.; Triki, A.; Lozano, C.; Barthelmebs, L.; Noguer, T. Selection of DNA aptamers against penicillin G using Capture-SELEX for the development of an impedimetric sensor. *Talanta* **2017**, *162*, 232–240, doi:10.1016/j.talanta.2016.09.058.

67. Lee, A.-Y.; Ha, N.-R.; Jung, I.-P.; Kim, S.-H.; Kim, A.-R.; Yoon, M.-Y. Development of a ssDNA aptamer for detection of residual benzylpenicillin. *Anal. Biochem.* **2017**, *531*, 1–7, doi:10.1016/j.ab.2017.05.013.

68. Rowe, A.A.; Miller, E.A.; Plaxco, K.W. Reagentless measurement of aminoglycoside antibiotics in blood serum via an electrochemical, ribonucleic acid aptamer-based biosensor. *Anal. Chem.* **2010**, *82*, 7090–7095, doi:10.1021/ac101491d.

69. Song, K.-M.; Cho, M.; Jo, H.; Min, K.; Jeon, S.H.; Kim, T.; Han, M.S.; Ku, J.K.; Ban, C. Gold nanoparticle-based colorimetric detection of kanamycin using a DNA aptamer. *Anal. Biochem.* **2011**, *415*, 175–181, doi:10.1016/j.ab.2011.04.007.

70. Chen, J.; Li, Z.; Ge, J.; Yang, R.; Zhang, L.; Qu, L.-B.; Wang, H.-Q.; Zhang, L. An aptamer-based signal-on bio-assay for sensitive and selective detection of Kanamycin A by using gold nanoparticles. *Talanta* **2015**, *139*, 226–232, doi:10.1016/j.talanta.2015.02.036.

71. Bai, X.; Hou, H.; Zhang, B.; Tang, J. Label-free detection of kanamycin using aptamer-based cantilever array sensor. *Biosens. Bioelectron.* **2014**, *56*, 112–116, doi:10.1016/j.bios.2013.12.068.

72. Niu, S.; Lv, Z.; Liu, J.; Bai, W.; Yang, S.; Chen, A. Colorimetric aptasensor using unmodified gold nanoparticles for homogeneous multiplex detection. *PloS one* **2014**, *9*, e109263, doi:10.1371/journal.pone.0109263.

73. Wang, C.; Chen, D.; Wang, Q.; Tan, R. Kanamycin detection based on the catalytic ability enhancement of gold nanoparticles. *Biosens. Bioelectron.* **2017**, *91*, 262–267, doi:10.1016/j.bios.2016.12.042.

74. Zhou, N.; Luo, J.; Zhang, J.; You, Y.; Tian, Y. A label-free electrochemical aptasensor for the detection of kanamycin in milk. *Anal. Methods* **2015**, *7*, 1991–1996, doi:10.1039/C4AY02710H.

75. Xu, Y.; Han, T.; Li, X.; Sun, L.; Zhang, Y.; Zhang, Y. Colorimetric detection of kanamycin based on analyte-protected silver nanoparticles and aptamer-selective sensing mechanism. *Anal. Chim. Acta* **2015**, *891*, 298–303, doi:10.1016/j.aca.2015.08.013.

76. Ha, N.-R.; Jung, I.-P.; Kim, S.-H.; Kim, A.-R.; Yoon, M.-Y. Paper chip-based colorimetric sensing assay for ultra-sensitive detection of residual kanamycin. *Process Biochem.* **2017**, *62*, 161–168, doi:10.1016/j.procbio.2017.07.008.

77. Liu, J.; Zeng, J.; Tian, Y.; Zhou, N. An aptamer and functionalized nanoparticle-based strip biosensor for on-site detection of kanamycin in food samples. *The Analyst* **2017**, *143*, 182–189, doi:10.1039/c7an01476g.

78. Wang, Y.; Wang, B.; Shen, J.; Xiong, X.; Deng, S. Aptamer based bare eye detection of kanamycin by using a liquid crystal film on a glass support. *Microchim. Acta* **2017**, *184*, 3765–3771, doi:10.1007/s00604-017-2405-y.

79. Khabbaz, L.S.; Hassanzadeh-Khayyat, M.; Zaree, P.; Ramezani, M.; Abnous, K.; Taghdisi, S.M. Detection of kanamycin by using an aptamer-based biosensor using silica nanoparticles. *Anal. Methods* **2015**, *7*, 8611–8616, doi:10.1039/C5AY01807B.

80.   Liu, C.; Lu, C.; Tang, Z.; Chen, X.; Wang, G.; Sun, F. Aptamer-functionalized magnetic nanoparticles for simultaneous fluorometric determination of oxytetracycline and kanamycin. *Microchim. Acta* **2015**, *182*, 2567–2575, doi:10.1007/s00604-015-1628-z.

81.   Robati, R.Y.; Arab, A.; Ramezani, M.; Langroodi, F.A.; Abnous, K.; Taghdisi, S.M. Aptasensors for quantitative detection of kanamycin. *Biosens. Bioelectron.* **2016**, *82*, 162–172, doi:10.1016/j.bios.2016.04.011.

82.   Ramezani, M.; Danesh, N.M.; Lavaee, P.; Abnous, K.; Taghdisi, S.M. A selective and sensitive fluorescent aptasensor for detection of kanamycin based on catalytic recycling activity of exonuclease III and gold nanoparticles. *Sens. Actuators, B* **2016**, *222*, 1–7, doi:10.1016/j.snb.2015.08.024.

83.   Xing, Y.-P.; Liu, C.; Zhou, X.-H.; Shi, H.-C. Label-free detection of kanamycin based on a G-quadruplex DNA aptamer-based fluorescent intercalator displacement assay. *Sci. Rep.* **2015**, *5*, 8125, doi:10.1038/srep08125.

84.   Li, H.; Sun, D.-e.; Liu, Y.; Liu, Z. An ultrasensitive homogeneous aptasensor for kanamycin based on upconversion fluorescence resonance energy transfer. *Biosens. Bioelectron.* **2014**, *55*, 149–156, doi:10.1016/j.bios.2013.11.079.

85.   Wang, Y.; Ma, T.; Ma, S.; Liu, Y.; Tian, Y.; Wang, R.; Jiang, Y.; Hou, D.; Wang, J. Fluorometric determination of the antibiotic kanamycin by aptamer-induced FRET quenching and recovery between MoS2 nanosheets and carbon dots. *Microchim. Acta* **2017**, *184*, 203–210, doi:10.1007/s00604-016-2011-4.

86.   Ha, N.-R.; Jung, I.-P.; La, I.-J.; Jung, H.-S.; Yoon, M.-Y. Ultra-sensitive detection of kanamycin for food safety using a reduced graphene oxide-based fluorescent aptasensor. *Scientific reports* **2017**, *7*, 40305, doi:10.1038/srep40305.

87.   Liao, Q.G.; Wei, B.H.; Luo, L.G. Aptamer based fluorometric determination of kanamycin using double-stranded DNA and carbon nanotubes. *Microchim. Acta* **2017**, *184*, 627–632, doi:10.1007/s00604-016-2050-x.

88.   Tang, Y.; Gu, C.; Wang, C.; Song, B.; Zhou, X.; Lou, X.; He, M. Evanescent wave aptasensor for continuous and online aminoglycoside antibiotics detection based on target binding facilitated fluorescence quenching. *Biosens. Bioelectron.* **2018**, *102*, 646–651, doi:10.1016/j.bios.2017.12.006.

89.   Leung, K.-H.; He, H.-Z.; Chan, D.S.-H.; Fu, W.-C.; Leung, C.-H.; Ma, D.-L. An oligonucleotide-based switch-on luminescent probe for the detection of kanamycin in aqueous solution. *Sens. Actuators, B* **2013**, *177*, 487–492, doi:10.1016/j.snb.2012.11.053.

90.   Zhao, M.; Zhuo, Y.; Chai, Y.-Q.; Yuan, R. Au nanoparticles decorated C60 nanoparticle-based label-free electrochemiluminesence aptasensor via a novel "on-off-on" switch system. *Biomaterials* **2015**, *52*, 476–483, doi:10.1016/j.biomaterials.2015.02.058.

91.   Hao, L.; Duan, N.; Wu, S.; Xu, B.; Wang, Z. Chemiluminescent aptasensor for chloramphenicol based on N-(4-aminobutyl)-N-ethylisoluminol-functionalized flower-like gold nanostructures and magnetic nanoparticles. *Anal. Bioanal. Chem.* **2015**, *407*, 7907–7915, doi:10.1007/s00216-015-8957-y.

92.   Hao, L.; Gu, H.; Duan, N.; Wu, S.; Wang, Z. A chemiluminescent aptasensor for simultaneous detection of three antibiotics in milk. *Anal. Methods* **2016**, *8*, 7929–7936, doi:10.1039/C6AY02304E.

93.   Li, R.; Liu, Y.; Cheng, L.; Yang, C.; Zhang, J. Photoelectrochemical aptasensing of kanamycin using visible light-activated carbon nitride and graphene oxide nanocomposites. *Anal. Chem.* **2014**, *86*, 9372–9375, doi:10.1021/ac502616n.

94.   Xin, Y.; Li, Z.; Zhang, Z. Photoelectrochemical aptasensor for the sensitive and selective detection of kanamycin based on Au nanoparticle functionalized self-doped TiO2 nanotube arrays. *Chem. Commun.* **2015**, *51*, 15498–15501, doi:10.1039/c5cc05855d.

95.   Lv, J.; Lei, Q.; Xiao, Q.; Li, X.; Huang, Y.; Li, H. Facile fabrication of an "off-on" photoelectrochemical aptasensor for kanamycin detection based on polypyrrole/CeO 2. *Anal. Methods* **2017**, *9*, 4754–4759, doi:10.1039/C7AY01611E.

96.   Zhou, N.; Zhang, J.; Tian, Y. Aptamer-based spectrophotometric detection of kanamycin in milk. *Anal. Methods* **2014**, *6*, 1569, doi:10.1039/c3ay41816b.

97. Sharma, A.; Istamboulie, G.; Hayat, A.; Catanante, G.; Bhand, S.; Marty, J.L. Disposable and portable aptamer functionalized impedimetric sensor for detection of kanamycin residue in milk sample. *Sens. Actuators, B* **2017**, *245*, 507–515, doi:10.1016/j.snb.2017.02.002.

98. Zhu, Y.; Chandra, P.; Song, K.-M.; Ban, C.; Shim, Y.-B. Label-free detection of kanamycin based on the aptamer-functionalized conducting polymer/gold nanocomposite. *Biosens. Bioelectron.* **2012**, *36*, 29–34, doi:10.1016/j.bios.2012.03.034.

99. Sun, X.; Li, F.; Shen, G.; Huang, J.; Wang, X. Aptasensor based on the synergistic contributions of chitosan-gold nanoparticles, graphene-gold nanoparticles and multi-walled carbon nanotubes-cobalt phthalocyanine nanocomposites for kanamycin detection. *Analyst* **2014**, *139*, 299–308, doi:10.1039/c3an01840g.

100. Li, F.; Guo, Y.; Sun, X.; Wang, X. Aptasensor based on thionine, graphene–polyaniline composite film, and gold nanoparticles for kanamycin detection. *Eur Food Res Technol* **2014**, *239*, 227–236, doi:10.1007/s00217-014-2211-2.

101. Xu, W.; Wang, Y.; Liu, S.; Yu, J.; Wang, H.; Huang, J. A novel sandwich-type electrochemical aptasensor for sensitive detection of kanamycin based on GR–PANI and PAMAM–Au nanocomposites. *New J. Chem.* **2014**, *38*, 4931–4937, doi:10.1039/C4NJ00858H.

102. Guo, W.; Sun, N.; Qin, X.; Pei, M.; Wang, L. A novel electrochemical aptasensor for ultrasensitive detection of kanamycin based on MWCNTs-HMIMPF6 and nanoporous PtTi alloy. *Biosens. Bioelectron.* **2015**, *74*, 691–697, doi:10.1016/j.bios.2015.06.081.

103. Qin, X.; Guo, W.; Yu, H.; Zhao, J.; Pei, M. A novel electrochemical aptasensor based on MWCNTs–BMIMPF 6 and amino functionalized graphene nanocomposite films for determination of kanamycin. *Anal. Methods* **2015**, *7*, 5419–5427, doi:10.1039/C5AY00713E.

104. Qin, X.; Yin, Y.; Yu, H.; Guo, W.; Pei, M. A novel signal amplification strategy of an electrochemical aptasensor for kanamycin, based on thionine functionalized graphene and hierarchical nanoporous PtCu. *Biosens. Bioelectron.* **2016**, *77*, 752–758, doi:10.1016/j.bios.2015.10.050.

105. Chen, M.; Gan, N.; Zhou, Y.; Li, T.; Xu, Q.; Cao, Y.; Chen, Y. An electrochemical aptasensor for multiplex antibiotics detection based on metal ions doped nanoscale MOFs as signal tracers and RecJf exonuclease-assisted targets recycling amplification. *Talanta* **2016**, *161*, 867–874, doi:10.1016/j.talanta.2016.09.051.

106. Song, H.-Y.; Kang, T.-F.; Li, N.-N.; Lu, L.-P.; Cheng, S.-Y. Highly sensitive voltammetric determination of kanamycin based on aptamer sensor for signal amplification. *Anal. Methods* **2016**, *8*, 3366–3372, doi:10.1039/c6ay00152a.

107. Wang, H.; Wang, Y.; Liu, S.; Yu, J.; Guo, Y.; Xu, Y.; Huang, J. Signal-on electrochemical detection of antibiotics based on exonuclease III-assisted autocatalytic DNA biosensing platform. *RSC Adv.* **2016**, *6*, 43501–43508, doi:10.1039/c6ra06061g.

108. Wang, H.; Wang, Y.; Liu, S.; Yu, J.; Guo, Y.; Xu, Y.; Huang, J. Signal-on electrochemical detection of antibiotics at zeptomole level based on target-aptamer binding triggered multiple recycling amplification. *Biosens. Bioelectron.* **2016**, *80*, 471–476, doi:10.1016/j.bios.2016.02.014.

109. Song, H.-Y.; Kang, T.-F.; Lu, L.-P.; Cheng, S.-Y. Highly sensitive aptasensor based on synergetic catalysis activity of MoS2-Au-HE composite using cDNA-Au-GOD for signal amplification. *Talanta* **2017**, *164*, 27–33, doi:10.1016/j.talanta.2016.10.100.

110. Huang, S.; Gan, N.; Li, T.; Zhou, Y.; Cao, Y.; Dong, Y. Electrochemical aptasensor for multi-antibiotics detection based on endonuclease and exonuclease assisted dual recycling amplification strategy. *Talanta* **2018**, *179*, 28–36, doi:10.1016/j.talanta.2017.10.016.

111. Nikolaus, N.; Strehlitz, B. DNA-aptamers binding aminoglycoside antibiotics. *Sensors* **2014**, *14*, 3737–3755, doi:10.3390/s140203737.

112. Stoltenburg, R.; Nikolaus, N.; Strehlitz, B. Capture-SELEX: Selection of DNA Aptamers for Aminoglycoside Antibiotics. *J. Anal. Methods Chem.* **2012**, *2012*, 415697, doi:10.1155/2012/415697.

113. Ma, L.; Sun, N.; Tu, C.; Zhang, Q.; Diao, A. Design of an aptamer – based fluorescence displacement biosensor for selective and sensitive detection of kanamycin in aqueous samples. *RSC Adv.* **2017**, *7*, 38512–38518, doi:10.1039/C7RA07052G.

2698   114. Liu, R.; Yang, Z.; Guo, Q.; Zhao, J.; Ma, J.; Kang, Q.; Tang, Y.; Xue, Y.; Lou, X.; He, M. Signaling-
2699   Probe Displacement Electrochemical Aptamer-based Sensor (SD-EAB) for Detection of
2700   Nanomolar Kanamycin A. *Electrochim. Acta* **2015**, *182*, 516–523,
2701   doi:10.1016/j.electacta.2015.09.140.
2702   115. Wallis, M.G.; Ahsen, U. von; Schroeder, R.; Famulok, M. A novel RNA motif for neomycin
2703   recognition. *Chem. Biol.* **1995**, *2*, 543–552, doi:10.1016/1074-5521(95)90188-4.
2704   116. Ling, K.; Jiang, H.; Zhang, L.; Li, Y.; Yang, L.; Qiu, C.; Li, F.-R. A self-assembling RNA aptamer-
2705   based nanoparticle sensor for fluorometric detection of Neomycin B in milk. *Anal. Bioanal. Chem.*
2706   **2016**, *408*, 3593–3600, doi:10.1007/s00216-016-9441-z.
2707   117. de-los-Santos-Alvarez, N.; Lobo-Castanon, M.J.; Miranda-Ordieres, A.J.; Tunon-Blanco, P.
2708   Modified-RNA aptamer-based sensor for competitive impedimetric assay of neomycin B. *J. Am.*
2709   *Chem. Soc.* **2007**, *129*, 3808–3809, doi:10.1021/ja0689482.
2710   118. de-los-Santos-Alvarez, N.; Lobo-Castanon, M.J.; Miranda-Ordieres, A.J.; Tunon-Blanco, P. SPR
2711   sensing of small molecules with modified RNA aptamers: detection of neomycin B. *Biosens.*
2712   *Bioelectron.* **2009**, *24*, 2547–2553, doi:10.1016/j.bios.2009.01.011.
2713   119. Wang, Y.; Rando, R.R. Specific binding of aminoglycoside antibiotics to RNA. *Chem. Biol.* **1995**,
2714   *2*, 281–290, doi:10.1016/1074-5521(95)90047-0.
2715   120. Spiga, F.M.; Maietta, P.; Guiducci, C. More DNA-Aptamers for Small Drugs: A Capture-SELEX
2716   Coupled with Surface Plasmon Resonance and High-Throughput Sequencing. *ACS Comb. Sci.*
2717   **2015**, *17*, 326–333, doi:10.1021/acscombsci.5b00023.
2718   121. Cappi, G.; Spiga, F.M.; Moncada, Y.; Ferretti, A.; Beyeler, M.; Bianchessi, M.; Decosterd, L.;
2719   Buclin, T.; Guiducci, C. Label-free detection of tobramycin in serum by transmission-localized
2720   surface plasmon resonance. *Anal. Chem.* **2015**, *87*, 5278–5285, doi:10.1021/acs.analchem.5b00389.
2721   122. Han, X.; Zhang, Y.; Nie, J.; Zhao, S.; Tian, Y.; Zhou, N. Gold nanoparticle based photometric
2722   determination of tobramycin by using new specific DNA aptamers. *Microchim. Acta* **2018**, *185*,
2723   340, doi:10.1007/s00604-017-2568-6.
2724   123. Ma, Q.; Wang, Y.; Jia, J.; Xiang, Y. Colorimetric aptasensors for determination of tobramycin in
2725   milk and chicken eggs based on DNA and gold nanoparticles. *Food chemistry* **2018**, *249*, 98–103,
2726   doi:10.1016/j.foodchem.2018.01.022.
2727   124. González-Fernández, E.; de-los-Santos-Álvarez, N.; Lobo-Castañón, M.J.; Miranda-Ordieres,
2728   A.J.; Tuñón-Blanco, P. Impedimetric aptasensor for tobramycin detection in human serum.
2729   *Biosens. Bioelectron.* **2010**, *26*, 2354–2360, doi:10.1016/j.bios.2010.10.011.
2730   125. González-Fernández, E.; de-los-Santos-Álvarez, N.; Lobo-Castañón, M.J.; Miranda-Ordieres,
2731   A.J.; Tuñón-Blanco, P. Aptamer-Based Inhibition Assay for the Electrochemical Detection of
2732   Tobramycin Using Magnetic Microparticles. *Electroanalysis* **2011**, *23*, 43–49,
2733   doi:10.1002/elan.201000567.
2734   126. González-Fernández, E.; de-los-Santos-Álvarez, N.; Miranda-Ordieres, A.J.; Lobo-Castañón,
2735   M.J. Monovalent labeling system improves the sensitivity of aptamer-based inhibition assays
2736   for small molecule detection. *Sens. Actuators, B* **2013**, *182*, 668–674, doi:10.1016/j.snb.2013.03.070.
2737   127. Schoukroun-Barnes, L.R.; Wagan, S.; White, R.J. Enhancing the analytical performance of
2738   electrochemical RNA aptamer-based sensors for sensitive detection of aminoglycoside
2739   antibiotics. *Anal. Chem.* **2014**, *86*, 1131–1137, doi:10.1021/ac4029054.
2740   128. Zhou, N.; Wang, J.; Zhang, J.; Li, C.; Tian, Y.; Wang, J. Selection and identification of
2741   streptomycin-specific single-stranded DNA aptamers and the application in the detection of
2742   streptomycin in honey. *Talanta* **2013**, *108*, 109–116, doi:10.1016/j.talanta.2013.01.064.
2743   129. Liu, Z.; Zhang, Y.; Xie, Y.; Sun, Y.; Bi, K.; Cui, Z.; Zhao, L.; Fan, W. An aptamer-based
2744   colorimetric sensor for streptomycin and its application in food inspection. *Chem. Res. Chin.*
2745   *Univ.* **2017**, *33*, 714–720, doi:10.1007/s40242-017-7029-6.
2746   130. Luan, Q.; Miao, Y.; Gan, N.; Cao, Y.; Li, T.; Chen, Y. A POCT colorimetric aptasensor for
2747   streptomycin detection using porous silica beads- enzyme linked polymer aptamer probes and
2748   exonuclease-assisted target recycling for signal amplification. *Sensors and Actuators B: Chemical*
2749   **2017**, *251*, 349–358, doi:10.1016/j.snb.2017.04.149.

2750 131. Zhao, J.; Wu, Y.; Tao, H.; Chen, H.; Yang, W.; Qiu, S. Colorimetric detection of streptomycin in
2751   milk based on peroxidase-mimicking catalytic activity of gold nanoparticles. *RSC Adv.* **2017**, *7*,
2752   38471–38478, doi:10.1039/C7RA06434A.
2753 132. Emrani, A.S.; Danesh, N.M.; Lavaee, P.; Ramezani, M.; Abnous, K.; Taghdisi, S.M. Colorimetric
2754   and fluorescence quenching aptasensors for detection of streptomycin in blood serum and milk
2755   based on double-stranded DNA and gold nanoparticles. *Food Chem.* **2016**, *190*, 115–121,
2756   doi:10.1016/j.foodchem.2015.05.079.
2757 133. Taghdisi, S.M.; Danesh, N.M.; Nameghi, M.A.; Ramezani, M.; Abnous, K. A label-free
2758   fluorescent aptasensor for selective and sensitive detection of streptomycin in milk and blood
2759   serum. *Food Chem.* **2016**, *203*, 145–149, doi:10.1016/j.foodchem.2016.02.017.
2760 134. Wu Caiye; Gan, N.; Ou, C.; Tang, H.; Zhou, Y.; Cao, J. A homogenous "signal-on" aptasensor
2761   for antibiotics based on a single stranded DNA binding protein-quantum dot aptamer probe
2762   coupling exonuclease-assisted target recycling for signal amplification. *RSC Adv.* **2017**, *7*, 8381–
2763   8387, doi:10.1039/C6RA27337H.
2764 135. Lin, B.; Yu, Y.; Cao, Y.; Guo, M.; Zhu, D.; Dai, J.; Zheng, M. Point-of-care testing for streptomycin
2765   based on aptamer recognizing and digital image colorimetry by smartphone. *Biosens. Bioelectron.*
2766   **2018**, *100*, 482–489, doi:10.1016/j.bios.2017.09.028.
2767 136. Xu, X.; Liu, D.; Luo, L.; Li, L.; Wang, K.; You, T. Photoelectrochemical aptasensor based on CdTe
2768   quantum dots-single walled carbon nanohorns for the sensitive detection of streptomycin. *Sens.*
2769   *Actuators, B* **2017**, *251*, 564–571, doi:10.1016/j.snb.2017.04.168.
2770 137. Ghanbari, K.; Roushani, M. A novel electrochemical aptasensor for highly sensitive and
2771   quantitative detection of the streptomycin antibiotic. *Bioelectrochemistry* **2018**, *120*, 43–48,
2772   doi:10.1016/j.bioelechem.2017.11.006.
2773 138. Danesh, N.; Ramezani, M.; Sarreshtehdar Emrani, A.; Abnous, K.; Taghdisi, S.M. A novel
2774   electrochemical aptasensor based on arch-shape structure of aptamer-complimentary strand
2775   conjugate and exonuclease I for sensitive detection of streptomycin. *Biosens. Bioelectron.* **2016**, *75*,
2776   123–128, doi:10.1016/j.bios.2015.08.017.
2777 139. Yin, J.; Guo, W.; Qin, X.; Pei, M.; Wang, L.; Ding, F. A regular "signal attenuation"
2778   electrochemical aptasensor for highly sensitive detection of streptomycin. *New J. Chem.* **2016**, *40*,
2779   9711–9718, doi:10.1039/C6NJ02209J.
2780 140. Yin, Y.; Qin, X.; Wang, Q.; Yin, Y. A novel electrochemical aptasensor for sensitive detection of
2781   streptomycin based on gold nanoparticle-functionalized magnetic multi-walled carbon
2782   nanotubes and nanoporous PtTi alloy. *RSC Adv.* **2016**, *6*, 39401–39408, doi:10.1039/C6RA02029A.
2783 141. Yin, J.; Guo, W.; Qin, X.; Zhao, J.; Pei, M.; Ding, F. A sensitive electrochemical aptasensor for
2784   highly specific detection of streptomycin based on the porous carbon nanorods and
2785   multifunctional graphene nanocomposites for signal amplification. *Sens. Actuators, B* **2017**, *241*,
2786   151–159, doi:10.1016/j.snb.2016.10.062.
2787 142. Lüllmann, H.; Mohr, K.; Wehling, M. *Pharmakologie und Toxikologie*. *Arzneimittelwirkungen*
2788   *verstehen - Medikamente gezielt einsetzen*, 14., komplett überarb. und neu gestaltete Aufl.; Thieme:
2789   Stuttgart, 1999.
2790 143. Koolman, J.; Röhm, K.-H. *Taschenatlas der Biochemie*, 2., überarb. und erw. Aufl.; Thieme:
2791   Stuttgart, 1998.
2792 144. He, L.; Zhi, W.; Wu, Y.; Zhan, S.; Wang, F.; Xing, H.; Zhou, P. A highly sensitive resonance
2793   scattering based sensor using unmodified gold nanoparticles for daunomycin detection in
2794   aqueous solution. *Anal. Methods* **2012**, *4*, 2266, doi:10.1039/c2ay25596k.
2795 145. Wochner, A.; Menger, M.; Orgel, D.; Cech, B.; Rimmele, M.; Erdmann, V.A.; Glokler, J. A DNA
2796   aptamer with high affinity and specificity for therapeutic anthracyclines. *Anal. Biochem.* **2008**,
2797   *373*, 34–42, doi:10.1016/j.ab.2007.09.007.
2798 146. Chandra, P.; Noh, H.-B.; Won, M.-S.; Shim, Y.-B. Detection of daunomycin using
2799   phosphatidylserine and aptamer co-immobilized on Au nanoparticles deposited conducting
2800   polymer. *Biosens. Bioelectron.* **2011**, *26*, 4442–4449, doi:10.1016/j.bios.2011.04.060.

147. Mehta, J.; van Dorst, B.; Rouah-Martin, E.; Herrebout, W.; Scippo, M.-L.; Blust, R.; Robbens, J. In vitro selection and characterization of DNA aptamers recognizing chloramphenicol. *J. Biotechnol.* **2011**, *155*, 361–369, doi:10.1016/j.jbiotec.2011.06.043.

148. Miao, Y.; Gan, N.; Li, T.; Zhang, H.; Cao, Y.; Jiang, Q. A colorimetric aptasensor for chloramphenicol in fish based on double-stranded DNA antibody labeled enzyme-linked polymer nanotracers for signal amplification. *Sens. Actuators, B* **2015**, *220*, 679–687, doi:10.1016/j.snb.2015.05.106.

149. Miao, Y.; Gan, N.; Ren, H.-X.; Li, T.; Cao, Y.; Hu, F.; Yan, Z.; Chen, Y. A triple-amplification colorimetric assay for antibiotics based on magnetic aptamer-enzyme co-immobilized platinum nanoprobes and exonuclease-assisted target recycling. *The Analyst* **2015**, *140*, 7663–7671, doi:10.1039/c5an01142f.

150. Miao, Y.-B.; Ren, H.-X.; Gan, N.; Zhou, Y.; Cao, Y.; Li, T.; Chen, Y. A triple-amplification SPR electrochemiluminescence assay for chloramphenicol based on polymer enzyme-linked nanotracers and exonuclease-assisted target recycling. *Biosens. Bioelectron.* **2016**, *86*, 477–483, doi:10.1016/j.bios.2016.07.007.

151. Miao, Y.-B.; Ren, H.-X.; Gan, N.; Cao, Y.; Li, T.; Chen, Y. Fluorescent aptasensor for chloramphenicol detection using DIL-encapsulated liposome as nanotracer. *Biosens. Bioelectron.* **2016**, *81*, 454–459, doi:10.1016/j.bios.2016.03.034.

152. Miao, Y.-B.; Gan, N.; Ren, H.-X.; Li, T.; Cao, Y.; Hu, F.; Chen, Y. Switch-on fluorescence scheme for antibiotics based on a magnetic composite probe with aptamer and hemin/G-quadruplex coimmobilized nano-Pt-luminol as signal tracer. *Talanta* **2016**, *147*, 296–301, doi:10.1016/j.talanta.2015.10.005.

153. Abnous, K.; Danesh, N.M.; Ramezani, M.; Emrani, A.S.; Taghdisi, S.M. A novel colorimetric sandwich aptasensor based on an indirect competitive enzyme-free method for ultrasensitive detection of chloramphenicol. *Biosens. Bioelectron.* **2016**, *78*, 80–86, doi:10.1016/j.bios.2015.11.028.

154. Alibolandi, M.; Hadizadeh, F.; Vajhedin, F.; Abnous, K.; Ramezani, M. Design and fabrication of an aptasensor for chloramphenicol based on energy transfer of CdTe quantum dots to graphene oxide sheet. *Mater. Sci. Eng. C* **2015**, *48*, 611–619, doi:10.1016/j.msec.2014.12.052.

155. Wu, S.; Zhang, H.; Shi, Z.; Duan, N.; Fang, C.; Dai, S.; Wang, Z. Aptamer-based fluorescence biosensor for chloramphenicol determination using upconversion nanoparticles. *Food Control* **2015**, *50*, 597–604, doi:10.1016/j.foodcont.2014.10.003.

156. Duan, Y.; Wang, L.; Gao, Z.; Wang, H.; Zhang, H.; Li, H. An aptamer-based effective method for highly sensitive detection of chloramphenicol residues in animal-sourced food using real-time fluorescent quantitative PCR. *Talanta* **2017**, *165*, 671–676, doi:10.1016/j.talanta.2016.12.090.

157. Wang, Y.; Gan, N.; Zhou, Y.; Li, T.; Cao, Y.; Chen, Y. Novel single-stranded DNA binding protein-assisted fluorescence aptamer switch based on FRET for homogeneous detection of antibiotics. *Biosens. Bioelectron.* **2017**, *87*, 508–513, doi:10.1016/j.bios.2016.08.107.

158. Feng, X.; Gan, N.; Lin, S.; Li, T.; Cao, Y.; Hu, F.; Jiang, Q.; Chen, Y. Ratiometric electrochemiluminescent aptasensor array for antibiotic based on internal standard method and spatial-resolved technique. *Sens. Actuators, B* **2016**, *226*, 305–311, doi:10.1016/j.snb.2015.11.131.

159. Feng, X.; Gan, N.; Zhang, H.; Yan, Q.; Li, T.; Cao, Y.; Hu, F.; Yu, H.; Jiang, Q. A novel "dual-potential" electrochemiluminescence aptasensor array using CdS quantum dots and luminol-gold nanoparticles as labels for simultaneous detection of malachite green and chloramphenicol. *Biosens. Bioelectron.* **2015**, *74*, 587–593, doi:10.1016/j.bios.2015.06.048.

160. Liu, Y.; Yan, K.; Okoth, O.K.; Zhang, J. A label-free photoelectrochemical aptasensor based on nitrogen-doped graphene quantum dots for chloramphenicol determination. *Biosens. Bioelectron.* **2015**, *74*, 1016–1021, doi:10.1016/j.bios.2015.07.067.

161. Wang, Y.; Bian, F.; Qin, X.; Wang, Q. Visible light photoelectrochemical aptasensor for chloramphenicol by using a TiO2 nanorod array sensitized with Eu(III)-doped CdS quantum dots. *Microchim. Acta* **2018**, *185*, 906, doi:10.1007/s00604-018-2711-z.

162. Pilehvar, S.; Dierckx, T.; Blust, R.; Breugelmans, T.; Wael, K. de. An electrochemical impedimetric aptasensing platform for sensitive and selective detection of small molecules such as chloramphenicol. *Sensors* **2014**, *14*, 12059–12069, doi:10.3390/s140712059.

2854   163. Pilehvar, S.; Mehta, J.; Dardenne, F.; Robbens, J.; Blust, R.; Wael, K. de. Aptasensing of
2855   chloramphenicol in the presence of its analogues: reaching the maximum residue limit. *Anal.*
2856   *Chem.* **2012**, *84*, 6753–6758, doi:10.1021/ac3012522.

2857   164. Pilehvar, S.; Dardenne, F.; Blust, R.; wael, K. de. Electrochemical sensing of phenicol antibiotics
2858   at gold. *Int. J. Electrochem. Sci* **2012**, 5000–5011.

2859   165. Yan, L.; Luo, C.; Cheng, W.; Mao, W.; Zhang, D.; Ding, S. A simple and sensitive electrochemical
2860   aptasensor for determination of Chloramphenicol in honey based on target-induced strand
2861   release. *J. Electroanal. Chem.* **2012**, *687*, 89–94, doi:10.1016/j.jelechem.2012.10.016.

2862   166. Yadav, S.K.; Agrawal, B.; Chandra, P.; Goyal, R.N. In vitro chloramphenicol detection in a
2863   Haemophilus influenza model using an aptamer-polymer based electrochemical biosensor.
2864   *Biosens. Bioelectron.* **2014**, *55*, 337–342, doi:10.1016/j.bios.2013.12.031.

2865   167. Bagheri Hashkavayi, A.; Bakhsh Raoof, J.; Ojani, R.; Hamidi Asl, E. Label-Free Electrochemical
2866   Aptasensor for Determination of Chloramphenicol Based on Gold Nanocubes-Modified Screen-
2867   Printed Gold Electrode. *Electroanalysis* **2015**, *27*, 1449–1456, doi:10.1002/elan.201400718.

2868   168. Hamidi-Asl, E.; Dardenne, F.; Blust, R.; Wael, K. de. An improved electrochemical aptasensor
2869   for chloramphenicol detection based on aptamer incorporated gelatine. *Sensors* **2015**, *15*, 7605–
2870   7618, doi:10.3390/s150407605.

2871   169. Rosy, R.; Goyal, R.N.; Shim, Y.-B. Glutaraldehyde sandwiched amino functionalized polymer
2872   based aptasensor for the determination and quantification of chloramphenicol. *RSC Adv.* **2015**,
2873   *5*, 69356–69364, doi:10.1039/C5RA11131E.

2874   170. Yan, Z.; Gan, N.; Wang, D.; Cao, Y.; Chen, M.; Li, T.; Chen, Y. A "signal-on" aptasensor for
2875   simultaneous detection of chloramphenicol and polychlorinated biphenyls using multi-metal
2876   ions encoded nanospherical brushes as tracers. *Biosens. Bioelectron.* **2015**, *74*, 718–724,
2877   doi:10.1016/j.bios.2015.07.024.

2878   171. Bagheri Hashkavayi, A.; Raoof, J.B.; Azimi, R.; Ojani, R. Label-free and sensitive aptasensor
2879   based on dendritic gold nanostructures on functionalized SBA-15 for determination of
2880   chloramphenicol. *Anal. Bioanal. Chem.* **2016**, *408*, 2557–2565, doi:10.1007/s00216-016-9358-6.

2881   172. Yan, Z.; Gan, N.; Li, T.; Cao, Y.; Chen, Y. A sensitive electrochemical aptasensor for multiplex
2882   antibiotics detection based on high-capacity magnetic hollow porous nanotracers coupling
2883   exonuclease-assisted cascade target recycling. *Biosens. Bioelectron.* **2016**, *78*, 51–57,
2884   doi:10.1016/j.bios.2015.11.019.

2885   173. Chen, M.; Gan, N.; Li, T.; Wang, Y.; Xu, Q.; Chen, Y. An electrochemical aptasensor for multiplex
2886   antibiotics detection using Y-shaped DNA-based metal ions encoded probes with NMOF
2887   substrate and CSRP target-triggered amplification strategy. *Anal. Chim. Acta* **2017**, *968*, 30–39,
2888   doi:10.1016/j.aca.2017.03.024.

2889   174. Liu, S.; Lai, G.; Zhang, H.; Yu, A. Amperometric aptasensing of chloramphenicol at a glassy
2890   carbon electrode modified with a nanocomposite consisting of graphene and silver
2891   nanoparticles. *Microchim. Acta* **2017**, *184*, 1445–1451, doi:10.1007/s00604-017-2138-y.

2892   175. Lavaee, P.; Danesh, N.M.; Ramezani, M.; Abnous, K.; Taghdisi, S.M. Colorimetric aptamer based
2893   assay for the determination of fluoroquinolones by triggering the reduction-catalyzing activity
2894   of gold nanoparticles. *Microchim. Acta* **2017**, *11*, 81, doi:10.1007/s00604-017-2213-4.

2895   176. Abnous, K.; Danesh, N.M.; Alibolandi, M.; Ramezani, M.; Taghdisi, S.M.; Emrani, A.S. A novel
2896   electrochemical aptasensor for ultrasensitive detection of fluoroquinolones based on single-
2897   stranded   DNA-binding   protein.   *Sens.   Actuators,   B*   **2017**,   *240*,   100–106,
2898   doi:10.1016/j.snb.2016.08.100.

2899   177. Han, S.R.; Yu, J.; Lee, S.-W. In vitro selection of RNA aptamers that selectively bind
2900   danofloxacin. *Biochem. Biophys. Res. Commun.* **2014**, *448*, 397–402, doi:10.1016/j.bbrc.2014.04.103.

2901   178. Liu, X.; Su, L.; Zhu, L.; Gao, X.; Wang, Y.; Bai, F.; Tang, Y.; Li, J. Hybrid material for enrofloxacin
2902   sensing based on aptamer-functionalized magnetic nanoparticle conjugated with upconversion
2903   nanoprobes. *Sens. Actuators, B* **2016**, *233*, 394–401, doi:10.1016/j.snb.2016.04.096.

2904   179. Liu, X.; Ren, J.; Su, L.; Gao, X.; Tang, Y.; Ma, T.; Zhu, L.; Li, J. Novel hybrid probe based on
2905   double recognition of aptamer-molecularly imprinted polymer grafted on upconversion

nanoparticles for enrofloxacin sensing. *Biosens. Bioelectron.* **2017**, *87*, 203–208, doi:10.1016/j.bios.2016.08.051.

180. Pilehvar, S.; Reinemann, C.; Bottari, F.; Vanderleyden, E.; van Vlierberghe, S.; Blust, R.; Strehlitz, B.; Wael, K. de. A joint action of aptamers and gold nanoparticles chemically trapped on a glassy carbon support for the electrochemical sensing of ofloxacin. *Sens. Actuators, B* **2017**, *240*, 1024–1035, doi:10.1016/j.snb.2016.09.075.

181. Reinemann, C.; Freiin von Fritsch, U.; Rudolph, S.; Strehlitz, B. Generation and characterization of quinolone-specific DNA aptamers suitable for water monitoring. *Biosens. Bioelectron.* **2016**, *77*, 1039–1047, doi:10.1016/j.bios.2015.10.069.

182. Li, S.; Liu, C.; Yin, G.; Zhang, Q.; Luo, J.; Wu, N. Aptamer-molecularly imprinted sensor base on electrogenerated chemiluminescence energy transfer for detection of lincomycin. *Biosens. Bioelectron.* **2017**, *91*, 687–691, doi:10.1016/j.bios.2017.01.038.

183. Niazi, J.H.; Lee, S.J.; Kim, Y.S.; Gu, M.B. ssDNA aptamers that selectively bind oxytetracycline. *Bioorg. Med. Chem.* **2008**, *16*, 1254–1261, doi:10.1016/j.bmc.2007.10.073.

184. Kim, Y.S.; Niazi, J.H.; Gu, M.B. Specific detection of oxytetracycline using DNA aptamer-immobilized interdigitated array electrode chip. *Anal. Chim. Acta* **2009**, *634*, 250–254, doi:10.1016/j.aca.2008.12.025.

185. Kim, K.; Gu, M.-B.; Kang, D.-H.; Park, J.-W.; Song, I.-H.; Jung, H.-S.; Suh, K.-Y. High-sensitivity detection of oxytetracycline using light scattering agglutination assay with aptasensor. *Electrophoresis* **2010**, *31*, 3115–3120, doi:10.1002/elps.201000217.

186. Kim, Y.S.; Kim, J.H.; Kim, I.A.; Lee, S.J.; Jurng, J.; Gu, M.B. A novel colorimetric aptasensor using gold nanoparticle for a highly sensitive and specific detection of oxytetracycline. *Biosens. Bioelectron.* **2010**, *26*, 1644–1649, doi:10.1016/j.bios.2010.08.046.

187. Kim, Y.S.; Kim, J.H.; Kim, I.A.; Lee, S.J.; Gu, M.B. The affinity ratio - its pivotal role in gold nanoparticle-based competitive colorimetric aptasensor. *Biosens. Bioelectron.* **2011**, *26*, 4058–4063, doi:10.1016/j.bios.2011.03.030.

188. Kim, C.-H.; Lee, L.-P.; Min, J.-R.; Lim, M.-W.; Jeong, S.-H. An indirect competitive assay-based aptasensor for detection of oxytetracycline in milk. *Biosens. Bioelectron.* **2013**, *51*, 426–430, doi:10.1016/j.bios.2013.08.003.

189. Stoltenburg, R.; Reinemann, C.; Strehlitz, B. FluMag-SELEX as an advantageous method for DNA aptamer selection. *Anal. Bioanal. Chem.* **2005**, *383*, 83–91, doi:10.1007/s00216-005-3388-9.

190. Niazi, J.H.; Lee, S.J.; Gu, M.B. Single-stranded DNA aptamers specific for antibiotics tetracyclines. *Bioorg. Med. Chem.* **2008**, *16*, 7245–7253, doi:10.1016/j.bmc.2008.06.033.

191. Kwon, Y.S.; Ahmad Raston, N.H.; Gu, M.B. An ultra-sensitive colorimetric detection of tetracyclines using the shortest aptamer with highly enhanced affinity. *Chem. Commun.* **2014**, *50*, 40–42, doi:10.1039/c3cc47108j.

192. Meng, F.; Ma, X.; Duan, N.; Wu, S.; Xia, Y.; Wang, Z.; Xu, B. Ultrasensitive SERS aptasensor for the detection of oxytetracycline based on a gold-enhanced nano-assembly. *Talanta* **2017**, *165*, 412–418, doi:10.1016/j.talanta.2016.12.088.

193. Hou, H.; Bai, X.; Xing, C.; Gu, N.; Zhang, B.; Tang, J. Aptamer-based cantilever array sensors for oxytetracycline detection. *Anal. Chem.* **2013**, *85*, 2010–2014, doi:10.1021/ac3037574.

194. Seo, H.B.; Kwon, Y.S.; Lee, J.-e.; Cullen, D.; Noh, H.M.; Gu, M.B. A novel reflectance-based aptasensor using gold nanoparticles for the detection of oxytetracycline. *The Analyst* **2015**, *140*, 6671–6675, doi:10.1039/c5an00726g.

195. Yuan, F.; Zhao, H.; Zhang, Z.; Gao, L.; Xu, J.; Quan, X. Fluorescent biosensor for sensitive analysis of oxytetracycline based on an indirectly labelled long-chain aptamer. *RSC Adv.* **2015**, *5*, 58895–58901, doi:10.1039/C5RA04025F.

196. Xu, Y.; Shi, G.; Duan, X. Self-Assembled Three-Dimensional Graphene Macrostructures: Synthesis and Applications in Supercapacitors. *Acc. Chem. Res.* **2015**, *48*, 1666–1675, doi:10.1021/acs.accounts.5b00117.

197. Tan, B.; Zhao, H.; Du, L.; Gan, X.; Quan, X. A versatile fluorescent biosensor based on target-responsive graphene oxide hydrogel for antibiotic detection. *Biosens. Bioelectron.* **2016**, *83*, 267–273, doi:10.1016/j.bios.2016.04.065.

198. Zhang, H.; Fang, C.; Wu, S.; Duan, N.; Wang, Z. Upconversion luminescence resonance energy transfer-based aptasensor for the sensitive detection of oxytetracycline. *Anal. Biochem.* **2015**, *489*, 44–49, doi:10.1016/j.ab.2015.08.011.

199. Yan, K.; Liu, Y.; Yang, Y.; Zhang, J. A Cathodic "Signal-off" Photoelectrochemical Aptasensor for Ultrasensitive and Selective Detection of Oxytetracycline. *Anal. Chem.* **2015**, *87*, 12215–12220, doi:10.1021/acs.analchem.5b03139.

200. Li, Y.; Tian, J.; Yuan, T.; Wang, P.; Lu, J. A sensitive photoelectrochemical aptasensor for oxytetracycline based on a signal "switch off-on" strategy. *Sens. Actuators, B* **2017**, *240*, 785–792, doi:10.1016/j.snb.2016.09.042.

201. Zheng, D.; Zhu, X.; Zhu, X.; Bo, B.; Yin, Y.; Li, G. An electrochemical biosensor for the direct detection of oxytetracycline in mouse blood serum and urine. *Analyst* **2013**, *138*, 1886–1890, doi:10.1039/c3an36590e.

202. Xu, W.; Liu, S.; Yu, J.; Cui, M.; Li, J.; Guo, Y.; Wang, H.; Huang, J. An ultrasensitive HRP labeled competitive aptasensor for oxytetracycline detection based on grapheme oxide–polyaniline composites as the signal amplifiers. *RSC Adv.* **2014**, *4*, 10273, doi:10.1039/c3ra47368f.

203. Zhang, J.; Zhang, B.; Wu, Y.; Jia, S.; Fan, T.; Zhang, Z.; Zhang, C. Fast determination of the tetracyclines in milk samples by the aptamer biosensor. *Analyst* **2010**, *135*, 2706–2710, doi:10.1039/c0an00237b.

204. Liu, S.; Wang, Y.; Xu, W.; Leng, X.; Wang, H.; Guo, Y.; Huang, J. A novel sandwich-type electrochemical aptasensor based on GR-3D Au and aptamer-AuNPs-HRP for sensitive detection of oxytetracycline. *Biosens. Bioelectron.* **2017**, *88*, 181–187, doi:10.1016/j.bios.2016.08.019.

205. Aslipashaki, S.N.; Khayamian, T.; Hashemian, Z. Aptamer based extraction followed by electrospray ionization-ion mobility spectrometry for analysis of tetracycline in biological fluids. *J. Chromatogr. B* **2013**, *925*, 26–32, doi:10.1016/j.jchromb.2013.02.018.

206. Liu, Y.; Yan, K.; Zhang, J. Graphitic Carbon Nitride Sensitized with CdS Quantum Dots for Visible-Light-Driven Photoelectrochemical Aptasensing of Tetracycline. *CS Appl. Mater. Interfaces* **2015**, 28255–28264, doi:10.1021/acsami.5b08275.

207. Müller, M.; Weigand, J.E.; Weichenrieder, O.; Suess, B. Thermodynamic characterization of an engineered tetracycline-binding riboswitch. *Nucleic Acids Res.* **2006**, *34*, 2607–2617, doi:10.1093/nar/gkl347.

208. Jeong, S.; Rhee Paeng, I. Sensitivity and selectivity on aptamer-based assay: the determination of tetracycline residue in bovine milk. *Scientific World J.* **2012**, *2012*, 159456, doi:10.1100/2012/159456.

209. Wang, S.; Yong, W.; Liu, J.; Zhang, L.; Chen, Q.; Dong, Y. Development of an indirect competitive assay-based aptasensor for highly sensitive detection of tetracycline residue in honey. *Biosens. Bioelectron.* **2014**, *57*, 192–198, doi:10.1016/j.bios.2014.02.032.

210. Wang, S.; Liu, J.; Yong, W.; Chen, Q.; Zhang, L.; Dong, Y.; Su, H.; Tan, T. A direct competitive assay-based aptasensor for sensitive determination of tetracycline residue in honey. *Talanta* **2015**, *131*, 562–569, doi:10.1016/j.talanta.2014.08.028.

211. Luo, Y.; He, L.; Zhan, S.; Wu, Y.; Le Liu; Zhi, W.; Zhou, P. Ultrasensitive resonance scattering (RS) spectral detection for trace tetracycline in milk using aptamer-coated nanogold (ACNG) as a catalyst. *J. Agric. Food. Chem.* **2014**, *62*, 1032–1037, doi:10.1021/jf403566e.

212. Li, H.; Chen, Q.; Mehedi Hassan, M.; Chen, X.; Ouyang, Q.; Guo, Z.; Zhao, J. A magnetite/PMAA nanospheres-targeting SERS aptasensor for tetracycline sensing using mercapto molecules embedded core/shell nanoparticles for signal amplification. *Biosens. Bioelectron.* **2017**, *92*, 192–199, doi:10.1016/j.bios.2017.02.009.

213. He, L.; Luo, Y.; Zhi, W.; Wu, Y.; Zhou, P. A Colorimetric Aptamer Biosensor Based on Gold Nanoparticles for the Ultrasensitive and Specific Detection of Tetracycline in Milk. *Aust. J. Chem.* **2013**, *66*, 485, doi:10.1071/CH12446.

214. He, L.; Luo, Y.; Zhi, W.; Zhou, P. Colorimetric Sensing of Tetracyclines in Milk Based on the Assembly of Cationic Conjugated Polymer-Aggregated Gold Nanoparticles. *Food Anal. Methods* **2013**, *6*, 1704–1711, doi:10.1007/s12161-013-9577-9.

215. Luo, Y.; Xu, J.; Li, Y.; Gao, H.; Guo, J.; Shen, F.; Sun, C. A novel colorimetric aptasensor using cysteamine-stabilized gold nanoparticles as probe for rapid and specific detection of tetracycline in raw milk. *Food Control* **2015**, *54*, 7–15, doi:10.1016/j.foodcont.2015.01.005.

216. Ramezani, M.; Mohammad Danesh, N.; Lavaee, P.; Abnous, K.; Mohammad Taghdisi, S. A novel colorimetric triple-helix molecular switch aptasensor for ultrasensitive detection of tetracycline. *Biosens. Bioelectron.* **2015**, *70*, 181–187, doi:10.1016/j.bios.2015.03.040.

217. Wang, R.; Zhou, X.; Liedberg, B.; Zhu, X.; Memon, A.G.; Shi, H. Screening Criteria for Qualified Antibiotic Targets in Unmodified Gold Nanoparticles-Based Aptasensing. *ACS Appl. Mater. Interfaces* **2017**, *9*, 35492–35497, doi:10.1021/acsami.7b12796.

218. Tang, Y.; Zhang, J.; Liu, J.-H.; Gapparov, I.; Wang, S.; Dong, Y.; Su, H.; Tan, T. The development of a graphene oxide-based aptasensor used for the detection of tetracycline in honey. *Anal. Methods* **2017**, *9*, 1133–1140, doi:10.1039/C6AY03412H.

219. Jalalian, S.H.; Taghdisi, S.M.; Danesh, N.M.; Bakhtiari, H.; Lavaee, P.; Ramezani, M.; Abnous, K. Sensitive and fast detection of tetracycline using an aptasensor. *Anal. Methods* **2015**, *7*, 2523–2528, doi:10.1039/C5AY00225G.

220. Chen, T.-X.; Ning, F.; Liu, H.-S.; Wu, K.-F.; Li, W.; Ma, C.-B. Label-free fluorescent strategy for sensitive detection of tetracycline based on triple-helix molecular switch and G-quadruplex. *CCL* **2017**, *28*, 1380–1384, doi:10.1016/j.cclet.2017.01.006.

221. Ouyang, Q.; Liu, Y.; Chen, Q.; Guo, Z.; Zhao, J.; Li, H.; Hu, W. Rapid and specific sensing of tetracycline in food using a novel upconversion aptasensor. *Food Control* **2017**, *81*, 156–163, doi:10.1016/j.foodcont.2017.06.004.

222. Sun, C.; Su, R.; Bie, J.; Sun, H.; Qiao, S.; Ma, X.; Sun, R.; Zhang, T. Label-free fluorescent sensor based on aptamer and thiazole orange for the detection of tetracycline. *Dyes and Pigments* **2018**, *149*, 867–875, doi:10.1016/j.dyepig.2017.11.031.

223. Li, H.; Li, J.; Qiao, Y.; Fang, H.; Fan, D.; Wang, W. Nano-gold plasmon coupled with dual-function quercetin for enhanced photoelectrochemical aptasensor of tetracycline. *Sens. Actuators, B* **2017**, *243*, 1027–1033, doi:10.1016/j.snb.2016.12.032.

224. Zhang, X.; Zhang, R.; Yang, A.; Wang, Q.; Kong, R.; Qu, F. Aptamer based photoelectrochemical determination of tetracycline using a spindle-like ZnO-CdS@Au nanocomposite. *Microchim. Acta* **2017**, *184*, 4367–4374, doi:10.1007/s00604-017-2477-8.

225. Le, T.H.; van Pham, P.; La, T.H.; Phan, T.B.; Le, Q.H. Electrochemical aptasensor for detecting tetracycline in milk. *Adv. Nat. Sci: Nanosci. Nanotechnol.* **2016**, *7*, 15008, doi:10.1088/2043-6262/7/1/015008.

226. Xu, Q.-C.; Zhang, Q.-Q.; Sun, X.; Guo, Y.-M.; Wang, X.-Y. Aptasensors modified by antimony tin oxide nanoparticle-chitosan based on interdigitated array microelectrodes for tetracycline detection. *RSC Adv.* **2016**, *6*, 17328–17335, doi:10.1039/C5RA25922C.

227. Zhao, G.; Xu, Q.; Zhang, Q.; Guo, Y.; Sun, X.; Wang, X. Study on Aptasensors Modified by Ionic Liquid–Fe3O4 Based on Microarray Electrodes for Tetracycline Detection. *Int. J. Electrochem. Sci.* **2016**, 1699–1706.

228. Hou, W.; Shi, Z.; Guo, Y.; Sun, X.; Wang, X. An interdigital array microelectrode aptasensor based on multi-walled carbon nanotubes for detection of tetracycline. *Bioprocess and biosystems engineering* **2017, doi:**10.1007/s00449-017-1799-6.

229. Kim, Y.-J.; Kim, Y.S.; Niazi, J.H.; Gu, M.B. Electrochemical aptasensor for tetracycline detection. *Bioprocess Biosyst* **2010**, *33*, 31–37, doi:10.1007/s00449-009-0371-4.

230. Zhou, L.; Li, D.-J.; Gai, L.; Wang, J.-P.; Li, Y.-B. Electrochemical aptasensor for the detection of tetracycline with multi-walled carbon nanotubes amplification. *Sens. Actuators, B* **2012**, *162*, 201–208, doi:10.1016/j.snb.2011.12.067.

231. Chen, D.; Yao, D.; Xie, C.; Liu, D. Development of an aptasensor for electrochemical detection of tetracycline. *Food Control* **2014**, *42*, 109–115, doi:10.1016/j.foodcont.2014.01.018.

232. Shen, G.; Guo, Y.; Sun, X.; Wang, X. Electrochemical Aptasensor Based on Prussian Blue-Chitosan-Glutaraldehyde for the Sensitive Determination of Tetracycline. *Nano-Micro Lett.* **2014**, *6*, 143–152, doi:10.1007/BF03353778.

3063   233. Guo, Y.; Wang, X.; Sun, X. A label-free Electrochemical Aptasensor Based on Electrodeposited
3064   Gold Nanoparticles and Methylene Blue for Tetracycline Detection. *Int. J. Electrochem. Sci.* **2015**,
3065   3668–3679.

3066   234. Benvidi, A.; Tezerjani, M.D.; Moshtaghiun, S.M.; Mazloum-Ardakani, M. An aptasensor for
3067   tetracycline using a glassy carbon modified with nanosheets of graphene oxide. *Microchim. Acta*
3068   **2016**, *183*, 1797–1804, doi:10.1007/s00604-016-1810-y.

3069   235. Guo, Y.; Zhang, Q.; Xu, Q.; Ma, N.; Sun, X.; Wang, X.Y. Fabrication of aptasensors modified by
3070   MWCNTs-CS/Fe3O4-CS based on SPEs. *Int. J. Electrochem. Sci.* **2016**, 1691–1698.

3071   236. Jahanbani, S.; Benvidi, A. Comparison of two fabricated aptasensors based on modified carbon
3072   paste/oleic acid and magnetic bar carbon paste/Fe3O4@oleic acid nanoparticle electrodes for
3073   tetracycline detection. *Biosens. Bioelectron.* **2016**, *85*, 553–562, doi:10.1016/j.bios.2016.05.052.

3074   237. Taghdisi, S.M.; Danesh, N.M.; Ramezani, M.; Abnous, K. A novel M-shape electrochemical
3075   aptasensor for ultrasensitive detection of tetracyclines. *Biosens. Bioelectron.* **2016**, *85*, 509–514,
3076   doi:10.1016/j.bios.2016.05.048.

3077   238. Zhan, X.; Hu, G.; Wagberg, T.; Zhan, S.; Xu, H.; Zhou, P. Electrochemical aptasensor for
3078   tetracycline using a screen-printed carbon electrode modified with an alginate film containing
3079   reduced graphene oxide and magnetite (Fe3O4) nanoparticles. *Microchim. Acta* **2016**, *183*, 723–
3080   729, doi:10.1007/s00604-015-1718-y.

3081   239. Xu, Q.; Liu, Z.; Fu, J.; Zhao, W.; Guo, Y.; Sun, X.; Zhang, H. Ratiometric electrochemical
3082   aptasensor based on ferrocene and carbon nanofibers for highly specific detection of tetracycline
3083   residues. *Scientific reports* **2017**, *7*, 14729, doi:10.1038/s41598-017-15333-5.

3084   240. Song, K.-M.; Jeong, E.; Jeon, W.; Jo, H.; Ban, C. A coordination polymer nanobelt (CPNB)-based
3085   aptasensor   for   sulfadimethoxine.   *Biosens.   Bioelectron.*   **2012**,   *33*,   113–119,
3086   doi:10.1016/j.bios.2011.12.034.

3087   241. Chen, A.; Jiang, X.; Zhang, W.; Chen, G.; Zhao, Y.; Tunio, T.M.; Liu, J.; Lv, Z.; Li, C.; Yang, S.
3088   High sensitive rapid visual detection of sulfadimethoxine by label-free aptasensor. *Biosens.*
3089   *Bioelectron.* **2013**, *42*, 419–425, doi:10.1016/j.bios.2012.10.059.

3090   242. Liu, J.; Guan, Z.; Lv, Z.; Jiang, X.; Yang, S.; Chen, A. Improving sensitivity of gold nanoparticle
3091   based fluorescence quenching and colorimetric aptasensor by using water resuspended gold
3092   nanoparticle. *Biosens. Bioelectron.* **2014**, *52*, 265–270, doi:10.1016/j.bios.2013.08.059.

3093   243. Yan, J.; Huang, Y.; Zhang, C.; Fang, Z.; Bai, W.; Yan, M.; Zhu, C.; Chen, A. Aptamer based
3094   photometric assay for the antibiotic sulfadimethoxine based on the inhibition and reactivation
3095   of the peroxidase-like activity of gold nanoparticles. *Microchim. Acta* **2017**, *184*, 59–63,
3096   doi:10.1007/s00604-016-1994-1.

3097   244. Wang, A.; Zhao, H.; Chen, X.; Tan, B.; Zhang, Y.; Quan, X. A colorimetric aptasensor for
3098   sulfadimethoxine detection based on peroxidase-like activity of graphene/nickel@palladium
3099   hybrids. *Anal. Biochem.* **2017**, *525*, 92–99, doi:10.1016/j.ab.2017.03.006.

3100   245. Liu, X.; Gao, T.; Gao, X.; Ma, T.; Tang, Y.; Zhu, L.; Li, J. An aptamer based sulfadimethoxine
3101   assay that uses magnetized upconversion nanoparticles. *Microchim. Acta* **2017**, *184*, 3557–3563,
3102   doi:10.1007/s00604-017-2378-x.

3103   246. Okoth, O.K.; Yan, K.; Liu, Y.; Zhang, J. Graphene-doped Bi2S3 nanorods as visible-light
3104   photoelectrochemical aptasensing platform for sulfadimethoxine detection. *Biosens. Bioelectron.*
3105   **2016**, *86*, 636–642, doi:10.1016/j.bios.2016.07.037.

3106   247. Gao, H.; Gan, N.; Pan, D.; Chen, Y.; Li, T.; Cao, Y.; Fu, T. A sensitive colorimetric aptasensor for
3107   chloramphenicol detection in fish and pork based on the amplification of a nano-peroxidase-
3108   polymer. *Anal. Methods* **2015**, *7*, 6528–6536, doi:10.1039/C5AY01379H.

3109

3110   **Table 1.** Aptamer sequence, dissociation constant (K_D), limit of detection (LOD), real sample analysis (RSA) and realized sensor type and measuring method for the
3111   different antibiotic targets, mentioned in the corresponding reference (Ref). AC = alternating current, AEC = amperometric electrochemical,
3112   CA = chronoamperometry, CAN = cantilever, CO = colorimetric, CV = cyclic voltammetry, Cy = Cyanin dye, DPV = differential pulse voltammetry, ELAA = enzyme-
3113   linked aptamer assay, ESI-IMS = electrospray ionization-ion mobility spectrometry, FL = fluorometric, EBFC = enzyme biofuel cell, ECL = electrochemiluminescent,
3114   EIS = electrochemical impedance spectrometry, FAM = Fluorescein amidite, FIS = Faradeic impedance spectroscopy, IEC = impedimetric electrochemical,
3115   LCA = liquid crystal assay, LSPIA = of light scattering particle immunoagglutination assay, LSV = linear sweep voltammetry, MB = methylene blue, mut = mutated
3116   aptamer, OCV = open circuit voltage, PEC = photoelectrochemical, SPR = surface plasmon resonance, SWV = square wave voltammetry, apt = aptamer, b = buffer,
3117   bs = blood serum, bsa = bovine serum albumin, c = chicken, ce = chicken egg, cap = capture probe, cDNA = complementary DNA, d = drugs, f = fish, dw = distilled
3118   water, h = honey, hs = human serum, hp = human plasma, hu = human urine, lw = lake water, m = milk, me = meat, mb = mouse blood, mu = mouse urine, ms = mouse
3119   serum, p = pork, rs = rat serum, rw = river water, sa = salvia, st = standard, tw = tap water, sw = spiked water, ww = waste water, uw = ultrapure water.

Antibiotic target	5´ linker & spacer	Aptamer sequence 5´→ 3´	3´ linker & spacer	K_D [nM]	LOD [nM]	RSA	Sensor type/ method	Ref [1]
Ampicillin	FAM	I: GCG GGC GGT TGT ATA GCG G II: TTA GTT GGG GTT CAG TTG G III: CAC GGC ATG GTG GGC GTC GTG	-	I: 13.4 II: 9.8 III: 9:4	I: 1.4 (dw, FL) I: 5.7 (m, FL) I: 14.3 (dw, CO) I: 28.6 (m, CO)	m	FL,CO/ UV-Vis	[54]
	-	apt I: GCG GGC GGT TGT ATA GCG GTT TTT TT apt II: GCG GGC GGT TGT ATA GCG GTT TTT TT cDNA I: AAC CGC CCG CTT TC CTC AGC cDNA II: AAC CGC CCG CTT TAC CTC AGC cDNA III: AAC CGC CCG CTT TAC CTC AGC A cDNA IV: AAC CGC CCG CTT TAC CTC AGC A cDNA V: ACC GCC CGC TTT ACC TCA GCA cDNA VI: CAA CCG CCC GCT TTA CCT CAG CA cDNA VII: ACA ACC GCC CGC TTT ACC TCA GCA	apt I: SH apt II:	-	0.2 (b) (0.07·10^{-6} g/L)	rw	FL	[56]

3120
3121
3122

Antibiotic target	5′ linker & spacer	Aptamer sequence 5′→ 3′	3′ linker & spacer	K_D [nM]	LOD [nM]	RSA	Sensor type/ method	Ref [1]
Ampicillin	NH$_2$-C$_6$	GCG GGC GGT TGT ATA GCG G	-	13.4	0.1 (b)	m	IEC/ EIS	[55, 54]
	poly(T)-poly(C)	GCG GGC GGT TGT ATA GCG G	-	-	0.1 (b)	-	IEC/ EIS	[57, 58]
	-	-	-	-	0.001 (b)	m	AEC/ DPV	[59]
	MB	GCG GGC GGT TGT ATA GCG G	A$_{10}$	-	0.004 (b)	m	AEC/ DPV	[60]
	apt: SH cDNA: SH	TGG GGG TTG AGG CTA AGC CGA C cDNA: GTC TTA GCC TCA ACC CCC A	-	-	0.00038 (b)	m	AEC/ DPV	[61]
	SH-(CH$_2$)$_6$	TTA GTT GGG GTT CAG TTG G	MB		1000 (AC) 30000 (SWV)	bsa, sa, m	AEC/ AC, SWV	[62]
	SH-(CH$_2$)$_6$	apt: TTA GTT GGG GTT CAG TTG G cDNA I: CCA ACT AA cDNA II: CCC AAC TA cDNA III: CCC AAC TAA cDNA IV: CCC CAA CTA cDNA V: CCC CAA CTA A cDNA VI: ACC CCA ACT AA cDNA VII:AAC CCC AAC TAA cDNA VIII: GAA CCC CAA CTA A cDNA IX: TGA ACC CCA ACT AA	MB	-	30 (b)	hu, w, m, sa	AEC/ AC	[63]
	apt: NH$_2$-(CH$_2$)$_6$ cDNA: SH-(CH$_2$)$_6$	TTT TGC GGG CGG TTG TAT AGC GG cDNA: TTT TTT TTT CCG CTA TAC AAC CGC C	-	-	0.003 (b)	m	EBFC/ CV, OCV	[64]

Antibiotic target	5′ linker & spacer	Aptamer sequence 5′→ 3′	3′ linker & spacer	K_D [nM]	LOD [nM]	RSA	Sensor type/ method	Ref [1]
Penicillin G	-	GGG AGG ACG AAG CGG AAC GAG ATG TAG ATG AGG CTC GAT CCG AAT GCG TGA CGT CTA TCG GAA TAC TCG TTT TTA CGC CTC ATA AGA CAC GCC CGA CA	-	-	0.49 (b) $(0.17 \cdot 10^{-6}$ g/L)	m	IEC/ EIS	[66]
	FAM	GGG TCT GAG GAG TGC GCG GTG CCA GTG AGT	-	383.4	9.2 (b)	m	FL	[67]
Penicillin [2]	NH₂	CTG AAT GGA TCT CTT CTT GAG CGA TCT CCA CA	-	-	0.057 (b)	m	IEC/ EIS	[65]
Gentamicin	I: SH II: SH III: SH	I: GGG ACU UGG UUU AGG UAA UGA GUC CC II: (fully O-methylated) GGG ACU UGG UUU AGG UAA UGA GUC CC III: GGG ACT TGG TTT AGG TAA TGA GTC CC	I: NH-MB II: NH-MB III: NH-MB	I: 72000 II: ≈ 80000 III: ≈ 200000	-	hs	AEC/ SWV	[68, 119]
Kanamycin	SH-(CH₂)₆	TGG GGG TTG AGG CTA AGC CGA C	-	-	50000 (b)	-	CAN	[71]
	-	TGG GGG TTG AGG CTA AGC CGA	-	78.8	25 (b)	-	CO/ UV-Vis	[69]
	-	TGG GGG TTG AGG CTA AGC CGA	-	78.8	-	-	CO/ UV-Vis	[72, 69]
	-	TGG GGG TTG AGG CTA AGC CGA	-	8.38	1.49 (b)	-	CO	[30, 69]
	SH-(CH₂)₆	TGG GGG TTG AGG CTA AGC CGA	-	-	0.014 (b)	m	CO/ UV-Vis	[96, 69]
	-	TGG GGG TTG AGG CTA AGC CGA	-	-	4.5 (b) $(2.6 \cdot 10^{-6}$ g/L)	m	CO	[75]
	-	CGG AAG CGC GCC ACC CCA TCG GCG GGG GCG AAG CTT GCG	-	-	3.35 (b)	m	CO	[76, 86]
	apt: SH-(CH₂)₆ cDNA I: SH-(CH₂)₆ cap: biotin	apt: TGG GGG TTG AGG CTA AGC CGA cDNA I: TCA GTC GGC TTA GCC GTC AAC GT CAG ATC C cap: CCG ATG GAT CTG ACG T	apt: biotin		0.0778 (b)	m, h	CO	[77]

Antibiotic target	5′ linker & spacer	Aptamer sequence 5′→ 3′	3′ linker & spacer	K_D [nM]	LOD [nM]	RSA	Sensor type/ method	Ref [1]
Kanamycin	-	TGG GGG TTG AGG CTA AGC CGA	NH$_2$-(CH$_2$)$_6$ -	-	< 1 (b)	-	LCA	[78, 69]
	apt: biotin cDNA: FAM	apt: AGA TGG GGG TTG AGG CTA AGC CGA cDNA: CTT AGC CTC AAC CCC CAT CT	-	-	0.612 (b) 0.453 (rs)	rs	FL	[79]
	apt: biotin cDNA: ROX	apt: TGG GGG TTG AGG CTA AGC CGA cDNA: TCG GCT TAG CCT CAA CCC CCA	-	-	1.58 (b) (0.92·10^{-6} g/L)	m, h, p	FL	[80, 69]
	-	AGA TGG GGG TTG AGG CTA AGC CGA	-	-	0.321 (b) 0.476 (m) 0.568 (rs)	m, rs	FL	[82, 69]
	-	apt: TGG GGG TTG AGG CTA AGC CGA	-	-	59 (b)	m	FL	[83, 69]
	NH$_2$	AGA TGG GGG TTG AGG CTA AGC CGA	-	-	0.009 (b) 0.018 (bs)	bs	FL	[84]
	NH$_2$-C$_6$	TGG GGG TTG AGG CTA AGC CGA C	-	-	1100 (b)	m	FL	[85]
	II: FAM	I: ATG CGG ATC CCG CGC GAC CAA CGG AAG CGC GCC ACC CCA TCG GCG GGC GCG AAG CTT GCG C II: CGG AAG CGC GCC ACC CCA TCG GCG GGC GCG AAG CTT GCG	-	II: 92.3	I: 6.25 (b) II: 6.25 (b) II: 0.001 (st) II: 0.1 (bs) II: 0.02 (m)	m, bs	FL	[86]
	apt I: FAM	apt I: TGG GGG TTG AGG CTA AGC CGA apt II: TGG GGG TT FAM GAG GCT AAG CCG A apt III: TGG GGG TTG AGG CTA AGC CGA cDNA I: AAC CCC cDNA II: AAC CCC A cDNA III: AAC CCC CAA CT	cDNA I: FAM cDNA II: FAM cDNA III: FAM	-	0.4 (b)	m	FL	[87]

Antibiotic target	5´ linker & spacer	Aptamer sequence 5´→ 3´	3´ linker & spacer	K_D [nM]	LOD [nM]	RSA	Sensor type/ method	Ref [1]
Kanamycin	apt II: Cy3 apt III: Cy5 anchor apt: NH_2 cDNA II: Cy3	apt I: TGG GGG TTG AGG CTA AGC CGA apt II: TGG GGG TTG AGG CTA AGC CGA apt III: TGG GGG TTG AGG CTA AGC CGA apt IV: TGG GGG TTG AGG CTA AGC CGA anchor apt: TTT TTT TGG GGG TTG AGG CTA AGC CGA cDNA I: TAG CCT CAA cDNA II: TCG GCT TAG CCT	apt IV: Cy3 cDNA I: Cy3		26 (b)	m	FL	[88, 69]
	-	TGG GGG TTG AGG CTA AGC CGA	-	78.8	143 (b)	f	ECL	[89, 69]
	SH-$(CH_2)_6$-T_5	TGG GGG TTG AGG CTA AGC CGA G-quadruplex: GGT TGG TGT GGT TGG TAG CCT CAA GGT TGG TGT GGT TGG	-	-	0.045 (b)	m	ECL	[90]
	apt: biotin cDNA: SH-$(CH_2)_6$	apt: TGG GGG TTG AGG CTA AGC CGA cDNA: TTA GCC TCA A	-	-	0.034 (b) (0.002·10^{-6} g/L)	m	ECL	[92]
	-	TGG GGG TTG AGG CTA AGC CGA	-	-	0.2 (b)	-	PEC	[93]
	SH-$(CH_2)_6$	TGG GGG TTG AGG CTA AGC CGA	-	-	0.1 (b)	-	PEC/ EIS, CA	[94]
	SH-$(CH_2)_6$	TGG GGG TTG AGG CTA AGC CGA	-	-	7.2 (b) (3.5·10^{-6} g/L)	m	PEC/ EIS	[95, 94]
	-	TGG GGG TTG AGG CTA AGC CGA	-	-	1.0 (b)	m	IEC/ EIS	[74]
	-	TGG GGG TTG AGG CTA AGC CGA	-	-	0.23 (0.11·10^{-6} g/L)	m	IEC/ EIS	[97, 69]
	I: SH II: SH III: SH	I: GGG ACU UGG UUU AGG UAA UGA GUC CC II: (fully O-methylated) GGG ACU UGG UUU AGG UAA UGA GUC CC III: GGG ACT TGG TTT AGG TAA TGA GTC CC	I: NH-MB II: NH-MB III: NH-MB	I: 281000 II: ≈ 450000 III: ≈ 600000	-	hs	AEC/ SWV	[68, 119]

Antibiotic target	5′ linker & spacer	Aptamer sequence 5′→3′	3′ linker & spacer	K_D [nM]	LOD [nM]	RSA	Sensor type/ method	Ref [1]
Kanamycin	NH$_2$	TGG GGG TTG AGG CTA AGC CGA C	-	78.8	9.4 ± 0.4 (b) 10.8 ± 0.6 (m)	m	AEC/ SWV	[98]
	I: NH$_2$ II: biotin	I: TGG GGG TTG AGG CTA AGC CGA C II: TGG GGG TTG AGG CTA AGC CGA C	-	-	5.8 (b)	m	AEC/ DPV	[99]
	I NH$_2$ II biotin	I: TGG GGG TTG AGG CTA AGC CGA C II: TGG GGG TTG AGG CTA AGC CGA C	-	-	8.6 (b)	m	AEC/ DPV	[100]
	biotin	TGG GGG TTG AGG CTA AGC CG	-	-	0.0079 (b) (4,6·10^{-9} g/L)	m	AEC/ DPV	[101]
	NH$_2$	AGA TGG GGG TTG AGG CTA AGC CGA	-	-	0.0037 (b)	m	AEC/ DPV	[102]
	PO$_4$	AGA TGG GGG TTG AGG CTA AGC CGA	-		0.87 (b)	m, p, c	AEC/ DPV	[103]
	NH$_2$	AGA TGG GGG TTG AGG CTA AGC CGA	-	-	0.00042 (b)	m, p, c	AEC/ DPV	[104]
	-	TCT GGG GGT TGA GGC TAA GCC GAC	(CH$_2$)$_6$- NH$_2$	78.8	0.00015 (b)	m	AEC/ SWV	[105, 99]
	apt: SH cDNA: apt	apt: TGG GGG TTG AGG CTA AGC CGA C cDNA: GTC GGC TTA CGG TCA ACC CCC A	-	-	0.01 (b) (0.005·10^{-6} g/L)	m	AEC/ SWV	[106]
	-	TGG GGG TTG AGG CTA AGC CG	-	-	0.00074 (b)	m	AEC/ DPV	[107]
	-	TGG GGG TTG AGG CTA AGC CGA C	-	-	0.0000013 (b)	m	AEC/ DPV	[108]
	apt: NH$_2$-(CH$_2$)$_6$ cDNA: NH$_2$-(CH$_2$)$_6$	apt: TGG GGG TTG AGG CTA AGC CGA C cDNA: CGT TAG CCT CAA CCC	-	-	0.00016 (b)	m	AEC/ SWV	[47]
	SH	TGG GGG TTG AGG CTA AGC CGA	-	-	0.00137 (b) (0.008·10^{-9} g/L)	m	AEC/ DPV	[109]
	apt I: SH	apt: TGG GGG TTG AGG CTA AGC CGA			0.000035 (b)	m	AEC/ SWV	[110, 69]

Antibiotic target	5´ linker & spacer	Aptamer sequence 5´→ 3´	3´ linker & spacer	K_D [nM]	LOD [nM]	RSA	Sensor type/ method	Ref [1]
Kanamycin A	FAM	ATA CCA GCT TAT TCA ATT AGC CCG GTA TTG AGG TCG ATC TCT TAT CCT ATG GCT TGT CCC CCA TGG CTC GGT TAT ATC CAG ATA GTA AGT GCA ATC T	-	3900	5000 (ww)	ww	FL	[111]
	FAM	TGG GGG TTG AGG CTA AGC CGA	-	115 ± 2.76	0.3 (b)	m	FL	[70, 69]
	-	apt: TGG GGG TTG AGG CTA AGC CGA mut I: TGG AGG TTG AG CTA AGC CGA mut II: TGG AGG TTG AGG CTA AGC CGA mut III: TGG AGG TTG AAG CTA AAC CGA mut IV: TAA AAA TTA AAA CTA AAC CAA	-	-	0.3 (b)	m	FL	[113, 69]
	NH$_2$-C$_6$	TGG GGG TTG AGG CTA AGC CGA	-	78.8	10 (b)	m	IEC/ EIS	[55, 69]
	cDNA I: ferrocene-(CH$_2$)$_6$ cDNA II: SH-(CH$_2$)$_6$	apt I: TGG GGG TTG AGG CTA AGC CGA GTC ACT AT cDNA I: GTG ACT CGG CTT apt II: TGG GGG TTG AGG CTA AGC CGA GTC ACT AT cDNA II: TAT GTG ACT CGG CTT	apt I: (CH$_2$)$_3$-SH apt II: (CH$_2$)$_3$-ferrocene	78.8	1.0 (b)	lw	IEC/ EIS	[114, 69]
Neomycin B	FAM	GGA CUG GGC GAG AAG UUU AGU CC	(T)$_{15}$–(A)$_{12}$	115 ± 25	10 (m)	m	FL	[116, 115]
	-	(fully O-methylated) GGC CUG GGC GAG AAG UUU AGG CC	-	-	< 1000 (b)	m	IEC/ FIS	[117]
	-	(fully O-methylated) GGC CUG GGC GAG AAG UUU AGG CC	-	2500 ± 900	5 (b, SPR)	-	IEC/ FIS SPR	[118]

Antibiotic target	5´ linker & spacer	Aptamer sequence 5´→ 3´	3´ linker & spacer	K_D [nM]	LOD [nM]	RSA	Sensor type/ method	Ref [1]
Tobramycin	SH	TCC GTG TAT AGG TCG GGT CTC TTG CCA ACT GAT TCG TTG AAA AGT ATA GCC CCG CAG GG	-	260	500 (b) 3400 (bs)	bs	SPR	[121, 120]
	-	I: TAG GGA ATT CGT CGA CGG ATC CAT GGC ACG TTA TGC GGA GGC GGT ATG ATA GCG CTA CTG CAG GTC GAC GCA TGC GCC G II: CGT CGA CGG ATC CAT GGC ACG TTA TGC GGT ATG ATA GCG CAG GTC GAC G III: CGT CGA CGG ATC CAT GGC ACG TTA TAG GTC GAC G	-	I: 56.9 II: 46.8 III: 48.4	37.9 (b)	h	CO	[122]
	-	GGG ACT GGT TTT AGG TAA TGA GTC CC	-	-	23.3 (b)	m, ce	CO	[123]
	-	I: (O-methylated RNA except **U12** position) GGC ACG AGG UU**U** AGC UAC ACU CGU GCC II: (fully O-methylated) GGC ACG AGG UUU AGC UAC ACU CGU GCC	-	I: 600 II: 400	I: 700 (b) II: 400 (b)	hs	IEC/ FIS	[124, 119]
	I: SH II: SH III: SH	I: GGG ACU UGG UUU AGG UAA UGA GUC CC II: (fully O-methylated) GGG ACU UGG UUU AGG UAA UGA GUC CC III: GGG ACT TGG TTT AGG TAA TGA GTC CC	I: NH-MB II: NH-MB III: NH-MB	I 319000 II: ≈ 180000 III: ≈ 1380000	-	hs	AEC/ SWV	[68, 119]
	biotin	(O-methylated except **U12** position) GGC ACG AGG UU**U** AGC UAC ACU CGU GCC	-	-	5000 (b)	-	AEC/ DPV	[125, 119]
	fluorescein	(O-methylated except **U12** position) GGC ACG AGG UU**U** AGC UAC ACU CGU GCC	-	-	100 (b)	hs	AEC/ DPV, CA	[126]
	I: SH-C₆ II: SH-C₆ III: SH-C₆ IV: SH-C₆	I: GGG ACU UGG UUU AGG UAA UGA GUC CC II: ACU UGG UUU AGG UAA UGA GU III: CUU GGU UUA GGU AAU GAG IV: GGG ACU UGG UUU AGG UAA UGA GU	I: MB II: MB III: MB IV: MB	I: 16000 ± 3000 II: 220 ± 50 III: 510 ± 70 IV: 2900 ± 900 III: 148000 ± 4000 (s)	-	bsa	AEC/ SWV	[127, 119]

Antibiotic target	5′ linker & spacer	Aptamer sequence 5′→ 3′	3′ linker & spacer	K_D [nM]	LOD [nM]	RSA	Sensor type/ method	Ref [1]
Streptomycin	-	I: GGG GTC TGG TGT TCT GCT TTG TTC TGT CGG GTC GT II: TGA AGG GTC GAC TCT AGA GGC AGG TGT TCC TCA GG III: AGC TTG GGT GGG GCC ACG TAG AGG TAT AGC TTG TT IV: TGT GTG TTC GGT GCT GTC GGG TTG TTT CTT GGT TT	-	I: 199.1 II: 221.3 III: 272.0 IV: 340.6	I: 200 (b) I: 200 (h)	h	CO/ UV-Vis	[128]
	I: FAM II: FAM III: FAM	I: CCC GTT AAA GT AGT TGA GAG TAT TCC GTT TCT TTG TGT C II: GTG CGT TAT AAA CTA GTT TTG ATT CAA TGT TGG GTG TGG G III: GGG CCT GTT TTG CCT TCA CGT TCT CTT CCT TGC CGT TCT G	I: biotin II: biotin III: biotin	I: 6.07 II: 8.56 III: 13.14	25 (b)	m, h	CO	[129]
	SH-(CH$_2$)$_6$	TAG GGA ATT CGT CGACGG ATC CGG GGT CTG GTG TTC TGC TTT GTT CTG TCG GGT CGTCTG CAG GTC GAC GCA TGC GCC G	-	-	0.0017 (b) ($1 \cdot 10^{-9}$ g/L)	m	CO	[130, 128]
	SH	TAG GGA ATT CGT CGA CGA ATC CGG GGT CTG GTG TTC TGC TTT GTT CGTB TCG GGT CGT CTG CAG GTC GAC GCA TGC GCC G	-	199.1	86 (b)	m	CO	[131, 128]
	cDNA: FAM	apt: TAG GGA ATT CGT CGA CGG ATG CGG GGT CTG GTG TTG TGC TTT GTT CTG TCG GGT CGT CTG CAG GTC GAC GCA TGC GCC G cDNA: CGG CGC ATG CGT CGA CCT GCA GAC GAC CCG ACA GAA CAA AGC AGA ACA CCA GAC CCC GGA TCC GTC GAC GAA TTC CCT A	-	-	73.1 (b, CO) 102.4 (bs, CO) 108.7 (m, CO) 47.6 (b, FL) 58.2 (bs, FL) 56.2 (m, FL)	m, bs	CO, FL/ UV-Vis	[132]
	-	apt: TAG GGA ATT CGT CGA CGG ATG CGG GGT CTG GTG TTG TGC TTT GTT CTG TCG GGT CGT CTG CAG GTC GAC GCA TGC GCC G cDNA: CGG CGCA TGC GTC GAC CTG CAG ACG ACC CGA CAG AAC AAA GCA GAA CAC CAG ACC CCG GAT CCG TCG ACG AAT TCC CTA	-	-	54.5 (b) 71.0 (rs) 76.05 (m)	m, bs	FL	[133]

3129

Antibiotic target	5′ linker & spacer	Aptamer sequence 5′→ 3′	3′ linker & spacer	K_D [nM]	LOD [nM]	RSA	Sensor type/ method	Ref [1]
Streptomycin	-	GGG GTC TGG TGT TCT GCT TTG TTC TGT CGG GTC GT	-	-	0.05 (b) (0.03·10^{-6} g/L)	m	FL	[134, 128]
	-	apt: TAG GGA ATT CGT CGA CGG ATC CGG GGT CTG GTG TTC TGC TTT GTT CTG TCG GGT CGT CTG CAG GTC GAC GCA TGC GCC G cDNA I: CGG CGGC ATG CGT CGA CCT GCA GAC GAC CCG ACA GAA CAA AGC AGA ACA CCA GAC CCC GGA TCC GTC GAC GAA TTC CCT A cDNA II: CAG ACG ACC CGA CAG AAC AAA GCA GAA CAC CAG ACC CCG GAT CCG TCG ACG AAT TCC CTA cDNA III: GAC AGA ACA AAG CAG AAC ACC AGA CCC CGG ATC CGT CGA CGA ATT CCC TA cDNA IV: AGC AGA ACA CCA GAC CCC GGA TCC GTC GAC GAA TTC CCT A	-	-	94 (b)	m, c	FL	[135, 130]
	-	TAG GGA ATT CGT CGA CGG ATC CGG GGT CTG GTG TTC TGC TTT GTT CTG TCG GGT CGT CTG CAG GTC GAC GCA TGC GCC G	NH$_2$	-	0.033 (b)	h	PEC	[136]
	-	TAG GGA ATT CGT CGA CGG ATG CGG GGT CTG GTG TTG TGC TTT GTT CTG TCG GGT CGT CTG CAG GTC GAC GCA TGC GCC G	SH	-	0.057·10^{-3} (b) (0.033·10^{-9} g/L)	hs	IEC	[137]
	-	TAG GGA ATT CGT CGA CGG ATG CGG GGT CTG GTG TTG TGC TTT GTT CTG TCG GGT CGT CTG CAG GTC GAC GCA TGC GCC G	SH	-	11.4 (b) 14.1 (m) 15.3 (rs)	m, rs	AEC/ DPV	[138]
	cap: SH-(CH$_2$)$_6$	apt: TAG GGA ATT CGT CGA CGG ATG CGG GGT CTG GTG TTG TGC TTT GTT CTG TCG GGT CGT CTG CAG GTC GAC GCA TGC GCC G cap: GGT GTT GGT GTT cDNA I: GAC AGA ACA AAG CAG AAC ACC A cDNA II: TTC TGT CTC TCG	cDNA II: biotin	-	10 (b)	m	AEC/ SWV	[39]

Antibiotic target	5´ linker & spacer	Aptamer sequence 5´→ 3´	3´ linker & spacer	K_D [nM]	LOD [nM]	RSA	Sensor type/ method	Ref [1]
Streptomycin	-	TAG GGA ATT CGT CGA CGG ATG CGG GGT CTG GTG TTG TGC TTT GTT CTG TCG GGT CGT CTG CAG GTC GAC GCA TGC GCC G	SH	-	0.036 (b)	m, h	AEC/ DPV	[139]
	NH₂	TAG GGA ATT CGT CGA CGG ATG CGG GGT CTG GTG TTG TGC TTT GTT CTG TCG GGT CGT CTG CAG GTC GAC GCA TGC GCC G	-		0.0078 (b)	m	AEC/ DPV	[140]
	-	TAG GGA ATT CGT CGA CGG ATG CGG GGT CTG GTG TTG TGC TTT GTT CTG TCG GGT CGT CTG CAG GTC GAC GCA TGC GCC G	SH	-	0.028 (b)	m	AEC/ DPV	[141]
Daunomycin	-	GGG AAT TCG AGC TCG GTA CCA TCT GTG TAA GGG GTA AGG GGT GGG GGT GGG TAC GTC TAG CTG CAG GCA TGC AAG CTT GG	-	20	15 (b) (8.4·10⁻⁶ g/L)	-	FL ELAA SPR	[145]
	-	GGG AAT TCG AGC TCG GTA CCA TCT GTG TAA GGG GTA AGG GGT GGG GGT GGG TAC GTC TAG CTG CAG GCA TGC AAG CTT GG	-	20	17.6 (b)	-	CO, FL	[144, 145]
	poly-TTBA-NH₂	GGG AAT TCG AGC TCG GTA CCA TCT GTG TAA GGG GTA AGG GGT GGG GGT GGG TAC GTC TAG CTG CAG GCA TGC AAG CTT GG	-	20	0.052 ± 0.002 (b)	hu	AEC/ DPV	[146, 145]
Chloramphenicol	-	I: ACT TCA GTG AGT TGT CCC ACG GTC GGC GAG TCG GTG GTA G II: ACT GAG GGC ACG GAC AGG AGG GGG AGA GAT GGC GTG AGG T	-	I 766 II 1160	-	-	FL	[147]
	apt: SH-(CH₂)₆ cDNA: SH-(CH₂)₆	apt: ACT TCA GTG AGT TGT CCC ACG GTC GGC GAG TCG GTG GTA G cDNA: TTT TCT ACC ACC GAC TCG C	-	766	0.062 (b) (0.02·10⁻⁶ g/L)	f, p	CO/ UV-Vis	[247, 147]
	apt: (CH₂)₆ cDNA: SH-(CH₂)₆	apt: ACT TCA GTG AGT TGT CCC ACG GTC GGC GAG TCG GTG GTA G cDNA: CTA CCA CCG ACT CGC CGA CCG TGG GAC AAC TCA CTG AAG T	-	-	0.046 (b) (0.015·10⁻⁶ g/L)	m	CO/ UV-Vis	[148, 147]

3132
3133

Antibiotic target	5′ linker & spacer	Aptamer sequence 5′→ 3′	3′ linker & spacer	K_D [nM]	LOD [nM]	RSA	Sensor type/ method	Ref [1]
Chloramphenicol	apt: $(CH_2)_6$ cDNA: SH-$(CH_2)_6$	apt: ACT TCA GTG AGT TGT CCC ACG GTC GGC GAG TCG GTG GTA G cDNA: CTA CCA CCG ACT CGCG CGA CCG TGG GAC AAC TCA CTG AAG T	-	-	0.00093 (b) $(0.3 \cdot 10^{-9}$ g/L)	m	CO/ UV-Vis	[149]
	-	ACT TCA GTG AGT TGT CCC ACG GTC GGC GAG TCG GTG GTA G	biotin	-	0.451 (b) 0.697 (m) 0.601 (rs)	m, rs	CO/ UV-Vis	[153]
	NH_2-C_6	AGC AGC ACA GAG GTC AGA TGC ACT CGG ACC CCA TTC TCC TTC CAT CCC TCA TCC GTC CAC CCT ATG CGT GCT ACC GTG AA	-	-	0.098 (b) 0.761 (m)	m	FL	[154]
	apt: biotin cDNA: NH_2	apt: AGC AGC ACA GAG GTC AGA TGA CTT CAG TGA GTT GTC CCA CGG TCG GCG AGT CGG TGG TAG CCT ATG CGT GCT ACC GTG AA cDNA: CGA CCG TGG GAC AAC TCA	-	-	0.031 (b) $(0.01 \cdot 10^{-6}$ g/L)	m	FL	[155]
	apt: $(CH_2)_6$ cDNA: SH-$(CH_2)_6$	apt: ACT TCA GTG AGT TGT CCC ACG GTC GGC GAG TCG GTG GTA G cDNA: CTA CCA CCG ACT CGC CGA CCG TGG GAC AAC TCA CTG AAG T	-	-	0.0006 (b) $(0.0002 \cdot 10^{-6}$ g/L)	f	FL	[40, 147]
	apt: $(CH_2)_6$ cDNA: SH-$(CH_2)_6$ G-quadruplex: SH-$(CH_2)_6$	apt: ACT TCA GTG AGT TGT CCC ACG GTC GGC GAG TCG GTG GTA G cDNA: CTA CCA CCG ACT CGC CGA CCG TGG GAC AAC TCA CTG AAG T G-quadruplex: GGG TAG GGC GGG AA	-	-	0.0015 (b) $(0.0005 \cdot 10^{-6}$ g/L)	m	FL	[152, 147]
	$(CH_2)_6$	ACT TCA GTG AGT TGT CCC ACG GTC GGC GAG TCG GTG GTA G	-	-	0.001 (b)	f	FL	[151, 147]
	apt: SH-$(CH_2)_6$	apt: ACT TCA GTG AGT TGT CCC ACG GTC GGC GAG TCG GTG GTA G cDNA: CTA CCA CCG ACT CGC	-	-	0.0003 (b)	m	FL	[41, 147]

3134

Antibiotic target	5′ linker & spacer	Aptamer sequence 5′→ 3′	3′ linker & spacer	K_D [nM]	LOD [nM]	RSA	Sensor type/ method	Ref [1]
Chloramphenicol	-	apt: CAA TAA GCG ATG CGC CCT CGC CTG GGG GCC TAG TCC TCT CCT ATG CGT GCT ACC GTG AA cDNAI: TCG CTT ATT GAA AAA AAA AA cDNAII: CAT CGC TTA TTG AAA AAA AAA A cDNAIII: CGC ATC GCT TAT TGA AAA AAA AAA	cDNAI: biotin cDNAII: biotin cDNAIII: biotin	32.24	0.31 (b)	m	FL	[156]
	SH-$(CH_2)_6$	ACT TCA GTG AGT TGT CCC ACG GTC GGC GAG TCG GTG GTA G	-	766	0.093 (b) (0.003·10^{-6} g/L)	m	FL	[157, 147]
	cDNA: SH-$(CH_2)_6$	apt: ACT TCA GTG AGT TGT CCC ACG GTC GGC GAG TCG GTG GTA G cDNA: TTT TTC TAC CAC CGA CTC	apt: COOH	-	0.07 (b)	-	ECL	[159, 166]
	apt: biotin cDNA: SH-$(CH_2)_6$	apt: TTT TTA GCA GCA CAG AGG TCA GAT GAC TTC AGT GAG TTG TCC CAC GGT CGG CGA GTC GGT AGC CTA TGC GTG CTA CCG TGA A cDNA: CAC GCA TAG GCT ACC A	-	-	0.031 (b) (0.01·10^{-6} g/L) 3.094 (m) (1.0 ·10^{-6} g/L)	m	ECL	[91, 147]
	cDNA: SH-$(CH_2)_6$	apt: ACT TCA GTG AGT TGT CCC ACG GTC GGC GAG TCG GTG GTA G cDNA: CTA CCA CCG ACT C	apt: $(CH_2)_6$-NH_2	-	0.03 (b)	f	ECL	[158, 166]
	apt: $(CH_2)_6$	apt: ACT TCA GTG AGT TGT CCC ACG GTC GGC GAG TCG GTG GTA G cDNA: CTC GCC GAC CGT GGG ACA ACT CAC TGA AGT	-	-	0.000034 (b)	f	ECL/ SPR	[150, 147]
	-	ACT TCA GTG AGT TGT CCC ACG GTC GGC GAG TCG GTG GTA G	-	-	3.1 (b)	d	PEC	[160]

Antibiotic target	5′ linker & spacer	Aptamer sequence 5′→ 3′	3′ linker & spacer	K_D [nM]	LOD [nM]	RSA	Sensor type/ method	Ref [1]
Chloramphenicol	NH$_2$	ACT TCA GTG AGT TGT CCC ACG GTC GGC GAG TCG GTG GTA G	-	-	0.00036 (b)	M	PEC	[161]
	SH-(CH$_2$)$_6$	AGC AGC ACA GAG GTC AGA TGA CTG AGG GCA CGG ACA GGA GGG GGA GAG ATG GCG TGA GGT CCT ATG CGT GCT ACC GTG AA	-	-	1.76 (b)	-	IEC/ EIS	[162, 147]
	SH-(CH$_2$)$_6$	AGC AGC ACA GAG GTC AGA TGA CTG AGG GCA CGG ACA GGA GGG GGA GAG ATG GCG TGA GGT CCT ATG CGT GCT ACC GTG AA	-	-	1000 (b)	-	AEC/ SWV	[164, 147]
	SH-(CH$_2$)$_6$	AGC AGC ACA GAG GTC AGA TGA CTG AGG GCA CGG ACA GGA GGG GGA GAG ATG GCG TGA GGT CCT ATG CGT GCT ACC GTG AA	-	766	1.6 (b) 1.6 (m)	w, m	AEC/ SWV	[163, 147]
	apt: SH-(CH$_2$)$_6$ cDNA: biotin	apt: TTT TTA GCA GCA CAG AGG TCA GAT GAC TTC AGT GAG TTG TCC CAC GGT CGG CGA GTC GGT GGT AGC CTA TGC GTG CTA CCG TGA A cDNA: TTT TCT ACC ACC GAC TCG C	-	-	0.29 (b)	h	AEC/ DPV	[165, 147]
	NH$_2$	ACT TCA GTG AGT TGT CCC ACG GTC GGC GAG TCG GTG GTA G	-	-	0.02 (b)	u, d	AEC/ SWV	[166, 147]
	SH-(CH$_2$)$_6$	AGC AGC ACA GAG GTC AGA TGA CTT CAG TGA GTT GTC CCA CGG TCG GCG AGT CGG TGG TAG CCT ATG CGT GCT ACC GTG AA	-	-	4.0 (b)	hs	AEC/ SWV	[167]
	SH-(CH$_2$)$_6$	AGC AGC ACA GAG GTC AGA TGA CTG AGG GCA CGG ACA GGA GGG CAT GGA GAG ATG GCG	-	766	0.183 (b)	m	AEC/ DPV	[168, 147]
	NH$_2$	ACT TCA GTG AGT TGT CCC ACG GTC GGC GAG TCG GTG GTA G	-	-	0.000011 (b) 0.000014 (u)	d	AEC/ SWV	[169, 166]

Antibiotic target	5′ linker & spacer	Aptamer sequence 5′→ 3′	3′ linker & spacer	K_D [nM]	LOD [nM]	RSA	Sensor type/ method	Ref [1]
Chloramphenicol	apt: SH-(CH$_2$)$_6$ cDNA: NH$_2$-(CH$_2$)$_6$	apt: ACT TCA GTG AGT TGT CCC ACG GTC GGC GAG TCG GTG GTA G cDNA: ACC ACC GAC TCG CCG	-		0.0009 (b) (0.3·10^{-9} g/L)	f	AEC/ SWV	[170]
	SH-(CH$_2$)$_6$	AGC AGC ACA GAG GTC AGA TGA CTT CAG TGA GTT GTC CCA CGG TCG GCG AGT CGG TGG TAG CCT ATG CGT GCT ACC GTG AA	-	-	4.0 (b)	hs	AEC/ DPV	[171]
	cDNA I: SH-(CH$_2$)$_6$ cDNA II: NH$_2$-(CH$_2$)$_6$	apt: ACT TCA GTG AGT TGT CCC ACG GTC GGC GAG TCG GTG GTA cDNA I: ACA CAA GGG GGC CAC CAC AA cDNA II: TTG TGG TGG CCC CCT TGT GT	cDNA I: (CH$_2$)$_6$-PHO	-	0.46 (b) (0.15·10^{-6} g/L)	m	AEC/ SWV	[172]
	cap: SH-(CH$_2$)$_6$	apt: AGC AGC ACA GAG GTC AGA TGA CTT CAG TGA GTT GTC CCA CGG TCG GCG AGT CGG TGG TAG CCT ATG CGT GCT ACC GTG AA cap: GAG GAT TCA GTG A cDNA I: CCG ACC GTG GGA CAA CTC AGT GAA cDNA II: ACG GTC GGT TAC A	cDNA II: biotin	-	5 (b)	m	AEC/ SWV	[39]
	apt: NH$_2$-(CH$_2$)$_6$ cDNA: NH$_2$-(CH$_2$)$_6$	apt: ACT TCA GTG AGT TGT CCC ACG GTC GGC GAG TCG GTG GTA G cDNA: ACC GAC TCG CCG ACC	-	-	0.00019 (b)	m	AEC/ SWV	[47]
	cDNA I: NH$_2$-(CH$_2$)$_6$ cDNA II: SH-(CH$_2$)$_6$	apt: ACT TCA GTG AGT TGT CCC ACG GTC GGC GAG TCG GTG GTA GCC TAT GCA GTT T cDNA I: TTT CGC TGT GAC CTA CCA CCG ACT GC cDNA II: TTT GTG CAT AGG GTC ACA G	-	-	0.0000033 (b)	m	AEC/ SWV	[173]
	SH-(CH$_2$)$_6$	ACT TCA GTG AGT TGT CCC ACG GTC GGC GAG TCG GTG GTA G	-	-	2.0 (b)	m	AEC/ LSV	[174]
	apt: SH	apt: AGC AGC ACA GAG GTC AGA TGA CTG AGG GCA CGG ACA GGA GGG CAT GGA GAG ATG GCG		-	0.000021 (b)	m	AEC / SWV	[110, 147]

Antibiotic target	5′ linker & spacer	Aptamer sequence 5′→ 3′	3′ linker & spacer	K_D [nM]	LOD [nM]	RSA	Sensor type/ method	Ref [1]
Lincomycin	C dot	CGC GTG ATG TGG TCG ATG CGA TAC GGT GAG TCG CGC CAC GGC TAC ACA CGT CTC AGC GA	-	-	0.00016 (b)	me	ECL/ CV, AC	[182]
Ciprofloxacin	cDNA II: SH	apt: ATA CCA GCT TAT TCA ATT GCA GGG TAT CTG AGG CTT GAT CTA CTA AAT GTC GTG GGG CAT TGC TAT TGG CGT TGA TAC GTA CAA TCG TAA TCA GTT AG cDNA I: TTG AAT AAG CTG GTA TAA ACC cDNA II: AAA CCA CCT CCG AAT CCC AAG CCA CCG CCG CTA ACT GAT TAC GAT TGT	cDNA I: SH	-	1.3 (sw) 2.6 (s) 3.2 (m)	sw, hs, m	CO	[175, 181]
	SH	ATA CCA GCT TAT TCA ATT GCA GGG TAT CTG AGG CTT GAT CTA CTA AAT GTC GTG GGG CAT TGC TAT TGG CGT TGA TAC GTA CAA TCG TAA TCA GTT AG	-	-	0.263 (b)	m, hs	AEC/ DPV	[176]
Danofloxacin	FAM-oligo(dT)	UCA GGC UCC UGU GAA GCA ACC GAA UGG ACU GA	A_{16}	1.81 ± 0.18	-	-	FL SPR	[177]
Enrofloxacin	-	apt: CCC ATC AGG GGG CTA GGC TAA CAC GGT TCG GCT CTC TGA GCC CGG GTT ATT TCA GGG GGA cDNA: GTG TTA GCC TAG CCC CCT GAT	apt: biotin cDNA: biotin	-	0.56 (b) (0.02·10⁻⁶ g/L)	f	FL	[178]
	-	CCC ATC AGG GGG CTA GGC TAA CAC GGT TCG GCT CTC TGA GCC CGG GTT ATT TCA GGG GGA	biotin	-	0.11 (b) (0.04·10⁻⁶ g/L)	f	FL	[179]
Ofloxacin	SH-$(CH_2)_6$	ATA CCA GCT TAT TCA ATT AGT TGT GTA TTG AGG TTT GAT CTA GGC ATA GTC AAC AGA GCA CGA TCG ATC TGG CTT GTT CTA CAA TCG TAA TCA GTT AG	-	0.2	1.0 (b)	p, tp	AEC/ CV, DPV	[180, 181]

3136
3137
3138
3139

Antibiotic target	5′ linker & spacer	Aptamer sequence 5′→ 3′	3′ linker & spacer	K$_D$ [nM]	LOD [nM]	RSA	Sensor type/ method	Ref [1]
Ofloxacin	-	apt I: ATA CCA GCT TAT TCA ATT CGA TGG TAA GTG AGG TTC GTC CCT TTA ATA AAC TCG ATT AGG ATC TCG TGA GGT GTG CTC TAC AAT CGT AAT CAG TTA G apt II: ATA CCA GCT TAT TCA ATT GCA GGG TAT CTG AGG CTT GAT CTA CTA AAT GTC GTG GGG CAT TGC TAT TGG CGT TGA TAC GTA CAA TCG TAA TCA GTT AG apt III: ATA CCA GCT TAT TCA ATT AGT TGT GTA TTG AGG TTT GAT CTA GGC ATA GTC AAC AGA GCA CGA TCG ATC TGG CTT GTT CTA CAA TCG TAA TCA GTT AG	-	I: 56.9 ± 11.3 II: 0.11 ± 0.06 III: 0.20 ± 0.09	-	-	FL	[181]
Oxytetracycline	-	I: CGT ACG GAA TTC GCT AGC CGA CGC GCG TTG GTG GTG GAT GGT GTG TTA CAC GTG TTG TGG ATC CGA GCT CCA CGT G II: CGT ACG GAA TTC GCT AGC ACG TTG ACG CTG GTG CCC GGT TGT GGT GCG AGT GTT GTG T GG ATC CGA GCT CCA CGT G III: CGT ACG GAA TTC GCT AGC CGA GTT GAG CCG GGC GCG GTA CGG GTA CTG GTA TGT GTG G GG ATC CGA GCT CCA CGT G	-	I: 9.61 II: 12.08 III: 56.84	-	-	FL	[183, 190]
	-	AGG TGC AC	-	1.104	0.1 (b)	-	CO/ UV-Vis	[191]
	-	GGA ATT CGC TAG CAC GTT GAC GCT GGT GCC CGG TTG TGG TGC GAG TGT TGT GTG GAT CCG AGC TCC ACG TG	(CH$_2$)$_6$-SH		0.2 (b)	-	CAN	[193, 183]
	-	CGA ACG CGC GTT GGT GGT GGA TGG TGT GTT ACA CGT GTT GT	-	9.61	100 (b)	-	LSPIA	[185, 183]

Antibiotic target	5′ linker & spacer	Aptamer sequence 5′→ 3′	3′ linker & spacer	K_D [nM]	LOD [nM]	RSA	Sensor type/ method	Ref [1]
Oxytetracycline	-	I: CGA CGC ACA GTC GCT GGT GCG TAC CTG GTT GCC GTT GTG T II: GGC GCG GCA TGG TGT GGA CTC CAG GCG GTA GGG ATG TCG T III: GGC GAA GGA GTC ATG TAG GTG TGG TCG AGA CCG CTG TGC T IV: GAA AGG GAC GTT CCA AGT TCG TAT AAG CAG TCC TGT GCG T	-	I: 4.7 II: 8.0 III: 9.5 IV: 14.0	I: 26.7 (b) $(12.3 \cdot 10^{-6}$ g/L) I: 58.6 (m) $(27 \cdot 10^{-6}$ g/L)	m	ELAA	[188]
	biotin	ACC GCA CCA CCG TCA TGA GTG CGA ACT TAC GCA ATC ATG ACG GTG GTG CGG TGG TG	SH	-	0.000000009 (b) $(0.0435 \cdot 10^{-12}$ g/L)	f	SERS	[192, 191]
	-	CGT ACG GAA TTC GCT AGC GGG CGG GGG TGC TGG GGG AAT GGA GTG CTG CGT GCT GCG GGG ATC CGA GCT CCA CGT G	-	11.13	25 (b)	-	CO/ UV-Vis	[186, 183]
	-	CGT ACG GAA TTC GCT AGC GGG CGG GGG TGC TGG GGG AAT GGA GTG CTG CGT GCT GCG GGG ATC CGA GCT CCA CGT G	-	-	1 (b) 1 (tw)	tw	CO/ UV-Vis	[194, 183]
	FAM	CGT ACG GAA TTC GCT AGC GGG CGG GGG TGC GGG AAT GGA GTG CTG CGT GCT GCG GGG ATC CGA GCT CCA CGT G	-		10 (b)	lw	FL	[32, 183]
	apt: biotin cDNA: FAM	apt: GGA ATT CGC TAG CAC GTT GAC GCT GGT GCC CGG TTG TGG TGC GAG TGT TGT GTG GAT CCG AGC TCC ACG TG cDNA: ACA CAA CAC TCG CAC CAC AAC CGG GCA CCA GCG TCA ACG T	-	-	1.85 (b) $(0.85 \cdot 10^{-6}$ g/L)	m, h, p	FL	[80, 183]

3143
3144
3145
3146

Antibiotic target	5´ linker & spacer	Aptamer sequence 5´→ 3´	3´ linker & spacer	K_D [nM]	LOD [nM]	RSA	Sensor type/ method	Ref [1]
Oxytetracycline	-	apt: CGT ACG GAA TTC GCT AGC GGG CGG GGG TGC GGG AAT GGA GTG CTG CGT GCT GCG GGG ATC CGA GCT CCA CGT G cDNA I: AAT TCC GTA CG cDNA II: CGT ACG GAA TT	cDNA I: FAM	-	10 (b)	m, tw	FL	[195]
	FAM	CGT ACG GAA TTC GCT AGC GGG CGG GGG TGC TGG GGG AAT GGA GTG CTG CGT GCT GCG GGG ATC CGA GCT CCA CGT G	-	-	54.3 (b) $(25 \cdot 10^{-6}$ g/L)	tw, rw	FL	[197]
	apt: NH_2 cDNA: NH_2	apt: GGA ATT CGC TAG CAC GTT GAC GCT GGT GCC CGG TTG TGG TGC GAG TGT TGT GTG GAT CCG AGC TCC ACG TG cDNA: CGG ATC CAC ACA ACA	-	-	0.078 (b) $(0.036 \cdot 10^{-6}$ g/L)	m	ECL	[38, 183]
	apt: NH_2 cDNA: NH_2	apt: GGA ATT CGC TAG CAC GTT GAC GCT GGT GCC CGG TTG TGG TGC GAG TGT TGT GTG GAT CCG AGC TCC ACG TG cDNA: CAA CGT GCT AGC GAA	-	-	0.12 (b) $(0.054 \cdot 10^{-6}$ g/L)	m	ECL	[198, 183]
	apt: biotin cDNA: SH-$(CH_2)_6$	apt: GGA ATT CGC TAG CAC GTT GAC GCT GGT GCC CGG TTG TGG TGC GAG TGT GTG GAT CCG AGC TCC ACG TG cDNA: AAA ATC CAC ACA ACA	-	-	0.043 (b) $(0.02 \cdot 10^{-6}$ g/L)	m	ECL	[92]
	NH_2-$(CH_2)_6$	GGA ATT CGC TAG CAC GTT GAC GCT GGT GCC CGG TTG TGG TGC GAG TGT TGT GTG GAT CCG AGC TCC ACG TG	-	-	0.9 (b)	d	PEC/ EIS	[199, 183]

Antibiotic target	5´ linker & spacer	Aptamer sequence 5´→ 3´	3´ linker & spacer	K_D [nM]	LOD [nM]	RSA	Sensor type/ method	Ref [1]
Oxytetracycline	cDNA I: SH cDNA II: SH cDNA III: SH	apt: GGA ATT CGC TAG CAC GTT GAC GCT GGT GCC CGG TTG TGG TGC GAG TGT TGT GTG GAT CCG AGC TCC ACG TG cDNA I: CAC GTG GAG CTC GGA TCC ACA CAA CAC TCG CAC CAC AAC CGG GCA CCA GCG TCA ACG TGC TAG CGA ATT CC cDNA II: CAC GTG GAG CTC GGA TCC AC cDNA III: CAC GTG GAG CTC GGA TCC ACA CAA CAC TCG CAC CA	cDNA I: $(TTT)_{20}$-ACG TG-NH_2 cDNA II: $(TTT)_5$-ACG TG-NH_2 cDNA III: $(TTT)_{10}$-ACG TG-NH_2	-	0.19 (b)	m, w, c	PEC	[200]
	-	GGA ATT CGC TAG CAC GTT GAC GCT GGT GCC CGG TTG TGG TGC GAG TGT TGT GTG GAT CCG AGC TCC ACG TG	C_3-SH	11.13	1 (b)	-	AEC/ SWV	[184, 183]
	cDNA: SH-$(CH_2)_6$	apt: CGT ACG GAA TTC GCT AGC GGG CGG GGG TGC GGG AAT GGA GTG CTG CGT GCT GCG GGG ATC CGA GCT CCA CGT G cDNA: GCA TGC CTT AAG CGA TCG CCA TAT TAT AAG GCA TGC	cDNA: ferrocene	-	21.3 (b) (9.8·10^{-6} g/L)	mb, ms, mu	AEC/ SWV	[201]
	biotin C_3	GGA ATT CGC TAG CAC GTT GAC GCT GGT GCC CGG TTG TGG TGC GAG TGT TGT	-	-	0.005 (b) (2.3·10^{-9} g/L)	h	AEC/ CV	[202]
	-	TCA CGT TGA CGC TGG TGC CCG GTT GTG GTG GGA GTG TTG TGT	$(CH_2)_6$-NH_2	4.7	0.00018 (b)	m	AEC/ SWV	[105, 183]
	cDNA I: SH-$(CH_2)_6$ cDNA II: NH_2-$(CH_2)_6$	apt: ACG TTG ACG CTG GTG CCC GGT TGT GGT GGG AGT GTT GTG T cDNA I: CTA CCA TTT TTT CGC CGA CC cDNA II: GGT CGG CGA AAA AAT GGT AG	cDNA I: $(CH_2)_6$-PHO	-	0.22 (b) (0.1·10^{-6} g/L)	m	AEC/ SWV	[172]

3152

Antibiotic target	5′ linker & spacer	Aptamer sequence 5′→ 3′	3′ linker & spacer	K_D [nM]	LOD [nM]	RSA	Sensor type/ method	Ref [1]
Oxytetracycline	cDNA I: NH_2-$(CH_2)_6$ cDNA II: SH-$(CH_2)_6$	apt: ACG TTG ACG CTG GTG CCC GGT TGT GGT GCG AGT GTT GTG TCC TAT GCA GTT T cDNA I: TTT CGC TGT GAC ACA CAA CAC TCG GT cDNA II: TTT GTG CAT AGG GTC ACAG	-	-	0.0000048 (b)	m	AEC/ SWV	[173]
	SH	CGA CGC ACA GTC GCT GGT GCG TAC CTG GTT GCC GTT GTG T	-	-	0.498 (b)	h	AEC/ DPV	[204]
Tetracycline	-	I: CGT ACG GAA TTC GCT AGC CCC CCG GCA GGC CAC GGC TTG GGT TGG TCC CAC TGC GCG TGG ATC CGA GCT CCA CGT G II: CGT ACG GAA TTC GCT AGC GGG GGC ACA CAT GTA GGT GCT GTC AGT GTG GTT TGG TGG ATC CGA GCT CCA CGT G III: CGT ACG GAA TTC GCT AGC GGG CGG GGG TGC TGG GGG AAT GGA GTG CTG CGT GCT GCG G GG ATC CGA GCT CCA CGT G	-	I 63 II 70 III 100	-	-	-	[190]
	NH_2	CGT ACG GAA TTC GCT AGC CCC CCG GCA GGC CAC GGC TTG GGT TGG TCC CAC TGC GCG TGG ATC CGA GCT CCA CGT G	C_6	63.6	42.8 (u) $(0.019 \cdot 10^{-3}$ g/L) 83.3 (p) $(0.037 \cdot 10^{-3}$ g/L)	hu, hp	ESI-IMS	[205, 229]
	II biotin	I CGT ACG GAA TTC GCT AGC CCC CCG GCA GGC CAC GGC TTG GGT TGG TCC CAC TGC GCG TGG ATC CGA GCT CCA CGT G II GAG CCU AAA ACA UAC CAG AGA AAU CUG GAG AGG UGA AGA AUA CGA CCA CCU AGG CUC	I biotin	I: 63 II: 0.77	I: 32.7 (b) I: 95.2 (m) II: 21.0 (b) II: 35.1 (m)	m	ELAA	[208, 190, 207]

Antibiotic target	5′ linker & spacer	Aptamer sequence 5′→ 3′	3′ linker & spacer	K_D [nM]	LOD [nM]	RSA	Sensor type/ method	Ref [1]
Tetracycline								
	-	CGT ACG GAA TTC GCT AGC CCC CCG GCA GGC CAC GGC TTG GGT TGG TCC CAC TGC GCG TGG ATC CGA GCT CCA CGT G	biotin	63.6	0.018 (b) ($7.8 \cdot 10^{-9}$ g/L) 0.022 (h) ($9.6 \cdot 10^{-9}$ g/L)	h	ELAA	[209, 190]
	-	CGT ACG GAA TTC GCT AGC CCC CCG GCA GGC CAC GGC TTG GGT TGG TCC CAC TGC GCG TGG ATC CGA GCT CCA CGT G	biotin	-	0.15 (b) ($0.0659 \cdot 10^{-6}$ g/L) 0.22 (h) ($0.0978 \cdot 10^{-6}$ g/L)	h	ELAA	[210, 190]
	-	CGT ACG GAA TTC GCT AGC CCC CCG GCA GGC CAC GGC TTG GGT TGG TCC CAC TGC GCG TGG ATC CGA GCT CCA CGT G	-	-	11.6 (b)	m	SERS	[211, 190]
	apt: NH_2 cDNA: NH_2	apt: CGT ACG GAA TTC GCT AGC CCC CCG GCA GGC CAC GGC TTG GGT TGG TCC CAC TGC GCG TGG ATC CGA GCT CCA CGT G cDNA: CAA CGT GCT AGC GAA	apt: NH_2	-	0.0023 (b) ($0.001 \cdot 10^{-6}$ g/L)	m	SERS	[212]
	-	AGG TGC AC	-	1.067	0.1 (b)	-	CO/ UV-Vis	[191]
	-	CGT ACG GAA TTC GCT AGC CCC CCG GCA GGC CAC GGC TTG GGT TGG TCC CAC TGC GCG TGG ATC CGA GCT CCA CGT G	-	-	122 (b)	m	CO/ UV-Vis	[213, 190]
	-	CGT ACG GAA TTC GCT AGC CCC CCG GCA GGC CAC GGC TTG GGT TGG TCC CAC TGC GCG TGG ATC CGA GCT CCA CGT G	-	-	45.8 (uw)	m	CO/ UV-Vis	[214, 190]
	-	CGT ACG GAA TTC GCT AGC CCC CCG GCA GGC CAC GGC TTG GGT TGG TCC CAC TGC GCG TGG ATC CGA GCT CCA CGT G	-	63.6	87.8 (b) ($0.039 \cdot 10^{-3}$ g/L)	m	CO/ UV-Vis	[215, 190]

Antibiotic target	5′ linker & spacer	Aptamer sequence 5′→ 3′	3′ linker & spacer	K_D [nM]	LOD [nM]	RSA	Sensor type/ method	Ref [1]
Tetracycline	-	CTC TCT CGG TGG TGT CTC TC	-	-	0.266 (b) 0.347 (m) 0.393 (rs)	m, rs	CO/ UV-Vis	[216, 191]
	-	CGT ACG GAA TTC GCT AGC CCC CCG GCA GGC CAC GGC TTG GGT TGG TCC CAC TGC GCG TGG ATC CGA GCT CCA CGT G	-	3.4	-	-	CO/ UV-Vis	[217, 190, 191]
	-	CGT ACG GAA TTC GCT AGC CCC CCG GCA GGC CAC GGC TTG GGT TGG TCC CAC TGC GCG TGG ATC CGA GCT CCA CGT G	-	-	0.0023 (b) ($0.001 \cdot 10^{-6}$ g/L)	h	CO/ UV-Vis	[218]
	I: $(CT)_4$ II: $(CT)_4$C II: $(CT)_5$ cDNA: FAM	I, II, III: GGG GGC ACA CAT GTA GGT GCT GTC CAG GTG TGG TTG TGG T cDNA: GAG GAG AGA GAG AGA TCC TC	I: $(TC)_3$ II: $(CT)_3$C III: $(TC)_4$ cDNA: black hole quencher		I: 2.09 (b) I: 7.30 (tw) I: 8.48 (rs)	tw, rs	FL	[219]
	-	apt: TCC CTT CCG GTG GTG CTT CCC T G-quadruplex: ATG GGA AGG GAG GGA TGG GT	-	-	0.97 (b)	hs	FL	[220, 191]
	-	apt: CGT ACG GAA TTC GCT AGC CCC CCG GCA GGC CAC GGC TTG GGT TGG TCC CAC TGC GCG TGG ATC CGA GCT CCA CGT G cDNA: CAA CGT GCT AGC GAA	-	-	0.014 (b) ($6.2 \cdot 10^{-9}$ g/L)	m, p	FL	[221, 190]
	-	CGT ACG GAA TTC GCT AGC CCC CCG GCA GGC CAC GGC TTG GGT TGG TCC CAC TGC GCG TGG ATC CGA GCT CCA CGT G	-	-	0.65 (uw) ($0.29 \cdot 10^{-6}$ g/L)	m	FL	[222, 190]
	apt: biotin cDNA: SH-$(CH_2)_6$	apt: CGT ACG GAA TTC GCT AGC CCC CCG GCA GGC CAC GGC TTG GGT TGG TCC CAC TGC GCG TGG ATC CGA GCT CCA CGT G cDNA: GGA CCA ACC CAA	-	-	0.045 (b) ($0.02 \cdot 10^{-6}$ g/L)	m	ECL	[92]

3160

Antibiotic target	5´ linker & spacer	Aptamer sequence 5´→ 3´	3´ linker & spacer	K_D [nM]	LOD [nM]	RSA	Sensor type/ method	Ref [1]
Tetracycline	-	CGT ACG GAA TTC GCT AGC CCC CCG GCA GGC CAC GGC TTG GGT TGG TCC CAC TGC GCG TGG ATC CGA GCT CCA CGT G	-	-	5.3 (b)	lw	PEC	[206, 215]
	SH-(CH₂)₆	CGT ACG GAA TTC GCT AGC CCC CCG GCA GGC CAC GGC TTG GGT TGG TCC CAC TGC GCG TGG ATC CGA GCT CCA CGT G	-	-	0.1 (b)	m	PEC	[223, 210]
	-	CGT ACG GAA TTC GCT AGC CCC CCG GCA GGC CAC GGC TTG GGT TGG TCC CAC TGC GCG TGG ATC CGA GCT CCA CGT G		-	4.5 (b)	w	PEC	[224, 215]
	-	ACT CTT ATA CGG GAG CCA ACA CCA AAG CTT CTG CGC CAC ACC ATA TGA GAG CAG GTG GTA CGG ATA AGC T	-	52.5 ± 3.6	22.5 (b) (1·10⁻⁵ g/L)	m	IEC/ EIS	[225]
	SH-(CH₂)₆	GTC TCT GTG TGC GCC AGA GAA CAC TGG GGC AGA TAT GGG CCA GCA CAG AAT GAG GCC C	-	-	6.75 (b) (3.0·10⁻⁶ g/L)	m	IEC/ EIS	[226, 145]
	SH-(CH₂)₆	GTC TCT GTG TGC GCC AGA GAA CAC TGG GGC AGA TAT GGG CCA GCA CAG AAT GAG GCC C	-	-	1.0 (b)	m	IEC/ EIS	[227, 145]
	NH₂-CH₂	CGT ACG GAA TTC GCT AGC CCC CCG GCA GGC CAC GGC TTG GGT TGG TCC CAC TGC GCG TGG ATC CGA GCT CCA CGT G	-	-	1.0 (b)	m	IEC/ EIS	[228]
	biotin-T₅	TTT TTG GTA CGG AAT TCG CTA GCC CCC CHG CAG GCC ACG GCT TGG GTT GGT CCC ACT GCG CGT GGA TCC GAG CTC CAC GTG	-	63.6	10 (b)	-	AEC/ SWV	[229, 190]
	-	-	-	-	2.25 (b) (1.0·10⁻⁶ g/L)	m	AEC/ CV	[203]
	NH₂-CH₂	CGT ACG GAA TTC GCT AGC CCC CCG GCA GGC CAC GGC TTG GGT TGG TCC CAC TGC GCG TGG ATC CGA GCT CCA CGT G	-	-	5.0 (b)	m	AEC/ DPV	[230, 190]
	NH₂-(CH₂)₆	-	-	51800	2.25 (b) (1.0·10⁻⁶ g/L)	m	AEC/ DPV	[231]

Antibiotic target	5′ linker & spacer	Aptamer sequence 5′→ 3′	3′ linker & spacer	K_D [nM]	LOD [nM]	RSA	Sensor type/ method	Ref [1]
Tetracycline	NH_2-CH_2	CGT ACG GAA TTC GCT AGC CCC CCG GCA GGC CAC GGC TTG GGT TGG TCC CAC TGC GCG TGG ATC CGA GCT CCA CGT G	-	-	0.32 (b)	m	AEC/ DPV	[232, 190]
	NH_2-CH_2	CGT ACG GAA TTC GCT AGC CCC CCG GCA GGC CAC GGC TTG GGT TGG TCC CAC TGC GCG TGG ATC CGA GCT CCA CGT G	-	-	0.0042 (b)	m	AEC/ CV IEC/ EIS	[233, 190]
	NH_2	CGT ACG GAA TTC GCT AGC CCC CCG GCA GGC CAC GGC TTG GGT TGG TCC CAC TGC GCG TGG ATC CGA GCT CCA CGT G	-	-	0.000029 (b)	d	AEC/ DPV	[234]
	SH-$(CH_2)_6$	GTC TCT GTG TGC GCC AGA GAA CAC TGG GGC AGA TAT GGG CCA GCA CAG AAT GAG GCC C	-		10 (b)	m	AEC/ CV	[235, 145]
	NH_2	CGT ACG GAA TTC GCT AGC CCC CCG GCA GGC CAC GGC TTG GGT TGG TCC CAC TGC GCG TGG ATC CGA GCT CCA CGT G	-		aptasensor I: 0.0003 (b, EIS) 0.029 (b, DPV) apatsensor II: 0.0000038 (b, EIS) 0.00031 (b, DPV)	m, d, h, bs	AEC/ DPV IEC/ EIS	[236]
	cDNA I: SH cDNA II: SH	apt: CGT ACG GAA TTC GCT AGC CCC CCG GCA GGC CAC GGC TTG GGT TGG TCC CAC TGC GCG TGG ATC CGA GCT CCA CGT G cDNA I: CCA TCA GAC CTA CCA AAC ACG TGG AGC T cDNA II: AGA CCT ACC AAA CGA ACC CA cDNA III: AAT TCC GTA CGA AAC CAT CCA GAC TAC C	cDNA III: SH	63	0.45 (b) 0.74 (m) 0.71 (s)	m, hs	AEC/ DPV	[237, 190]

Antibiotic target	5′ linker & spacer	Aptamer sequence 5′→ 3′	3′ linker & spacer	K_D [nM]	LOD [nM]	RSA	Sensor type/ method	Ref [1]
Tetracycline	cap: SH-(CH₂)₆	apt: CGT ACG GAA TTC GCT AGC CCC CCG GCA GGC CAC GGC TTG GGT TGG TCC CAC TGC GCG TGG ATC CGA GCT CCA CGT G cap: ATG TAG CTA GGT G cDNA I: CGT GTA GCA CAG CAT CAC CAC CTA GC cDNA II: GCT ACA CGC GTT T	cS II: biotin	-	20 (b)	m	AEC/ SWV	[39]
	-	CGT ACG GAA TTC GCT AGC CCC CCG GCA GGC CAC GGC TTG GGT TGG TCC CAC TGC GCG TGG ATC CGA GCT CCA CGT G	-	-	0.6 (b)	-	AEC/ DPV	[238]
	SH-(CH₂)₆	CGT ACG GAA TTC GCT AGC CCC CCG GCA GGC CAC GGC TTG GGT TGG TCC CAC TGC GCG TGG ATC CGA GCT CCA CGT G	-	-	0.74 (b) (0.33·10⁻⁶ g/L)	m	AEC/ DPV	[239, 145]
Sulfadimethoxine	-	I: GTT AGA TGG GAG GTC ATA TAG C II: GAG GGC AAC GAG TGT TTA TAG A	-	I: 150 II: 84	II: 32.2 (b) II: 32.2 (m) (10·10⁻⁶ g/L)	m	FL	[240]
	-	GAG GGC AAC GAG TGT TTA TAG A	FAM	-	-	-	FL, CO/ UV-Vis	[240, 242]
	-	GAG GGC AAC GAG TGT TTA TAG A	-	-	161.1 (b) (50·10⁻⁶ g/L)	-	CO/ UV-Vis	[240, 241]
	-	GAG GGC AAC GAG TGT TTA TAG A	-	84	-	-	CO/ UV-Vis	[72, 240]
	-	GAG GGC AAC GAG TGT TTA TAG A	-	-	32.2 (b) (10·10⁻⁶ g/L)	m	CO/ UV-Vis	[243]
	-	GAG GGC AAC GAG TGT TTA TAG A	-	-	22.56 (b)	lw	CO	[244]
	-	apt: GAG GGC AAC GAG TGT TTA TAG A cDNA: CGT TGC CCT C	apt: biotin cDNA: biotin	-	0.35 (b) (0.11·10⁻⁶ g/L)	f	FL	[245, 240]
	NH₂	GAG GGC AAC GAG TGT TTA TAG A	FAM	-	0.55 (b)	m, d	PEC	[246]

3166   [1] when naming several references, the first always describes the realized sensor with associated LOD; aptamer sequence(s) and/or associated K_D values
3167   are derived from the additional reference(s)
3168   [2] the exact subcategory of the substance is not mentioned